SENSITIVITY ANALYSIS OF BRIDGE DECKS FOR HIGH-SPEED RAILWAY BRIDGES

A THESIS SUBMITTED TO
THE GRADUATE SCHOOL OF NATURAL AND APPLIED SCIENCES
OF
MIDDLE EAST TECHNICAL UNIVERSITY

BY

ABDULLAH RAHMAN

IN PARTIAL FULFILLMENT OF THE REQUIREMENTS
FOR
THE DEGREE OF MASTER OF SCIENCE
IN
CIVIL ENGINEERING

JANUARY 2020

Approval of the thesis:

SENSITIVITY ANALYSIS OF BRIDGE DECKS FOR HIGH-SPEED RAILWAY BRIDGES

submitted by **ABDULLAH RAHMAN** in partial fulfillment of the requirements for the degree of **Master of Science in Civil Engineering Department, Middle East Technical University** by,

Prof. Dr. Halil Kalıpçılar
Dean, Graduate School of **Natural and Applied Sciences** _____

Prof. Dr. Ahmet Türer
Head of Department, **Civil Engineering** _____

Prof. Dr. Alp Caner
Supervisor, **Civil Engineering, METU** _____

Examining Committee Members:

Prof. Dr. Mehmet Utku
Civil Engineering Dept., METU _____

Prof. Dr. Alp Caner
Civil Engineering, METU _____

Prof. Dr. Cem Topkaya
Civil Engineering Dept., METU _____

Prof. Dr. Eray Baran
Civil Engineering Dept., METU _____

Assist. Prof. Dr. Burcu Güldür Erkal
Civil Engineering Dept., Hacettepe University _____

Date: 31.01.2020

I hereby declare that all information in this document has been obtained and presented in accordance with academic rules and ethical conduct. I also declare that, as required by these rules and conduct, I have fully cited and referenced all material and results that are not original to this work.

Name, Surname: Abdullah Rahman

Signature:

ABSTRACT

SENSITIVITY ANALYSIS OF BRIDGE DECKS FOR HIGH-SPEED RAILWAY BRIDGES

Rahman, Abdullah
Master of Science, Civil Engineering
Supervisor: Prof. Dr. Alp Caner

January 2020, 167 pages

Continuous welded rail provides a smooth ride for railway traffic, the use of continuous welded rail allows the trains to reach higher speeds, where tracks are made to be continuous over supporting structure and discontinuities -embankment in front of and behind the bridge- the structure and the track jointly resist the longitudinal forces generated from rail traffic. Bridge structural properties can allow additional stresses in rail due to movement under variable actions. Bridge structure and track are interlinked by ballast. This interlink will result in an interaction between the track and structure. If the interaction between the track and structure kept under control, the track and bridge will continue to fulfill their function without any damage into the track. In this thesis, parameters affecting the track-structure interaction are identified to perform a sensitivity analysis. The parameters are bridge deck span, deck height, bending stiffness, and neutral axis location. The focus of this thesis is given to develop a simple method for calculating the combined effect with a live load amplification factor of 1.4 ($\alpha = 1.4$). The Eurocode provides a simple method, but it is only valid for classified loads with α factor = 1.

Keywords: Track-structure interaction, High-speed railway bridge, Continuous welded rail, Additional rail stress

ÖZ

HIZLI TREN DEMİRYOLU KÖPRÜLERİ ÜST YAPILARI İÇİN DUYARLILIK ANALİZİ

Rahman, Abdullah
Yüksek Lisans, İnşaat Mühendisliği
Tez Danışmanı: Prof. Dr. Alp Caner

Ocak 2020, 167 sayfa

Sürekli kaynaklı ray sistemi demiryolu için pürüzsüz bir sürüşü mümkün kılmaktadır, Sürekli kaynaklı raylı systemin kullanımı trenlerin yüksek hızlara çıkmasına imkan sağlar. Demiryolunun üzerinde bulunduğu yapı ve giriş-çıkışlarda bulunan dolgular gibi süreksizlikler üzerinde sürekli hale getirildiği durumlarda, yapı ve demiryolu üst yapısı tren trafiğinin oluşturduğu boyuna yöndeki kuvvetlere birlikte direnç gösterir. Köprünün yapısal özellikleri, değişken yükler altındaki hareketlerden kaynaklanan ilave ray gerilmelerine müsade edebilir. Demiryolu üst yapısı ve köprü ballast tabakası ile birbirine bağlanmaktadır ve bu bağlantı demiryolu ile yapı arasında bir etkileşim ortaya çıkarmaktadır. Demiryolu üst yapısı ve köprü arasındaki bu etkileşim kontrol altında tutulursa yapı ve demiryolu herhangi bir hasar olmaksızın görevlerini yapmaya devam edeceklerdir. Bu çalışmada ray yapı etkileşiminde rol alan parametreler duyarlılık analizi gerçekleştirmek için tariflenmiştir. Bu parametreler, köprü üstyapısı açıklığı, derinliği,,eğilme rijitliği ve nötral eksen konumudur. Bu tez kapsamında yapılan çalışmanın amacı, hareketli yük büyütme faktrönün 1.4 alındığı durum için (α = 1.4) bütün etkileri dikkate alacak şekilde basit bir hesap yöntemi geliştirmektir. Eurocode şartnamesi bunun için basit bir yöntem belirtmektedir ancak bu yöntem sadece haraketli yük artırma faktörünün 1.0 alındığı durum için geçerlidir.

Anahtar Kelimeler: Ray-Yapı etkileşimi, Yüksek hızlı tren, Sürekli kaynaklı ray, Ray ilave gerilmeleri

For my Family, Family is always first

ACKNOWLEDGEMENTS

Always thankful to God for helping me all the time. I would like to pay my special regards to my supervisor, Professor Alp Caner, for accepting me to work under his supervision and for helping and supporting me through this thesis, he convincingly guided and encouraged me to be professional and to do the right thing even when the road gets tough.

I wish to express my deepest gratitude to the thesis examining committee members, Prof. Dr. Mehmet Utku, Prof. Dr. Cem Topkaya, Prof. Dr. Eray Baran, Assist. Prof. Dr. Burcu Güldür Erkal for their insights and valuable suggestions.

I wish to show my gratitude to Prof. Dr. Sayed Tanvir Wasti for helping and supporting me through my entire graduate study.

I would like to thank my family, my father Hecham and my mother Razan, my sister Alya and my little brother, they have always supported me and helped me through my entire graduate study.

My sincere thanks also go to my chief Kamil Ergüner and his wife Merih Ergüner, for their support and helping me in my graduate study.

Last but not least, I would like to thank my friends, my coworkers, for their support.

TABLE OF CONTENTS

LIST OF TABLES

TABLES

LIST OF FIGURES

FIGURES

CHAPTER 1

INTRODUCTION

1.1. High-Speed Railway

Travelling by trains is recognized as one of the safest land transportation systems, and the railway transportation system is efficient in terms of energy and mobilization. Speed railways have experienced a lot of developments over the past decades, and the main goal is to achieve higher speeds and reduce transportation time. A new type of railways which emerged from the conventional one is the high-speed railway system, which can significantly reduce the amount of time required for traveling by the conventional system. Japan had the lead in high-speed railways industry when they introduced the first high-speed track in 1964 (Manovachirasan et al., 2018) known as the bullet train. Many countries wanted to develop a high-speed railway network, such as Germany, France, Turkey, Poland, Sweden, Spain, South Korea. The system of high-speed railway track consists of the track and the fasteners, sleepers and the filling material ballast, (Ruge and Birk., 2007), as shown in Figure 1.1, which are the components that provide a surface for the train wheels running along the track.

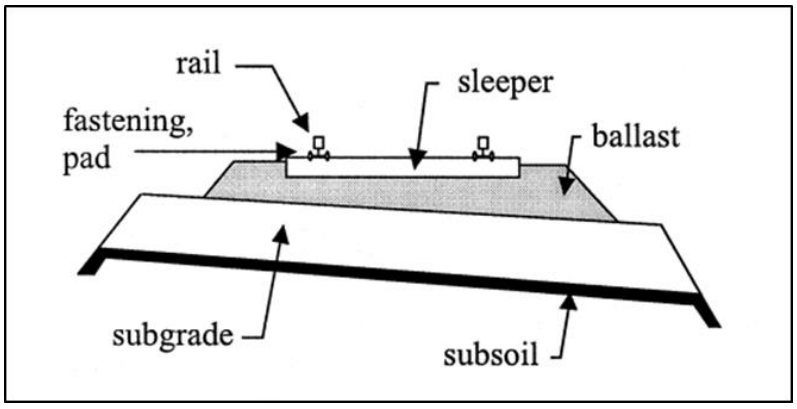

Figure 1.1. General Components of High-Speed Track System

1.2. Continuous Welded Rail (CWR)

In most of the conventional tracks, the rails are separated by gaps as shown in Figure 1.2 to allow for thermal expansion. Since the jointed track has a gap between the rails, the contact surface between the rail and the train wheel is reduced on the joint section. This reduction creates a dynamic force on the rails, requires a significant amount of maintenance, increases power consumption (Low., 2015) and limits the maximum speed of the train.

Introducing the Continuous Welded Track to the railway system will allow higher speeds and a smoother ride (Yeo and Lee., 2006) by reducing the vibrations created by the train wheels passing over the track joints (Müller et al., 1981). The CWR is produced by filling the gaps between the rails with filler material for several kilometers. The overall cost of the CWR track type is cheaper than the conventional type because the maintenance cost is reduced and the service life of the track is increased (Lei and Feng., 2004). The most significant difference in structural response between the continuously welded rails and the jointed type is the axial compression force in the longitudinal direction.

Figure 1.2. Jointed Rail (Engineering Materials-Jones., 2019)

1.3. Continuous Welded Rail for High-Speed Railways

The use of CWR instead of the jointed rail will result in a better track system. The CWR will allow higher speeds with low maintenance cost. However, because of the CWR is continuous it will result in an extra internal force due to thermal, braking and live loads. The jointed rail has small gaps allowing the rail to expand and contract under the thermal loads. These extra loads generated in the track should be resisted by the rail and the rail should withstand the stresses. These stresses can be compressive or tensile. Particular attention should be paid for the compression force because the compression force could reduce the compression resistance of the continuous welded rail due to buckling.

The first use of the continuous welded rail was in Germany in 1924 (Lonsdale., 1999) and it has become more common since the 1950's. The German Railways are always trying to increase the travelling speed. Therefore, they have designed most of their high-speed railways to allow speeds up to 250 km/hr (Müller et al., 1992). Similar to are in Spain and Turkey as shown in Figure 1.3.

Figure 1.3. High-Speed Network in Europe 2012 (UIC)

1.4. Continuous Welded Rail for Bridges

The major part of the rails is placed on a subgrade. Generally, the rail attached to the sleepers by fasteners laid on ballast bed supported by a subgrade, as shown in Figure 1.4 sleepers are typically spaced at 60 (cm) over ballast. However, in the application of bridges, the rail is attached to the sleepers by fasteners laid on ballast bed or concrete strip compatible with the filler used and then supported by the bridge deck. For the jointed rail system, the rail and the supporting structure are treated separately while, this is not the case for the continuously welded rail. Rail stresses needed to be checked for CWR case. The bridge has mechanical and geometrical properties such as bending stiffness, cross-section area, deck height. The superstructure is supported over bearings attached to the top of piers and abutments. Having a shear stiffness under lateral loads and axial stiffness under vertical loads, bearings will contribute to the structural response. Since the bridge could undergo some deformations due to vertical or horizontal force, the bridge movements are accommodated by the bearings and expansion joints on the top of the deck. Introducing a continuous welded rail at the top of the bridge will create a situation in which any movement of the bridge will affect the rail supported by the deck. The coupling between the bridge deck and the rail is achieved by ballast bed or by direct fastening.

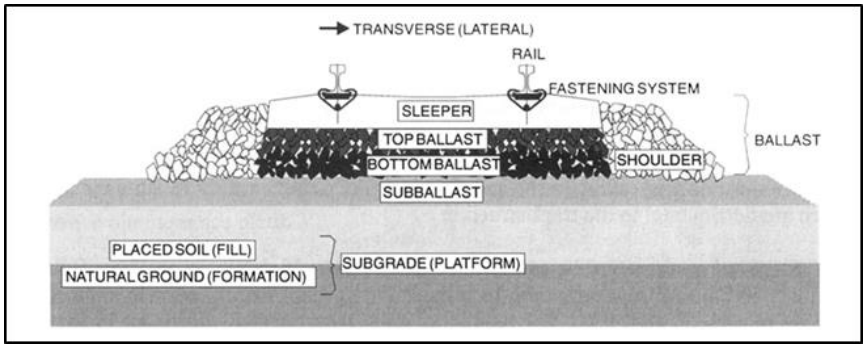

Figure 1.4. Cross Section View of Typical Ballast Track (Alabbasi and Hussein., 2019)

Since any movement of the bridge or the track will affect the other, this phenomenon is defined as interaction. The interaction between the structure supporting the track

and the track is discussed through this thesis by using interaction models, as shown in Figure 1.5. Generally, the bridges have large stiffness compared to tracks.

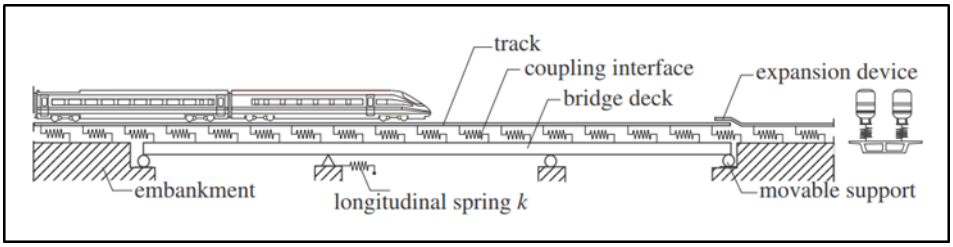

Figure 1.5. Track-Structure Interaction Model (Widarda., 2009)

1.5. Problem Statement and Thesis Objectives

The Structure and the Track are coupled by the ballast. This coupling action is described as the track structure interaction. The track-structure interaction is discussed well in the literature, and the physical event is defined in practice design codes, as reported in Chapter 2. The bridge structure has parameters affecting the behavior of the bridge deck and the interaction. The parameters are defined in the literature, but there are not any complete studies on how these parameters are affecting the interaction between the structure and the track. The aim of this thesis is to fill the gap in the literature regarding the parameters affecting the track-structure interaction phenomenon for a ballasted case without rail expansion device. Sensitivity analysis is performed for the parameters affecting the interaction to see how changing the parameters will affect the system of the track and the structure through mathematical models. Parameters affecting the interaction are defined and the response of the structure as a whole to variation of these parameters is discussed.

1.6. Organization of the Thesis

The thesis is organized as follows:

Chapter 1 is an introduction to the high-speed railway systems and the concept of continuous welded rail (CWR) and the interaction between the track and structure.

Chapter 2 is intended to discuss the Track-Structure interaction, deeply with the help of the literature and the design codes, the loads affecting the interaction, and the coupling nature between the track and the bridge deck. Also, later in this chapter, some bridge monitoring practices are reported, and lastly the areas covered by this work are defined.

Chapter 3 presents the mathematical modeling of the Track-Structure, differences between the modeling techniques, and the verification of the computer model used for the evaluation, according to UIC.

Chapter 4 focuses on the analysis types used for the evaluation. The two selected analysis types are the complete and simple separated type are defined, and the accuracy of each analysis is discussed. Moreover, a comparison between each analysis type is presented.

Chapter 5 is the evaluation of Track-Structure interaction. Sensitivity analysis is performed, and parameters affecting the interaction phenomenon are defined. The effect of each parameter on the rail stress is presented. At the end of the sensitivity analysis, a simple method is proposed for calculating the combined effect of Track-Structure interaction similar to the method given by Eurocode Annex G. The method is intended to cover higher classified loads with α factor up to 1.4, while Eurocode method only includes classified vertical loads with α factor equal to 1.

Chapter 6 presents a summary of the work done in this thesis, conclusion and some recommendations for future researches.

CHAPTER 2

TRACK-STRCTURE INTERACTION

Bridge and Track are interlinked, regardless of whether the system used for the track is the ballasted bed or it is directly fastened. Any force or deformation imposed on the track above or close to bridge structure will result in a force and deformation on the bridge structure or vice versa.

2.1. Track-Structure Interaction Development

After introducing the continuously welded rail to the high-speed railway network, a new problem started to arise for the designers -CWR- doesn't have any joints to accommodate the thermal movement of the rail as in case of jointed tracks. The most significant difference between the two types of tracks is the longitudinal forces generated in the rail due to thermal and variable actions. Back in the mid-70's the design for longitudinal forces could be based only to a very limited extent on the experience from road bridges (Prommersberger and Rojek., 1984). In the late 70's the designers started to take axial forces generated in the track due to interaction between the bridge deck and the track into consideration. Historically, the development of high-speed networks in Europe has been observed in several stages. The structural system (bridge-viaduct) proposed to support the track should satisfy some rules developed to ensure track safety. These rules typically have empirical limits based on actual site measurements of rail stress concentrations and experience approaches for rail stability and safety (Dutoit., 2008). To develop a design criterion for a continuous welded track-structure interaction, the International Union of Railways has commissioned a research team from the European Rail Research Institute (ERRI) in 1992 titled "Improve knowledge of CWR including switches". The research program was assigned to the (ERRI) special committee D-202 and it was composed of four main

tasks; development of theoretical models, experimental research to determine the input data for the model and the validation process of the models, non-destructive measurements of longitudinal rail stresses due to temperature action and revision of the International Union of Railways leaflets for the continuous welded rail (Esveld., 1996). The research concluded in three parts developed at TU Delft, The Netherlands and TU Krakow Poland and the three models were CWERRI, CREEP, TURN. CWERRI intended to analyze and study the (CWR) stability under various combinations, including vertical and longitudinal forces, dynamic effects and ballast yielding under combined load situation. Modeling CWR behavior in the longitudinal, vertical and lateral directions is possible with this method. As the CWR could be modeled, its behavior could be calculated integrally in a user-friendly environment. The model provides: rail-structure (bridge) interaction including the bending effect from vertical loads, multi span bridges with many rails aligned parallel, ballast yielding in three-dimensional behavior taking into account the vertical load effect, three-dimensional modelling and calculations, vertical and lateral rail stability under axial loads (Esveld., 1998).

2.2. Loads Considered by Interaction

Due to the fact that the track and structure are coupled by connection, the deformations and loads on each element affect others. The rail is used to support the train passing over it. The train has a vertical load with a rolling mass creating traction and braking forces, and the thermal loads induced by bridge expanding in summer and contracting in winter. The bridge interaction is also affected by creep shrinkage and temperature gradient, but the main loads affecting the track-structure interaction are thermal loads, vertical load, braking/acceleration loads (Ruge and Birk., 2007).

2.2.1. Braking-Acceleration Forces

Train movement along the bridge gives rise to a longitudinal (horizontal) force transferred through friction via the rails, fasteners, sleepers through ballast to bridge deck, bearings -if exists- finally to the supports. The rolling of the wheel at constant

speed creates a relatively small friction force. However, the friction force magnitude increases during movement at non-uniform speed, which takes place at breaking or acceleration. In this case, the adhesion forces between the train wheels and the tracks (Fryba., 1996).

The longitudinal force transferred to tracks in case of acceleration or deceleration is composed generally of air resistance due to vehicle drag, axle bearing and wheel flange friction. The latter two are considered negligible and the train traction force, which is related to the engine torque and gear ratio under the condition where no slippage occurs means complete adhesion (for modern locomotives with a software-controlled wheel slip). The maximum traction force that can be applied to the tracks is limited to μ the friction between the train wheel and the rail and to $W_{p,}$ the vertical load carried by the wheel (Unsworth., 2010). During load tests in the United States and Europe, it has been observed that the longitudinal forces resulted from braking or acceleration reach maximum force at low speeds as shown in Figure 2.1 when train starts to accelerate or just before stopping for braking, and it has been shown that forces exhibit almost static behavior (Fryba., 1996).

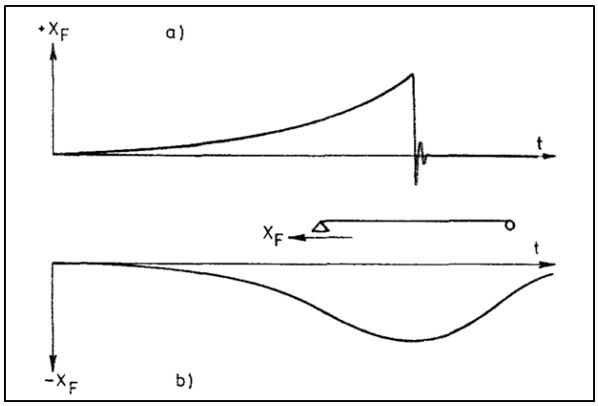

Figure 2.1. Time-history Under Horizontal force a) Braking, b) Acceleration (Fryba., 1996)

Where:

X_f : the longitudinal force due to braking of acceleration.

t : time.

The longitudinal force due to braking and acceleration has been examined extensively in the literature (Foutch et al., 1996, 1997), (LoPresti et al., 1998), (LoPresti and Otter., 1998), (Otter et al., 1996, 1997, 1999, 2000), (Tobias et al., 1999), (Uppal et al., 2001).

The latest research proposed a relationship between the braking/acceleration force and the length of the portion of the bridge under consideration, as shown in Figure 2.2, which overcome the complexities and numerical modeling effort.

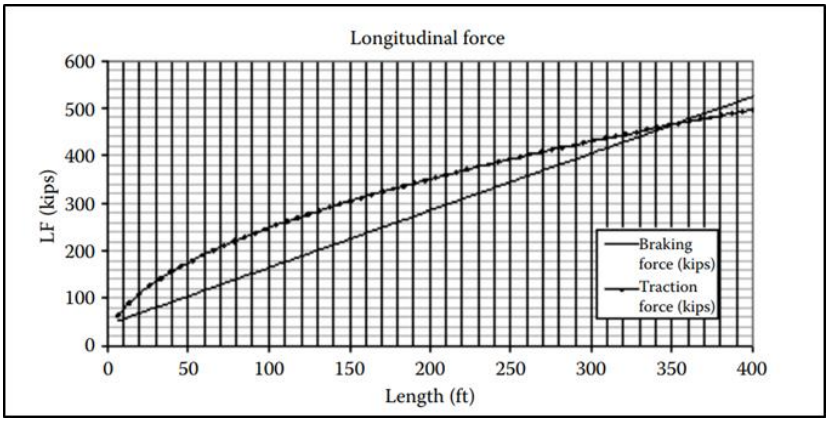

Figure 2.2. AREMA Design Longitudinal Forces

The load distribution of braking and traction forces depends on many factors, some of which are bridge members resisting the loads, bearing types and substructure stiffness, as shown in Chapter 5.

2.2.1.1. Braking Force

The braking force reaches its maximum magnitude just before stopping, and it is directly related to the weight of the train and the friction factor; hence, the largest beam longitudinal deformations could be approximately calculated from static longitudinal force equal to the coefficient of adhesion friction multiplied by the train weight (Fryba., 1996). The friction factor could achieve 40 % $\mu = 0.4$ (Prommersberger and Rojek., 1984). Due to the fact that braking force could be treated

as static load, the force could be distributed along the train length. This will make the computation much simpler and easier and more accurate at the same time.

2.2.1.2. Traction/Acceleration Force

The traction force reaches its peak just when the train starts to move (Unsworth., 2010), and it is directly related to the friction coefficient, torque produced by the engine, and the weight of the locomotive. It should be noted that the maximum traction force is limited by the weight supported by the traction wheels and the friction coefficient; otherwise, a slip will occur (Fryba., 1996). The weight of the locomotives containing the engines is higher than the normal wagons; thus, it could produce forces higher than braking forces, but on limited length. The horizontal forces due to acceleration and braking are summarized as follows; the span length doesn't affect the braking force since the emergency braking system is distributed along the train, the traction force and braking force are maximum at lower speeds, traction force generated from locomotives could affect a smaller length of the bridge (Otter et al., 2000).

2.2.2. Vertical Load

Vertical loads are transferred to the bridge deck through ballast bed. The bridge deck has a pre-defined bending stiffness, which will lead to superstructure end rotation under vertical loads, as shown in Figure 2.3. Deck rotation will impose a deformation on the track as shown in (Esveld., 1998).

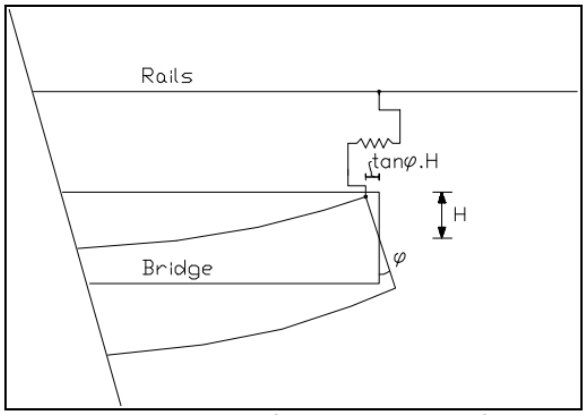

Figure 2.3. Influence of Bridge-end Rotation (Esveld., 1998)

The vertical loads for high-speed railways are primarily divided into two categories; the European and the United States load classification. Within the European region, the vertical loads are mainly based on LM-71 and the SW family load. The LM-71 load has been enhanced by the dynamic factor Φ, and by the load amplification factor α (Eurocode). The USA loads are based on maximum Cooper loads with Cooper E80 as the recommended load the other loads are scaled based on Cooper E80, such as 0.75 is used to determine Cooper E60 loads (AREMA., 2008). The total height of the deck and the natural axis ordinate have an effect on the force generated in the tracks.

2.2.3. Thermal Load

2.2.3.1. Thermal load on the Track

The continuous welded rail (CWR) is fixed to the sleeper by a fastener, which secures the rail in the sleeper by a clamping force. This clamping force is designed to provide the full transmit of all longitudinal movement of the track to the sleepers. The resistance of track/sleeper for sliding is greater than the resistance of ballast for horizontal movement. As a result, the track movement in the longitudinal direction under thermal action or traffic loads is restrained by the ballast stiffness, which will build up an axial force in the track. If a continuous welded rail laying on embankment without rail expansion device is subjected to the thermal load, the rail will be subjected to axial stress because the expansion and contraction of the rail are completely prevented. The CWR has a breathing zone -two zones- at each end, which could be opened till 50 (mm) for a distance up to 150 (m), as shown in Figure 2.4.

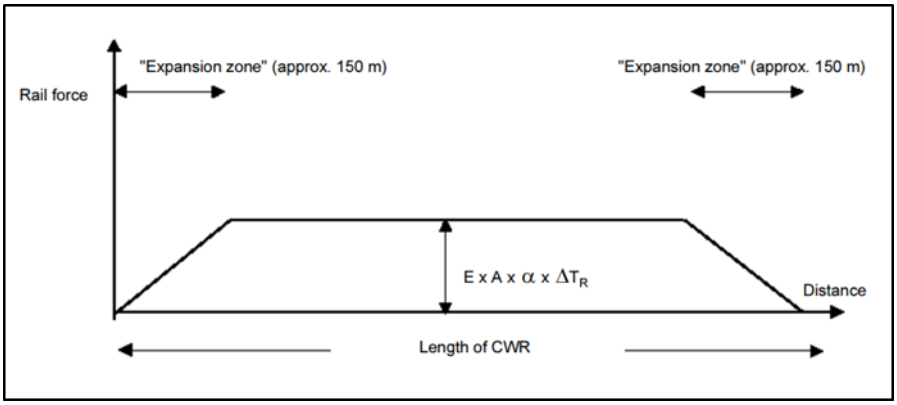

Figure 2.4. Thermal Longitudinal Force in CWR (UIC)

The stress within the CWR under thermal load is equal:

$$\sigma = E \times \propto \times \Delta Tr \qquad (2\text{-}1)$$

Where:

E: Young's Modulus of the rail (MPa)

ΔTr: Temperature change reference to laying temperature

ᾱ: Coefficient of thermal expansion

Experiments on rail temperature shows that the rail temperature increases to a maximum of 18 to 20 ºK above the surrounding air temperature (DIN-Fb 101).

2.2.3.2. Thermal Loads on the Bridge Deck

Bridges for high-speed railway expand and contract under thermal loads. Due to the movement, the bridge structure under thermal action induces additional forces on the continuously welded rail, which limits its use. The problem of continuous welded rail over bridge deck could be approached by considering the bridge deck and the rail as beam element interlinked by ballast (Fryba., 1996). The bridge has fixed, and movable supports and the bridge is typically free to move under thermal action. The bridge movement will generate a movement in the ballast and this movement will be

transmitted by ballast into the rails as a force. The force in the rails directly depends on the free expansion length of the bridge, as shown in Figure 2.13 and the difference between the laying temperature and the maximum or minimum temperature in the summer or winter. The parameters affecting the rail stress due to temperature action are discussed in detail in Chapter 5. The temperature variation depends on many factors such as coefficient of thermal expansion, as shown in Figure 2.6. Also, steel structures are more sensitive to temperature than concrete and composite structures, as shown in Figure 2.5 (DIN-Fb 101).

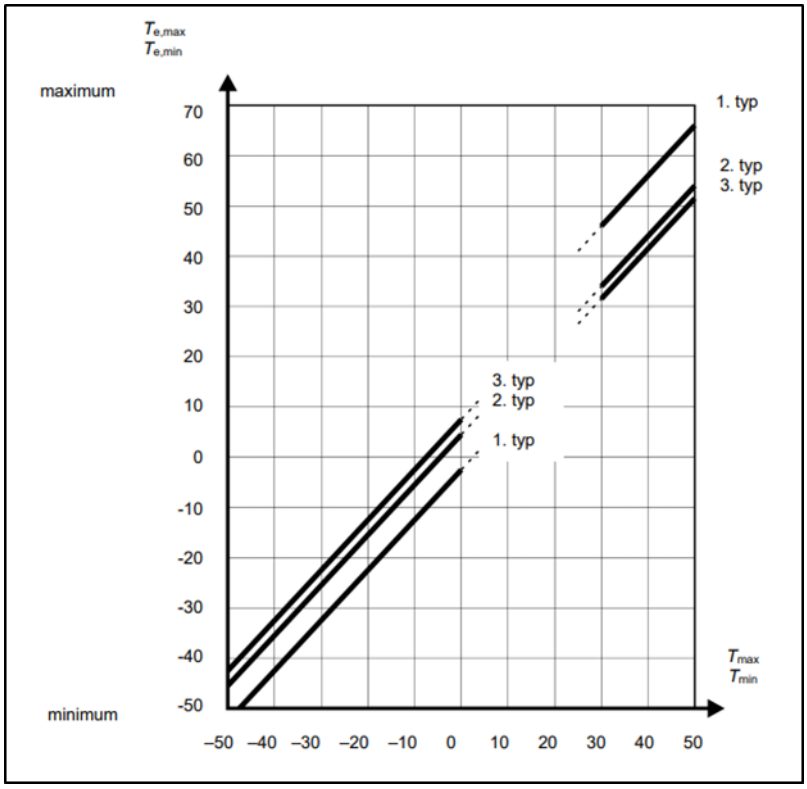

Figure 2.5. Correlation between Shade Air Temperature and Uniform Bridge Temperature Component (Holický and Marková., 2008)

$T_{e,max}$,$T_{e,min}$ are for the bridge deck, T_{max} , T_{min} for shade air temperature ºK, type-1 is steel deck, type-2 and type-3 are composite and concrete decks respectively.

Material	α_T (x 10^{-6} x $°C^{-1}$)
Aluminium, aluminium alloys	24
Stainless Steel	16
Structural steel	12
Concrete (except as specified below)	10
Concrete with light aggregates	7
Masonry	6-10
Timber, along to grain	5
Timber, across to grain	30-70

Figure 2.6. Coefficient of Thermal Expansion (EN 1991-1)

The thermal expansion coefficient for steel in composite and reinforced concrete deck is assumed to be equal to that of concrete (Holický and Marková., 2008).

2.3. Buckling of CWR

Temperature induces significant axial forces which can build up in CWR, threatening the stability of rail (Lim et al., 2008). Consideration of the CWR started in the early 30's, and the first computational model considering the buckling of CWR were developed in 1930 (Dosa and Unggureanu., 2007). Many finite element models and analytical models were developed by considering the ballast and the sleepers with the CWR, but they were mathematically very complex (Kerr.,1976). Later on, different finite element models were developed to investigate the CWR buckling (Samavedam et al., 1983). The models could be categorized as continuum models or discrete models. The 1D Winkler's foundation beam were mostly used among the other continuum models because of its simplicity. (Kish et al., 1982,1985), (Samavedam et al., 1983,1993) published many papers regarding the rail buckling using beam model. (Manovachirasan et al., 2017) developed a theoretical 3D finite element model for rail buckling analysis, as shown in Figure 2.7. This model takes into account the coupling change due to vertical loads and was developed to investigate the changes in the longitudinal stress distribution due to loads applied on the bridge and the track.

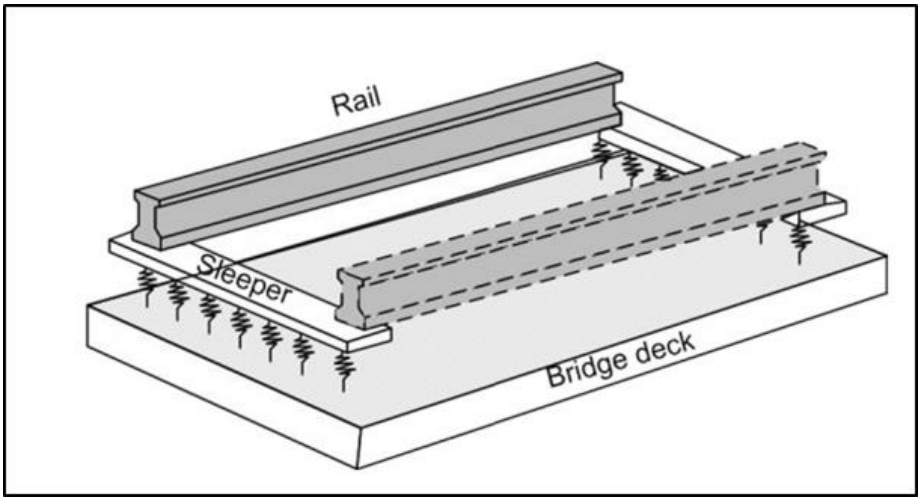

Figure 2.7. 3D Ballast Track Model (Manovachirasan et al., 2018)

2.4. Relative Displacement Criteria for Interaction

Movements of the rail relative to the deck are called relative displacement, as shown in Figure 2.8 and the stresses generated from this movement are identified as additional stresses on the rail (Low., 2015). Stresses generated from loads without relative displacement are not called additional stresses (Ramos et al., 2019). The term Track-Bridge interaction is all about the relative displacement between the bridge deck and the track crossing and running over it.

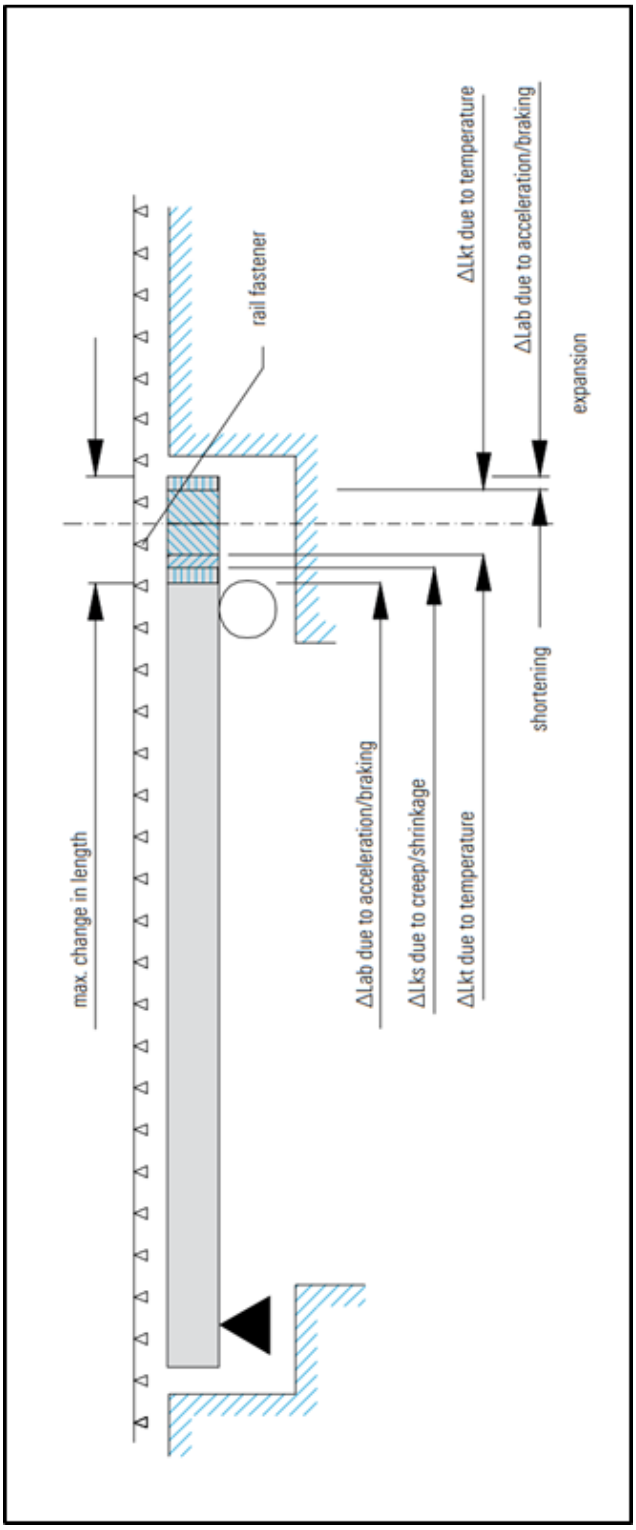

Figure 2.8. Bridge Movements Causing Relative Displacement

2.4.1.1. Loads with Relative Displacement for Interaction

Loads developing relative displacement between the track and the bridge deck are considered as loads with relative displacement induce additional stresses considered as additional stresses (Ramos et al., 2019). Vertical load from moving traffic movement is considered a load with relative displacement because the vertical loads will cause the bridge end to rotate, as shown in Figure 2.9 and this rotation will create a lateral movement on the top of the deck after the interaction with the rail. The stress resulted due to this displacement is considered as additional stress (Esveld., 1996).

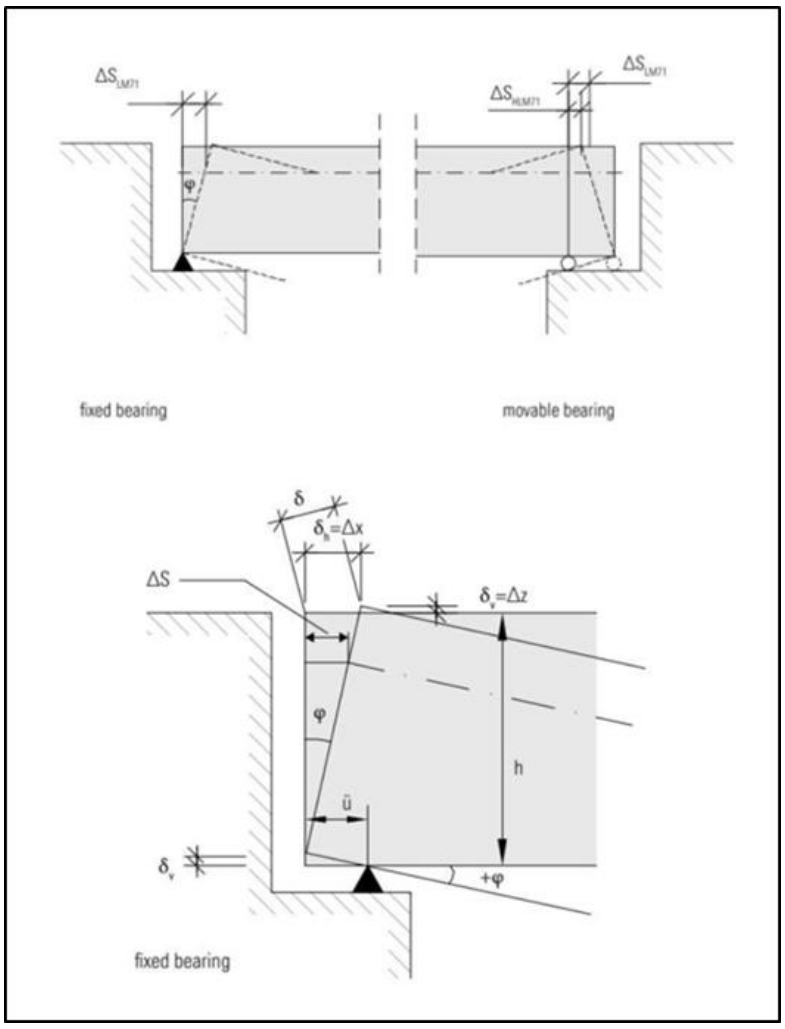

Figure 2.9. Bridge Top Deck Displacement Due to Vertical Loads

Braking/Traction forces applied on the CWR running over a bridge are considered as loads with relative displacement. The loads are transferred from the rails, fasteners, sleepers through ballast to the top of the bridge deck (Ruge and Birk., 2007). As the ballast will deform under the braking/acceleration force, relative displacement will be created between the track and the top of the deck, as shown in Figure 2.10. As a result, the stresses generated in the track due to braking/traction are considered as additional stresses.

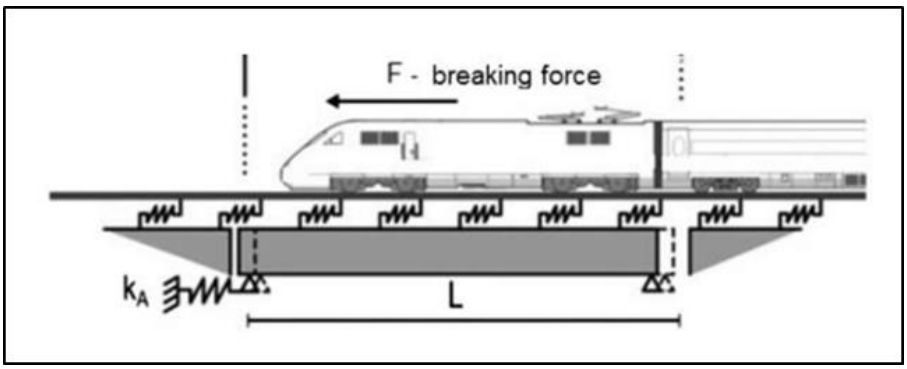

Figure 2.10. Braking Force with Relative Displacement

Thermal action and thermal loads tend to cause relative displacement between the track and the top of the bridge deck, as shown in Figure 2.11. There are two types of thermal actions. The first type is the thermal load on the continuous welded rail. If the rail is continuous on both sides of the bridge and there isn't any presence of a rail expansion device on the bridge, or close to the bridge, the thermal action won't generate any relative displacement and the thermal stress within the CWR is not considered as additional stress (UIC). If a rail thermal expansion device is used, there will be a relative displacement and the stresses within the CWR should be considered; nevertheless, the use of a rail expansion device is out of scoop of this study. The second type is the thermal load on the bridge deck structure. This type of load is different in nature from the previously presented loads. While the previous loads

follow the track-ballast-bridge deck path, the path for the thermal load is the opposite. The thermal load on bridge deck is directly influenced by the bridge structural system and supports condition. This effect is discussed in Chapter 5. The stresses within continuously welded rail generated from bridge movement under thermal load are considered as additional stresses.

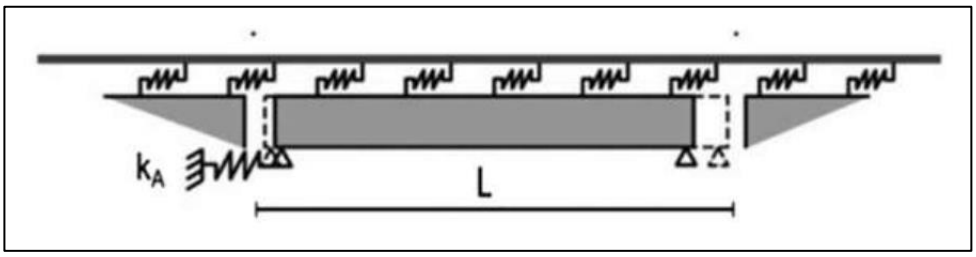

Figure 2.11. Bridge Movement under Thermal Action

2.4.1.2. Loads without Relative Displacement for Interaction

Thermal load is considered as a load producing relative displacement between the track and bridge deck. As mentioned before, the structural arrangement used for the bridge could affect the relative displacement case. If the bridge structure is restrained under the thermal action, there will be no relative displacement between the bridge deck and the track; thus, there is no additional stress. In fact, there will be no longer "maximum allowable expansion length". Temperature gradient has a very limited effect on the additional stresses and the relative displacement between the track and the bridge structure (Kumar and Upadhyay., 2012).

2.5. Development of Design Codes UIC and Eurocode

The axial loads in the continuous welded rail has raised a lot of concerns about how engineers should deal with CWR from the bridge designer point of view. Since the early 80's, the axial stresses and relative displacement and the combined response of the bridge with track have been a subject for researchers (Ramos et al., 2019). The

International Union of Railways initiated a set of researches and studies in the early 90's, especially in 1992. The research objective was to improve the knowledge of continuous welded rails (Esveld., 1998). ERRI (European Rail Research Institute) initiated studies and researches regarding the continuous welded rail and a number of committees are created like D-202 and D-213. The object of these committees is to provide more information about the behavior of CWR and how it will interact with structures. ERRI made researches and finalized its work with reports "Minutes of EERI D-213 committee meetings Strasbourg 1995", "Numerical simulations of track structure interaction effects due to thermal variation, braking forces and vertical loads case of single span bridges simplified one step model and complete multistep model 1996", "Design charts and formulate to evaluate track structure interaction effects for braking and temperature variations 1996", "Approximate analytical formulation of the track structure interaction due to end rotations revised version with extension to multiple track bridge and continuous deck bridges 1997", "Track bridge interactions in deck succession bridges summary diagrams 1997". These reports and other reports were the core of the UIC code the 774-3 R 2001 Track bridge Interaction recommendations for calculations. UIC code, among the other codes, is one of the most referred code for track bridge interaction. Most designers refer their designs to the UIC. The CEN Eurocode-1 EN 1991-2 Actions on structures – Part 2 Traffic loads on bridges with section-6 Rail traffic actions and other actions specifically for railway bridges is the basic design code for rail traffic on standard gauge within the European high-speed railway network. The Eurocode section-6.5.4 "Combined response of structure and track to variable actions" provides the main specifications for rail-structure interaction analysis. these specifications are identical to those from UIC with some modifications. Indeed, the Eurocode is based on UIC specifications. Eurocode defines the Track-Structure interaction as follows "where the rails are continuous over discontinuities in support to track (e.g. between a bridge structure and an embankment) the structure of the bridge (bridge deck, bearings and substructure) and the track (rails, ballast etc.) jointly resist the longitudinal actions due to traction or braking. Longitudinal actions are transmitted partly by the rails to the embankment

behind the abutment and partly by the bridge bearings and the substructure to the foundation. Where continuous rails restrain the free movement of the bridge deck, deformations of the bridge deck produce longitudinal forces in the rails and in fixed bridge bearings". UIC and Eurocode have limited the additional stress in continuously welded rail and the relative displacement and the total displacement of the deck according to the track configuration used for the design.

2.5.1. UIC and Eurocode Design Criteria for UIC-60 CWR

The following design criteria are only valid for continuously welded track UIC-CWR-60 (Rail 60 E1) type or complying with its geometrical and mechanical properties of UIC-60 are shown in Table 2.1 and Figure 2.12.

Table 2.1. *UIC-60 CWR Section Properties (EN 13674 – 1)*

Property	*Value*	*Unite*
Cross-sectional area	76.70	cm^2
Moment of inertia x-x	3038.30	cm^4
Moment of inertia y-y	512.30	cm^4
Section modulus top	333.60	cm^3
Section modulus bottom	375.50	cm^3
Section modulus y-y	68.30	cm^3
Indicative A	20.45	mm
Indicative B	52.05	mm
Bending axis-1	76.25	mm

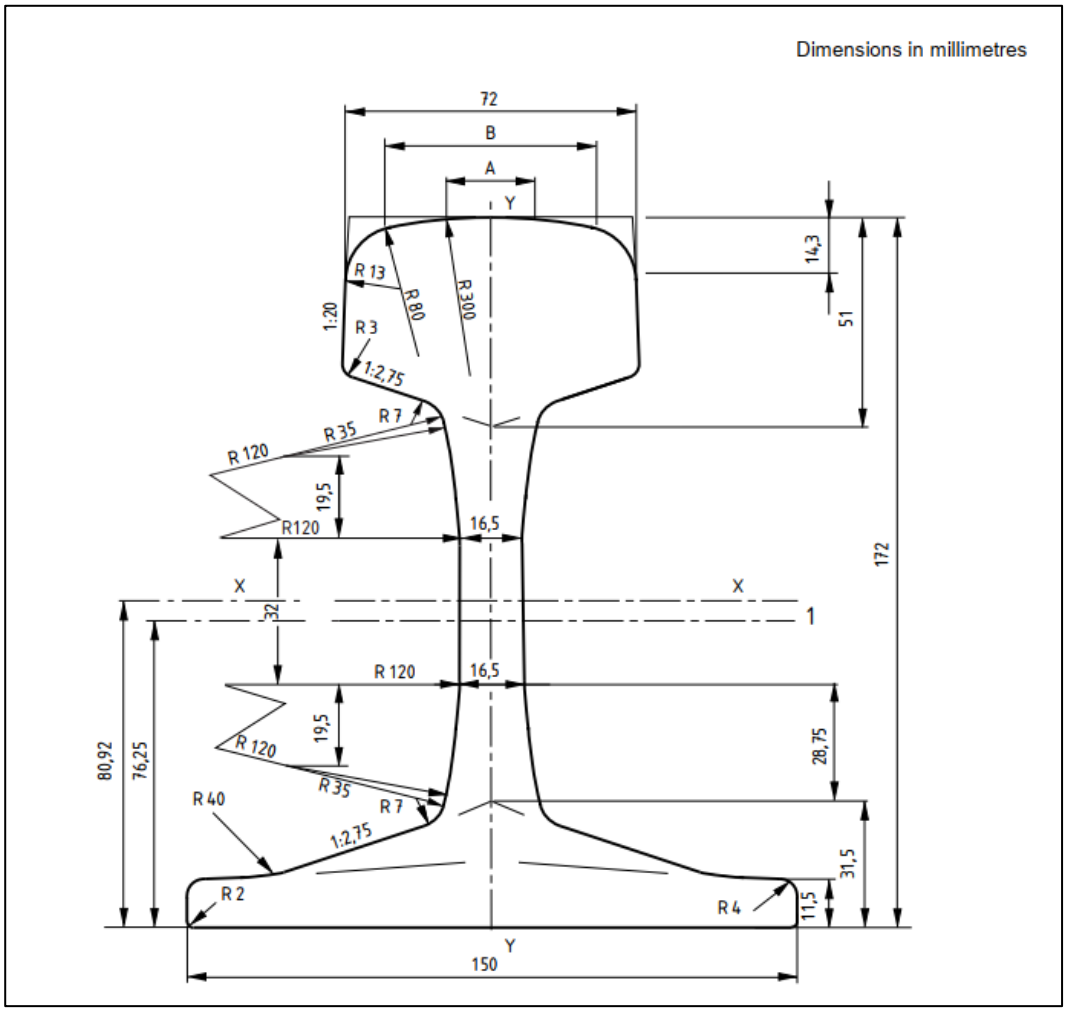

Figure 2.12. UIC-60 Rail Profile (EN 13674 – 1)

2.5.1.1. Design Criteria for UIC

UIC have limited the additional stresses in the continuously welded rail, total and relative displacement into specific values. UIC have limitations where these rules could be used. UIC specify UIC-60 CWR track type with at least 900 (MPa) strength steel grade and the minimum radius for curves is 1500 (m). The track should be fastened to concrete sleepers supported by a well consolidated ballast bed with at least 30 (cm) thickness. The stresses are defined as additional stresses on the continuous welded rail.

2.5.1.1.1. Compression Stress

UIC limits the maximum allowable additional compression stress in the rail for ballasted tracks to 72 (MPa). For directly fastened tracks and other track types UIC state that the limit should be specified by the local relevant authority.

2.5.1.1.2. Tension Stress

UIC limits the maximum allowable additional tension stress in the rail for ballasted track to 92 (MPa), For directly fastened tracks and other track types UIC state that the limit should be specified by the local relevant authority.

2.5.1.1.3. Relative Displacement

The maximum relative displacement between track and bridge deck or embankment allowed by UIC under the action of braking and traction forces is (4) mm.

2.5.1.1.4. Absolute Displacement

UIC allows the bridge deck to have an absolute horizontal displacement up to 5 (mm) under the action of braking and traction load.

2.5.1.1.5. Deck End Rotation

The UIC gives a maximum top deck horizontal displacement up to 8 (mm) resulted from bridge bending under vertical loads. Defined as LM-71 train load enhanced with dynamic factor Φ for bridge decks with one track.

2.5.1.1.6. Vertical Displacement

UIC has no specification regarding the top deck vertical displacement relative to the adjacent structure or embankment. UIC specifies that this displacement should be limited and relevant authorities could specify the maximum allowable value.

2.5.1.1.7. Maximum Bridge Expansion Length

UIC specifies the maximum allowable expansion length for a bridge without rail expansion device according to its type: for concrete and composite structures 90 (m) and for steel structures 60 (m).

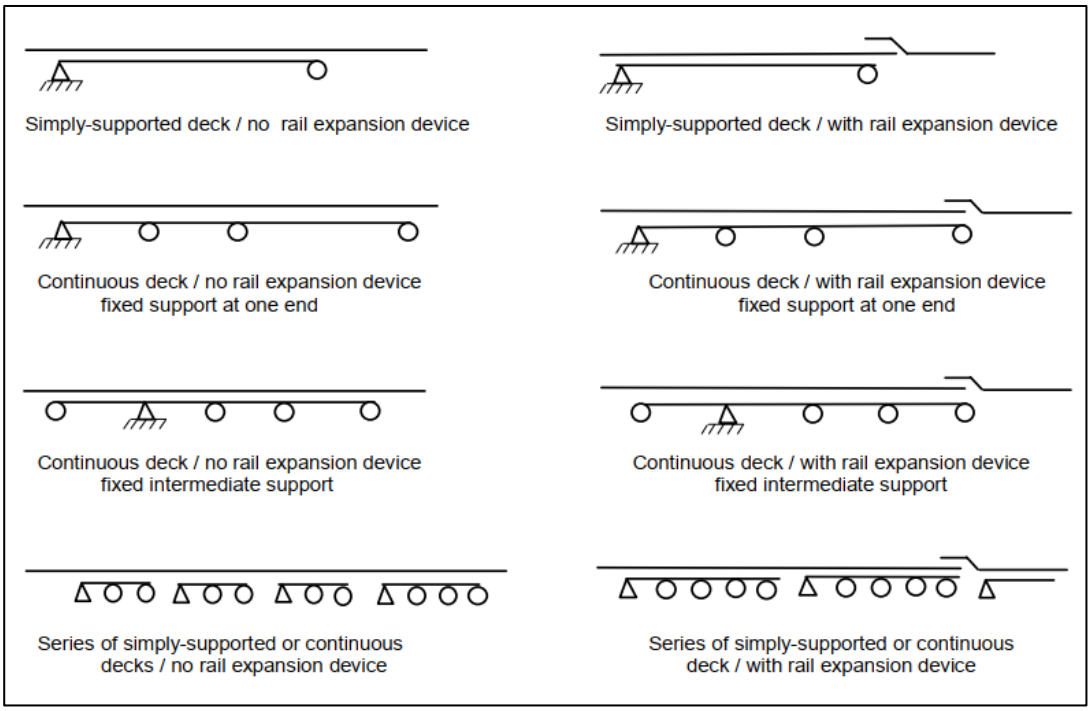

Figure 2.13. Expansion Length Examples (UIC)

2.5.1.1.8. Vertical Load

According to UIC, the vertical load which should be used for the track-structure interaction should be based on LM-71 enhanced with dynamic factor Φ for single track decks. UIC doesn't directly specify other loads or prevent the use of any other vertical load.

2.5.1.1.9. Braking Load

Per UIC, the braking force should be based on a uniformly distributed horizontal forces corresponding to a vertical load. The horizontal loads are 20 (kN/m) for load model LM-71 and SW/0 with a maximum total force not more than 6000 kN. The force for load model SW/2 is 35 (kN/m). These loads don't have to be enhanced by the dynamic factor Φ. For other traffic, the braking load could be considered as ¼ of the axle load of the concerned vehicle, but not exceeding the maximum total force limit.

2.5.1.1.10. Traction/Acceleration Load

UIC considers the acceleration load as uniformly distributed horizontal force corresponding with vertical load application to the track. The load is equal to 33 (kN/m) with a maximum total force equal to 1000 (kN). This load corresponds to load model LM-71 and load model SW/0. These loads don't have to be enhanced by the dynamic factor Φ. For other traffic, the acceleration load could be considered as ¼ of the axle load of the concerned vehicle but not exceeding the maximum total force limit.

2.5.1.1.11. Thermal Loads

According to UIC, there are two different thermal loads; thermal load on the bridge deck and thermal load on the rails. A thermal load on the rails should only be considered if a rail expansion device is used. The thermal variation should be applied to the reference temperature defined as the temperature when the rails are fixed into the bridge deck. The maximum variation applied to the rails should not deviate by

more than ± 50º C and the temperature difference between the deck and the rails should not exceed ± 20º C. Thermal load on the bridge deck should be considered not more than ± 35º C variation from the reference temperature. In case there isn't any rail thermal expansion device used on the bridge or the rail is continuous on the bridge ends, the thermal load is only considered on the bridge deck.

2.5.1.2. Design Criteria for Eurocode

Eurocode, like UIC, has limitations on the additional compression and tension stress on the continuous welded rail and the relative and absolute displacements. Eurocode defines conditions where these limits could be applied for design. The conditions are as follows: the track used should be UIC-60 or track complying with it, the steel grade used should at least provide 900 (MPa) tensile strength, the track should be straight or the minimum used radius should not be less than 1500 (m), the ballast under sleepers should be well consolidated with at least 30 (cm) thickness, the track should be fastened into heavy concrete sleepers with maximum spacing not more than 65 (cm).

2.5.1.2.1. Compression Stress

According to Eurocode, the maximum allowable additional compression stress in rail due to variable actions for ballasted tracks is 72 (MPa). For directly fastened tracks and for other types, the limit should be specified by the National Annex.

2.5.1.2.2. Tension Stress

The maximum allowable additional tension stress in the rail due variable actions for ballasted track is 92 (MPa). For direct fastened tracks and for other types, the limit should be specified by the National Annex.

2.5.1.2.3. Relative Displacement

According to Eurocode, the maximum relative displacement between the bridge deck end and adjacent abutment, or between two consecutive bridge decks, as shown in Figure 2.14, allowed by Eurocode under the action of braking and traction forces is 5 (mm).

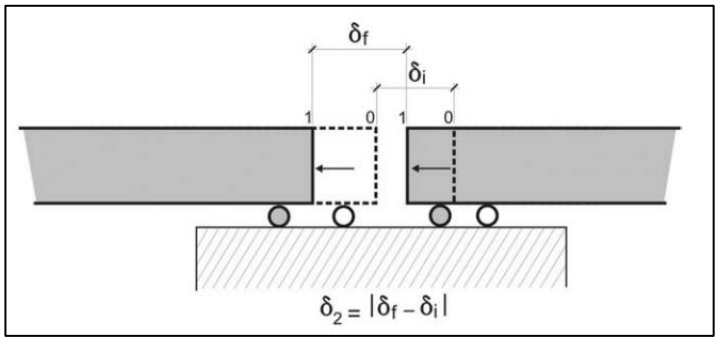

Figure 2.14. Relative Displacement (Goicolea., 2008)

2.5.1.2.4. Absolute Displacement

Eurocode does not have a direct specification for the absolute displacement of the bridge deck. Instead, Eurocode specifies a limit for the maximum deformation of the structure -which could be counted for the absolute displacement-, the maximum allowable structure deformation under the action of braking and traction is 5 (mm)

2.5.1.2.5. Deck End Rotation

Eurocode allows for a maximum top deck horizontal displacement up to 8 (mm) resulted from bridge bending under vertical loads, as shown in Figure 2.15. The vertical loads defined as LM-71 train load or SW/0 where required, the load could be enhanced with dynamic factor Φ or not, LM-71 load shall be multiplied by α factor as specified by Eurocode section 6.3.2 “actions shall be multiplied by α factor: combined response of structure and track to variable actions”.

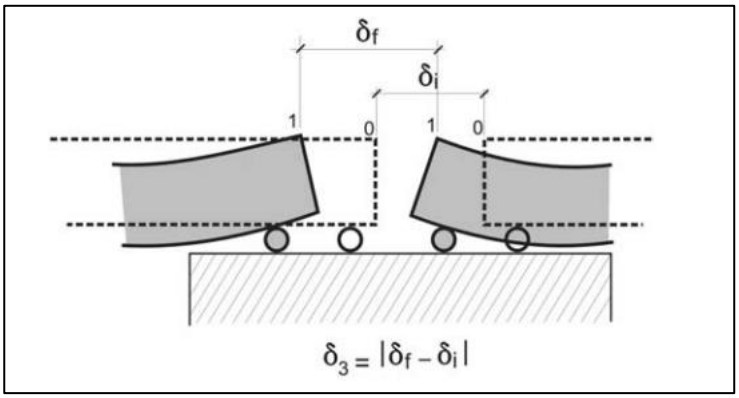

Figure 2.15. Horizontal Displacement due to Vertical Loads (Goicolea., 2008)

2.5.1.2.6. Vertical Displacement

Eurocode has limited the upper deck displacement relative to the adjacent abutment or the next bridge deck as shown in Figure 2.16 due to variable actions according to the maximum line speed

- Maximum line speed up to 160 (km/hr) allowable displacement 3 (mm)
- Maximum line speed over 160 (km/hr) allowable displacement 2 (mm)

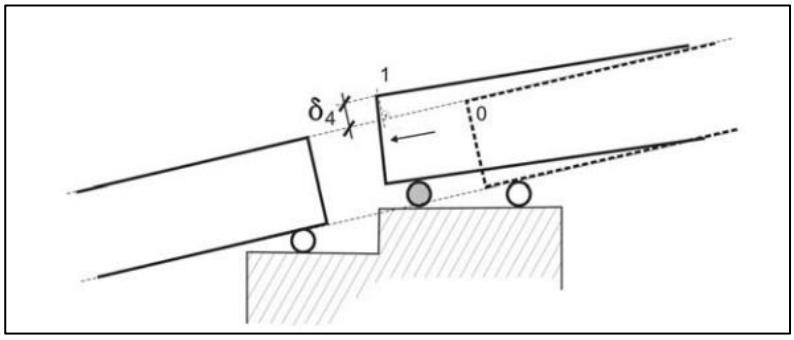

Figure 2.16. Relative Vertical Displacement (Goicolea., 2008)

2.5.1.2.7. Maximum Bridge Expansion Length

Eurocode doesn't specify a maximum allowable expansion length for a bridge without a rail expansion device. Instead, Eurocode within Annex G specifies a limit to the

maximum expansion length without rail expansion device according to the superstructure type, for concrete and composite structures 90 (m) and for steel structures 60 (m).

2.5.1.2.8. Vertical Loads

According to Eurocode, the vertical loads to be considered for the interaction are load model LM-71 shown in Figure 2.17 multiplied by α factor, SW/0 and SW/2 shown in Figure 2.18 where required, these loads my enhanced with Φ dynamic factor shown in Figure 2.19 or not. An alpha factor is defined in section 6.3.2 in Eurocode, the value of α factor 0.75 – 0.83 - 0.91 – 1 – 1.1 – 1.21 – 1.33 1.46. Some countries use a value not listed above e.g. Turkey α = 1.4.

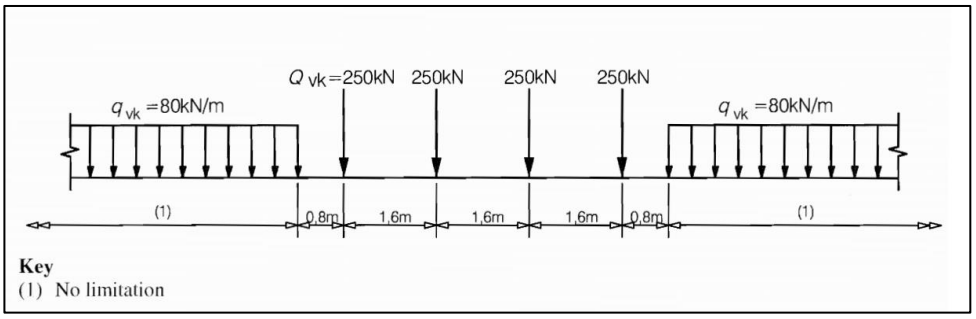

Figure 2.17. Load Model -71 (Eurocode)

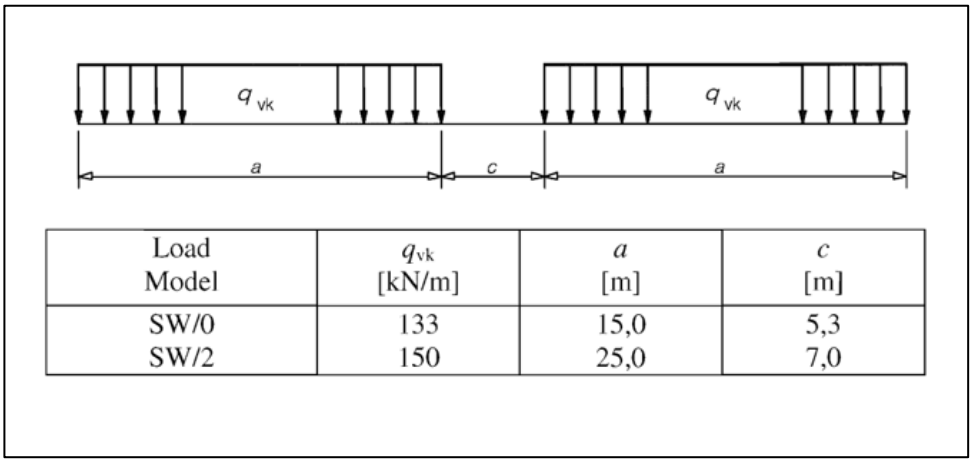

Load Model	q_{vk} [kN/m]	a [m]	c [m]
SW/0	133	15,0	5,3
SW/2	150	25,0	7,0

Figure 2.18. Load Model SW/0 and SW/2 (Eurocode)

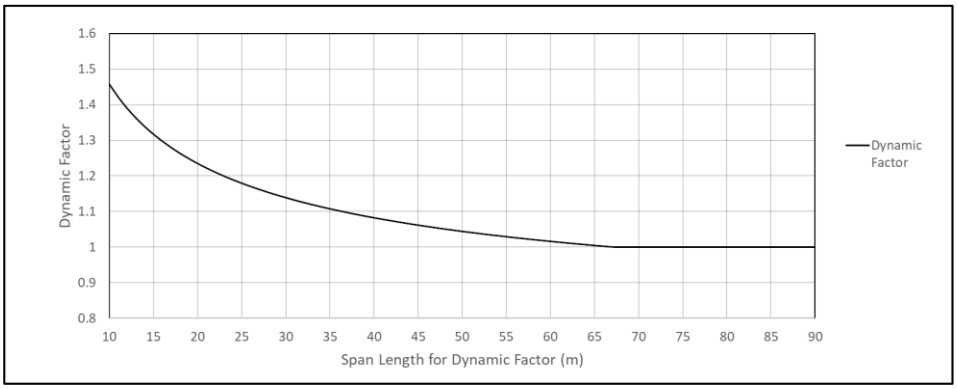

Figure 2.19. Dynamic Factor for Track with Standard Maintenance (Eurocode)

2.5.1.2.9. Braking Loads

According to Eurocode, the braking force should be based on a uniformly distributed horizontal forces corresponding with vertical load, the loads are 20 (kN/m) for load model LM-71 and SW/0 with a maximum total force not more than 6000 kN, the force for load model SW/2 is 35 (kN/m). These loads don't have to be enhanced by the dynamic factor Φ, but it should be multiplied by α factor Eurocode section (6.5.3), for other traffic the braking load could be considered as ¼ of the axle load of the concerned vehicle, but not exceeding the maximum total force limit.

2.5.1.2.10. Traction Load

According to Eurocode, the traction load should be considered as uniformly distributed horizontal force corresponding with vertical load application to the track. The load is equal to 33 (kN/m) with maximum total force equal to 1000 (kN). This load corresponds to load model LM-71 and load model SW/0 and SW/2. These loads don't have to be enhanced by the dynamic factor Φ, but it should be multiplied by α factor.

2.5.1.2.11. Thermal Load

According to Eurocode, thermal load on the bridge deck shall be considered for simplicity as ± 35º C variation from the reference temperature. Other values may be specified by the National Annex.

2.5.2. Additional Compression Stress

The track stresses are calculated according to admissible stresses theory, not for the ultimate limit state theory. The maximum allowable stress is different in design codes e.g. $\boldsymbol{\sigma}_{\text{allow}}$ = 600 (MPa) in Czechian standard (CSN 73 6203) and $\boldsymbol{\sigma}_{\text{allow}}$ = 470 (MPa) in German standards (DIN-Fb 101) as shown in Figure 2.21. These limits are for tensile stress. The case is different for compression. The stresses are limited at 290 (MPa), as shown in Figure 2.20 due to buckling (Chatkeo., 1985). The rail has already stresses resulted from traffic. Bad track condition could increase the stresses and bend in a curve, production, flat wheel condition, the additional stresses resulted from track-structure interaction are additive to the afore-mentioned stresses. Thus, the margins are relatively small. Also, the buckling temperature differences due to site conditions and the horizontal braking/traction forces will influence the buckling force, and the lateral forces resulted from the train movement. The maximum allowable additional compression stress was locked on $\boldsymbol{\sigma}_{\text{allow}}$ = 72 (MPa), this limit could be increased in ballast less tracks to 92 (MPa) because ballast-less tracks have much more advantageous behavior from the ballast bed track toward distortion (DIN-Fb 101). It should be noted that buckling is always related to temperature rise. In a hot summer day, to prevent the buckling of CWR, the maximum allowable expansion length is limited (Fryba., 1996).

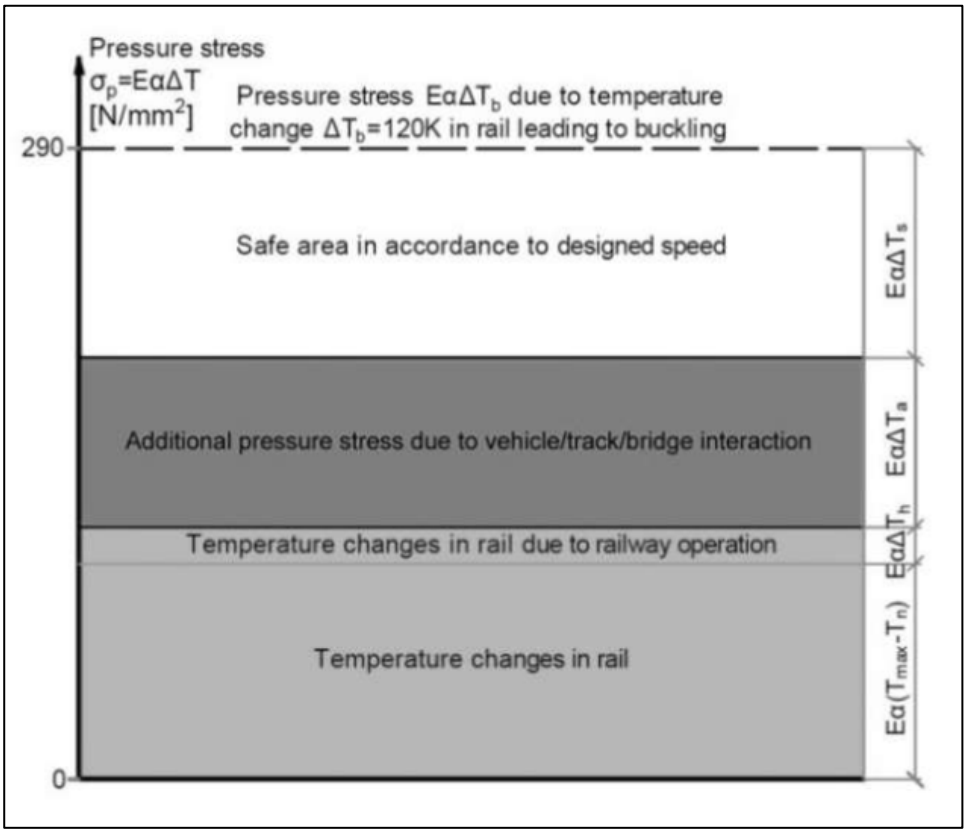

Figure 2.20. Compressive Stress in CWR UIC-60 due to Temperature (Mirković et al., 2018)

2.5.3. Additional Tensile Stress

The additional tensile stress in the continuous welded track is directly related to the fracture of the track. Cold weather will contribute to the fracture of the rail. Unfortunately, the steel resistance to fracture is lower when the temperature drops. The safety of high-speed railway traffic should be guaranteed even when the continuous welded rail cracks on the bridge as the gap has the most tendency to occur during low-temperature conditions (Fryba., 1996). The admissible width of the gap varies between 30 and 50 (mm), and this gap could result in the drop of the wheel center by 0.78 (mm), and impact will occur during the movement of the train. However, the impact doesn't depend on the gap width. Most design criteria depend on a maximum gap width less than 50 (mm) (Freyba., 1996). The fracture depends on all

factors the maximum expansion length and other criteria, fracture initiated from small transverse cracks in the rail which develops due to fatigue and starts due to sudden application of tensile stress, which could be resulted from wheel bearing on the contact area between the and the track, bending moment caused by the rail spans between the sleepers and that's why the design codes have limitations on the sleepers spacing, bending moment generated due to bending moments and shears across the bridge deck joint generated due to rotation, the axial stress generated from bridge rotation due to the rail is offset from the deck center rotation and that's why the design codes limit the end deck rotations to limit the additional stresses from the mentioned actions, and lastly, the axial stress generated due to braking and traction force due to bridge deck flexibility (Low., 2015).

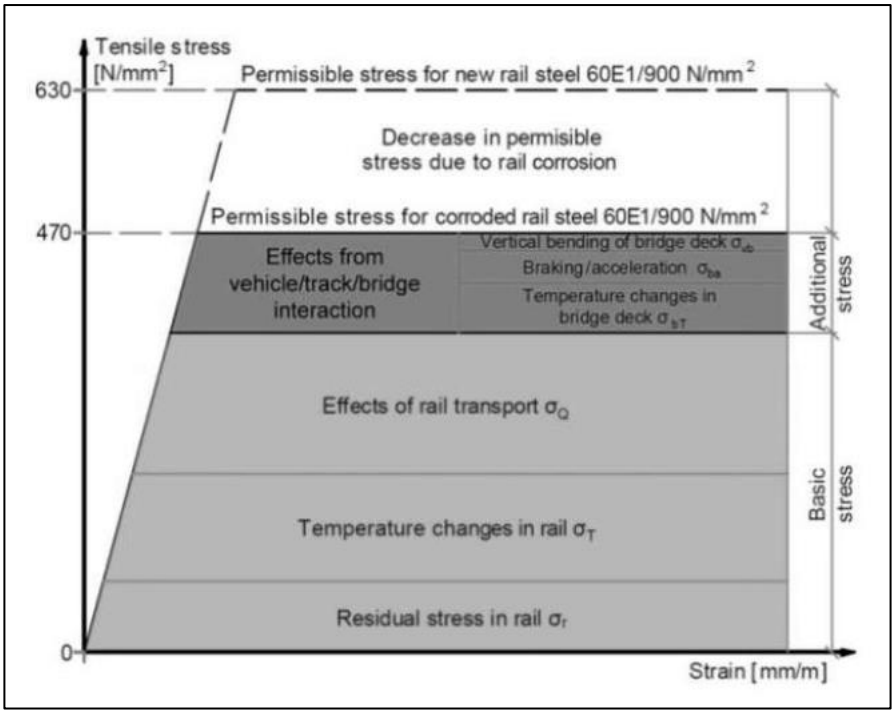

Figure 2.21. Tensile Stress in CWR (Mirković et al., 2018)

2.5.4. Absolute and Relative Displacement

The limits for the absolute and relative displacement under braking and traction are placed to prevent the excessive deconsolidation of the ballast bed. If deconsolidation occurs, it will create a stability problem and the limits used for design may not be valid anymore. Another approach is that limiting the displacement will limit the additional stresses indirectly. Top deck displacement under vertical loads is limited to guarantee the ballast stability. The displacement due to temperature is limited by the maximum expansion length. This limitation has two main components. It should be limited to avoid the rupture of the bolt joining the rail to the sleeper whether the system used is ballasted bed or direct fastening (Fryba., 1996). The other criterion is the track wearing. Bridge will expand and contract daily according to temperature, this will result in a daily movement of the track, and this movement will cause wear to the track. Limiting the maximum expansion length may limit the daily movement because there is another factor which it is the daily temperature changes, UIC consider 10-15 (mm) of daily movement and UIC directly specify even if the stresses and displacements are satisfied if the daily change of length due to temperature is exceeding 10-15 (mm) according to the level of maintenance, a rail thermal expansion device must be used.

2.5.5. Track Configuration

Track configuration is considered as the location of the rail relative to the natural axis, location of the rail thermal expansion device and the used coupling system. Mainly, there are two types of coupling; ballasted systems and non-ballasted system. Non-ballasted system is out of scoop of this study, yet ballasted system configuration will be discussed. Typically, ballast has a longitudinal stiffness and this stiffness is affected by the state of vertical loads. In design codes, UIC and Eurocode, the stiffness according to the state of vertical load is defined. In fact, the non-linearity in Track-Structure interaction is due to the ballast non-linear behavior. The ballast stiffness will change according to the state of vertical load, changes in the coupling force is

discussed in detail in (Ruge and Birk., 2007), (Widarda., 2009). Ballast behavior according to Eurocode is defined in section (6.5.4.4). The values used for yielding resistance of ballast are defined in the National Annex. The behavior of ballast is complex, and for simplicity, UIC and Eurocode provided a simple behavior of ballast as shown in Figure 2.22 and Figure 2.23, which considered being accurate.

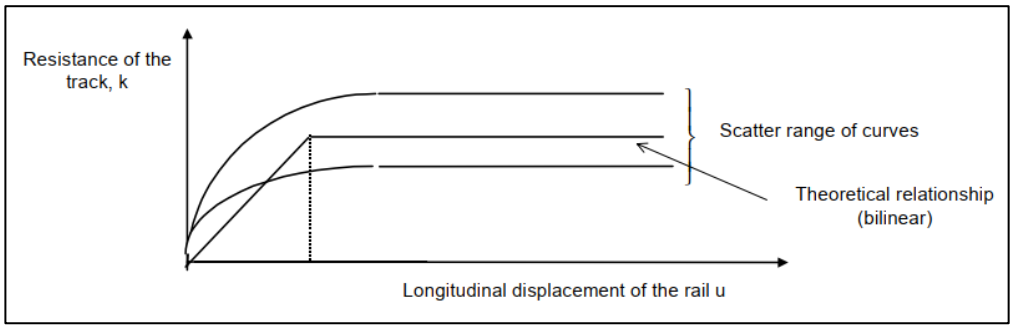

Figure 2.22. Longitudinal Resistance of Track on Ballast Bed (UIC)

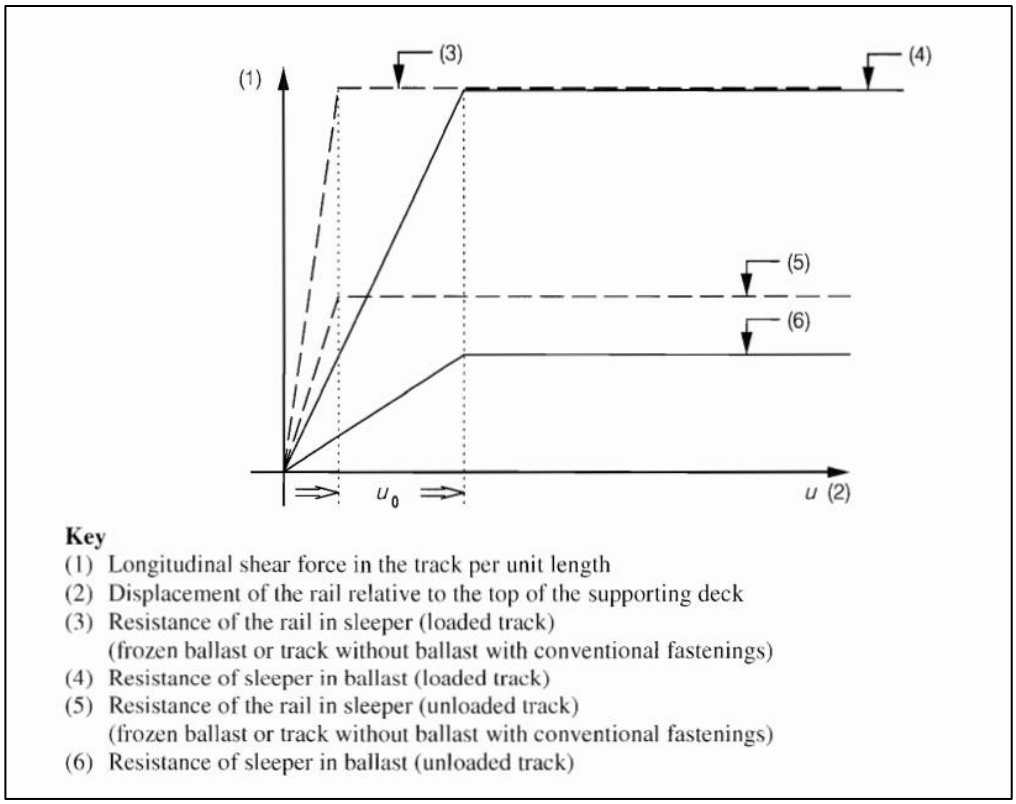

Figure 2.23. Resistance of Track per Unite Length as a Function of Longitudinal Displacement of the Track (Eurocode)

The relation between the resistance of the ballast calculated per unite length related to the longitudinal displacement of the track in UIC and Eurocode are identical to each other. The relation is bilinear with yielding threshold equal to 2 (mm) for ballasted tracks as shown in Table 2.2 two functions are given, one for the loaded track case, and the other for the unloaded track case. Unloaded track case is for thermal loads and loaded track case is for braking/acceleration and vertical loads.

Table 2.2. *Track Longitudinal Resistance Force Values per meter per Track (UIC)*

Case	*Resistance (kN)*	*Yielding (mm)*
Unloaded	20	2
Loaded	60	2

The above-mentioned values could vary according to local authorities. For the evaluation process of this study, the aforementioned values are used.

2.6. Interaction in Literature

Track-Bridge Interaction has been discussed a lot within the literature. There are many papers published regarding the bridge design practice for high-speed railway with CWR. Ballast stiffness is reviewed in many publications, and some structural health monitoring applications have been applied to some high-speed railway bridges to monitor the bridge movement and behavior under the variable loads action.

2.6.1. Ballast Stiffness in Horizontal Direction

The coupling between the track and the bridge deck is achieved by the ballast filling the gap between the track and the bridge deck. The ballast is used to provide vertical lateral and longitudinal support to track, and it is very good material for drainage and cost-effective. Ballast behavior has been studied in detail by the ERRI committee, and the result was the bilinear behavior used in Eurocode and UIC design codes, some tests performed by researchers concluded with the same results, ballast lateral

resistance increases by increasing the vertical loads and this holds true because the vertical forces will increase the friction between the ballast particles. (Min and Yun., 2016) performed a test on ballast bed with sleepers and CWR. The results were close to the results used in the design codes, as shown in Figure 2.24 and Figure 2.25.

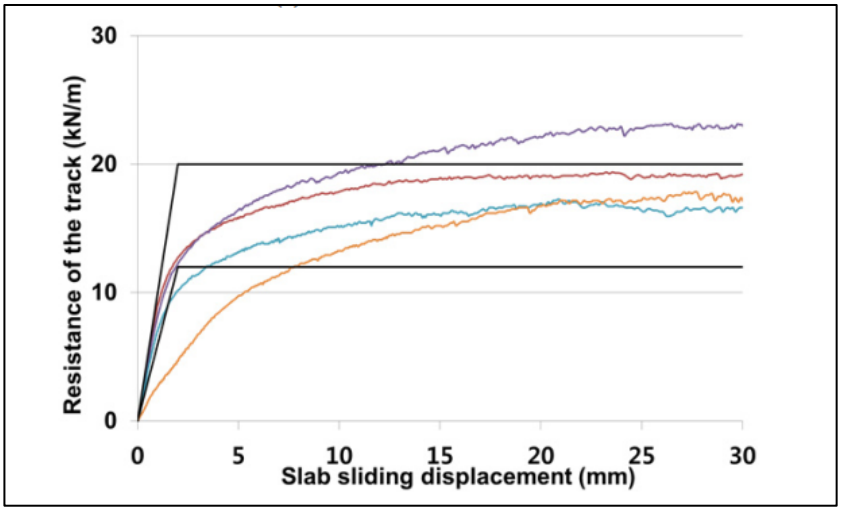

Figure 2.24. Un-loaded Ballast Test (Min and Yun., 2016)

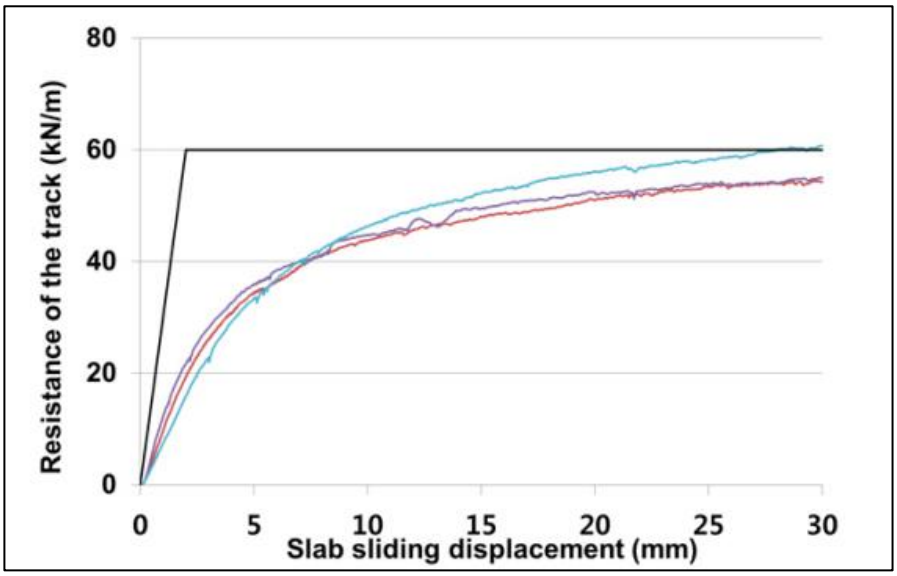

Figure 2.25. Loaded Ballast Test (Min and Yun., 2016)

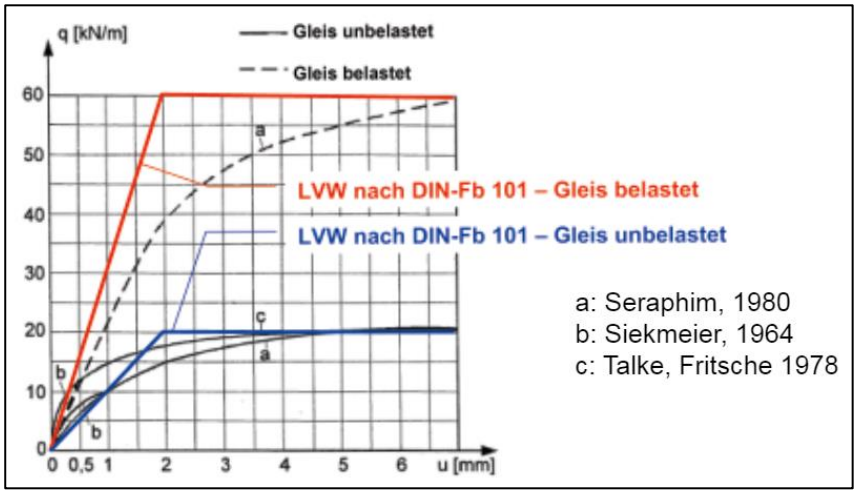

Figure 2.26. Ballast Resistance loaded, Unloaded (Freystein and Geibler., 2013)

(Wenner et al., 2016), in the state-of-the-art paper, reviewed the ballast resistance, as shown in Figure 2.26. Figure 2.27 shows that the ballast from tests agrees with stiffness proposed by the design codes.

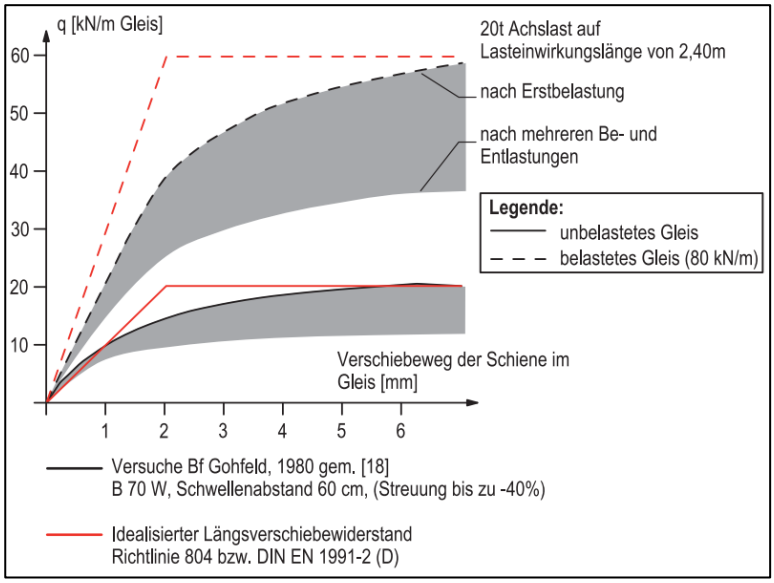

Figure 2.27. Ballast Resistance (Wenner et al., 2016)

2.6.2. Structural Health Monitoring Applications

The investigation of the longitudinal stresses generated in the continuous welded rail has been discussed a lot over the past years. Most researches are based on the UIC and Eurocode recommendation. These codes use a bilinear stiffness law for the ballast resistance under longitudinal deformation. Many structural health monitoring applications have been applied to the bridge to monitor and to validate the bridge behavior under thermal and variable actions. (Strauss et al., 2018) performed structural health monitoring on L110 bridge in Austria, shown in Figure 2.28. The objective of their work is to establish a monitoring-based nonlinear finite element modeling using advanced beam spring interaction laws. The analysis results had been compared with results from another analysis (Widarda., 2009), and the results from the finite element model were found to be in good agreement with results from the monitoring of the bridge, as shown in Figure 2.29 and Figure 2.30.

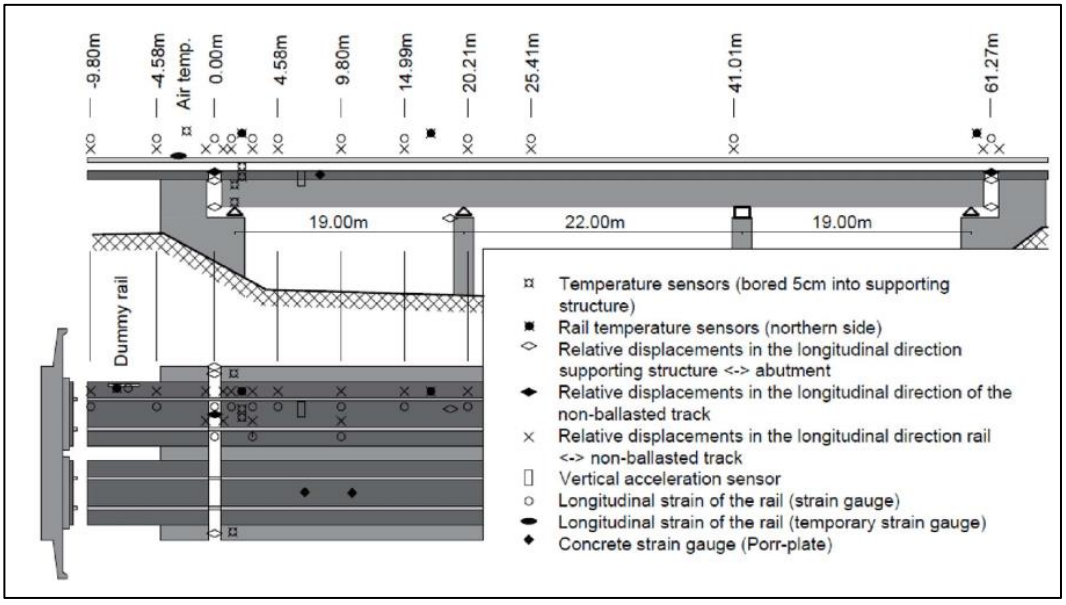

Figure 2.28. Static Scheme and the Monitoring System (Strauss et al., 2018)

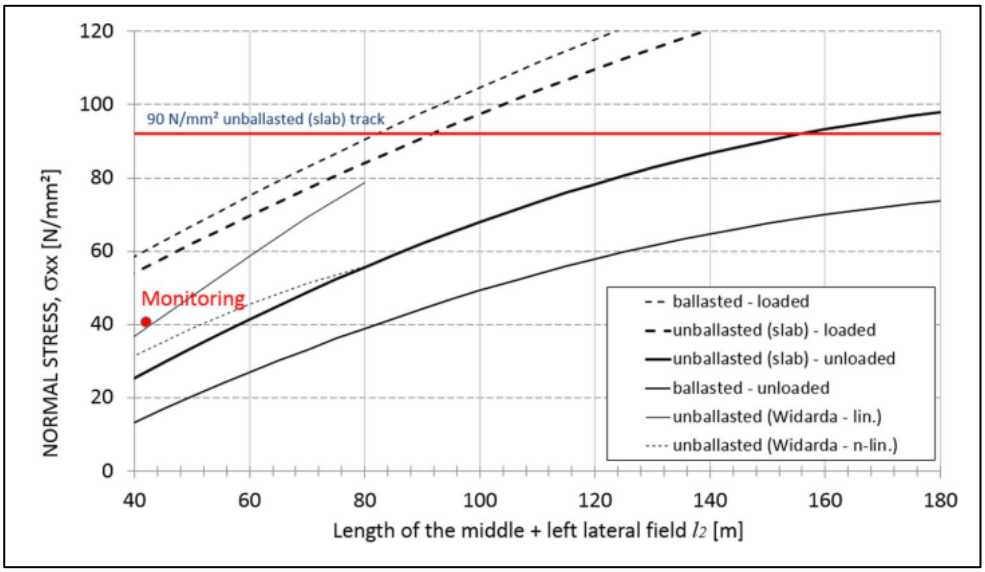

Figure 2.29. Axial Stress Under Temperature Drop for Variable length (Strauss et al., 2018)

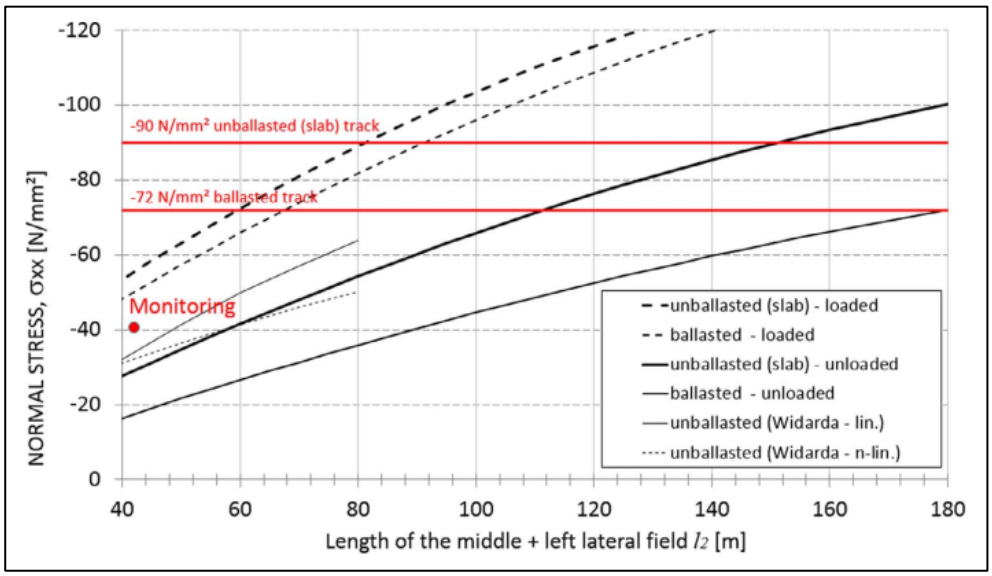

Figure 2.30. Axial Stress Under Temperature Rise for Variable length (Strauss et al., 2018)

(Strauss et al., 2018) concluded their results as follows: the stress calculated according to design codes are considered very conservative due to heating and a cooling of a bridge structure of 30º C each is not a real situation, possible maximum expansion

length for bridge could be extended to 150 (m), the situation where traffic loads and thermal warming happen at the same time is not probable. (Ryjáček and Vokáč., 2014) Performed long term monitoring of Kolin bridge in the Czech Republic shown in Figure 2.31. The bridge is a newly constructed railway bridge, and the monitoring devices were mounted at the rail fixation time. Mathematical models were constructed, and the results were compared from the monitoring results, (Ryjáček and Vokáč., 2014) proposed a new function for the longitudinal resistance of ballast bed. The bridge was a steel truss bridge with four spans. The structural system is simply supported beam. The structural arrangement is as follows: 32 + 49 + 28 + 20 (m). The bridge due to clearance problems has ballast bed track configuration followed by direct fastening track configuration. The bridge was monitored for a period just more than one year. The hot summer and the cold winter temperatures were covered in the monitoring period and they found the maximum change in CWR stress equal to 270 (MPa).

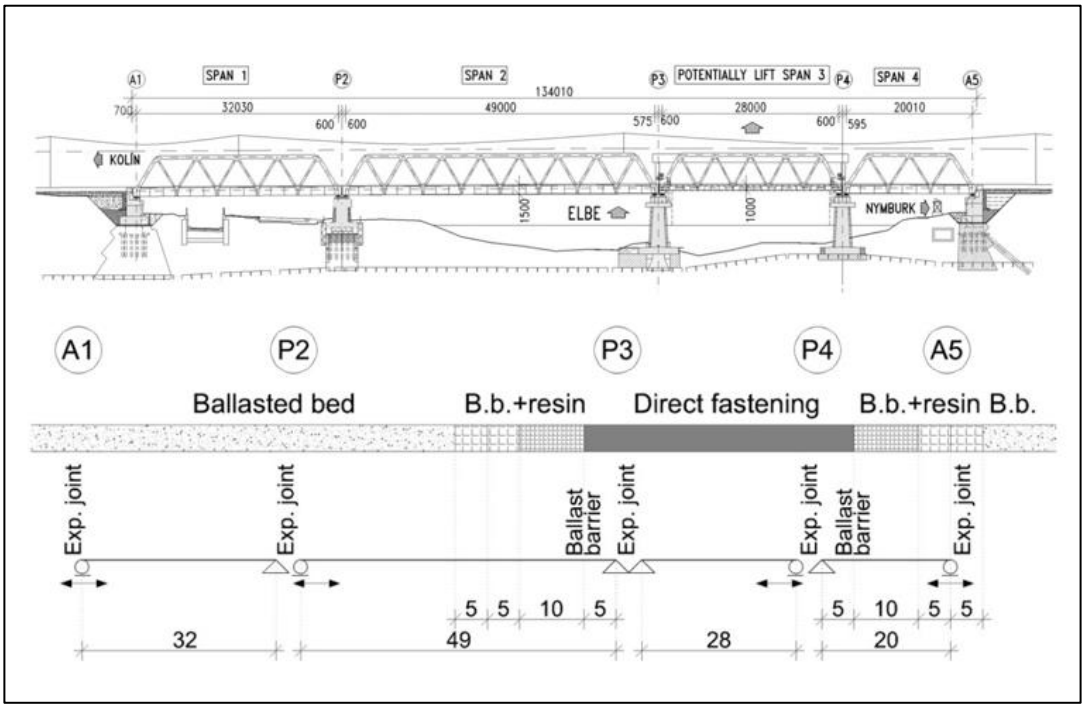

Figure 2.31. Kolin Bridge Configuration (Ryjáček and Vokáč, 2014)

The thermal expansion coefficient resulted from the monitoring application is very different from the results obtained by another application as (Fryba., 1996). The author concludes this difference could be as the result of the structure type, and the main steel parts are exposed directly to the sun. The study found that ballast stiffness is temperature depended. This cause is dealt within Eurocode considering frozen ballast. FEM models were created with different ballast resistance value, they reported that ballast resistance close to 30 (kN/m) are the closest to the monitored results with yielding displacement at 2.5 (mm), the most correlated ballast bed stiffens is 18 (kN/mm/m), as shown in Figure 2.32 and Figure 2.33.

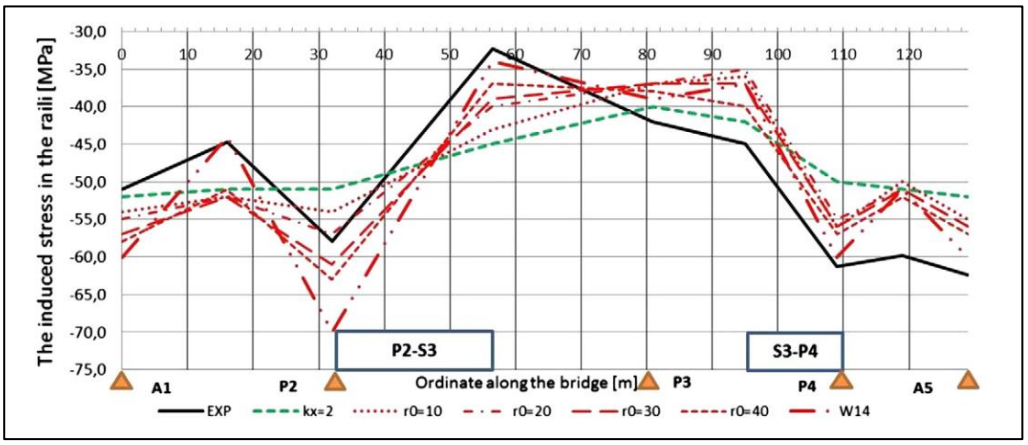

Figure 2.32. Rail Stress Numerical and Monitoring Temperature Rise -13 to 6 ºC (Ryjáček and Vokáč., 2014)

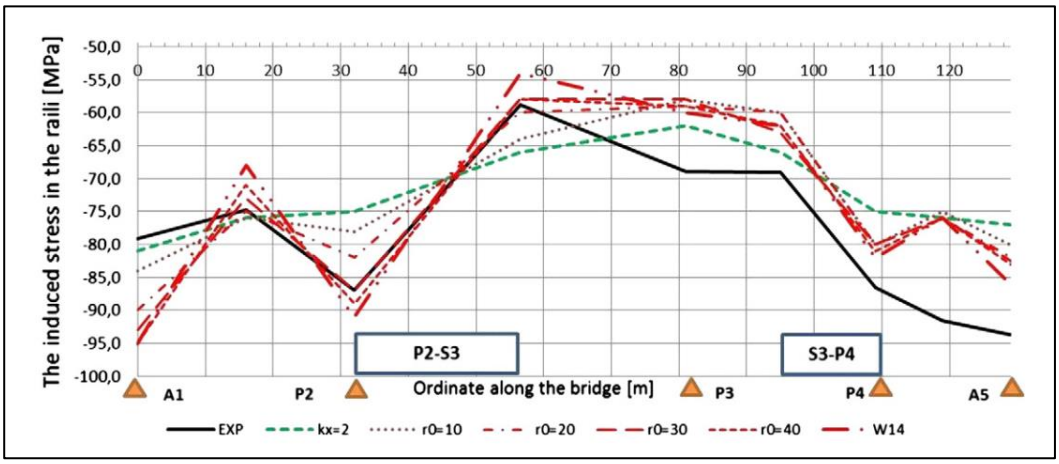

Figure 2.33. Rail Stress Numerical and Monitoring Temperature Rise 20 to 50 ºC (Ryjáček and Vokáč., 2014)

The author concluded that the ballast resistance found by the monitoring application is higher than the ballast resistance specified in Eurocode or UIC, the thermal expansion coefficient is higher than the coefficient reported in previous studies like (Fryba., 1996), but still lower than the value specified by Eurocode.

CHAPTER 3

NUMERICAL FEM MODELING OF TRACK BRIDGE INTERACTION

3.1. Modeling Approach to Track-Bridge Interaction in Computer Programs

Computer software could be used for simulating the track-structure interaction phenomena. Since the nature of the analysis is non-linear, the amount of time required for the computations is very long, and the computations itself are very complex; thus, computer software could reduce the time required for the analysis. The non-linear nature of the analysis is due to the non-linear behavior of the ballast mentioned in the previous chapter. The rails are laid on a ballast bed where the ballast has a predefined horizontal stiffness. After a specified amount of lateral displacement, the ballast yields and it behaves in a perfectly plastic behavior. The ballast behavior has been discussed in the previous chapter. Also, the ballast stiffness changes according to the ballast state of the vertical load. The vertical load could change the ballast stiffness. In fact, it will increase the ballast lateral stiffness and the yielding resistance threshold.

3.1.1. Bridge Modeling in FEM Software

The numerical modelling of the track-structure interaction has discussed widely in a lot of publications. There are many different approaches for the modeling techniques in the literature, some of which are more focused on the temperature effect on the interaction (Kumar and Upadhyay., 2012), where they investigated the effect of temperature gradient on the track structure interaction phenomena. (Liu W-S et al., 2013) discussed the temperature effect on rail structure interaction for CWR laid on X-style arch bridge.

(Chen et al., 2013) used a special modeling technique to investigate the temperature variation effect on the CWR laid on cable-stayed bridges, as shown in Figure 3.2.

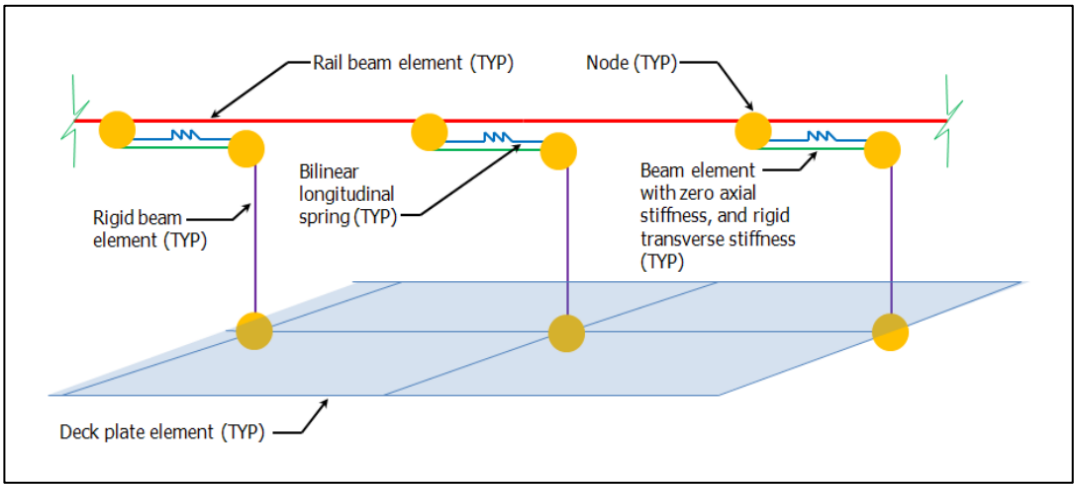

Figure 3.1. FEM model by (Baxter et al 2012)

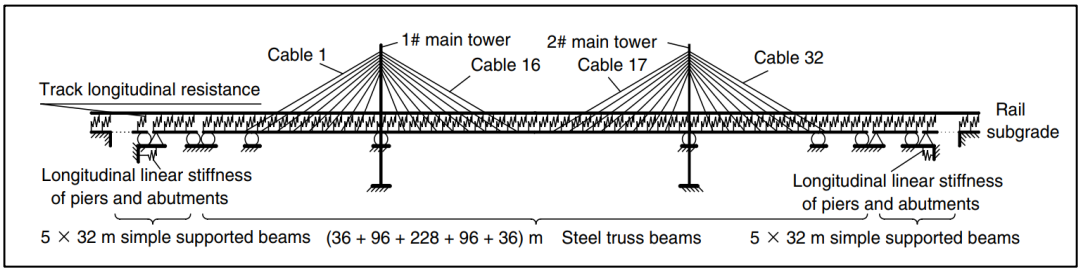

Figure 3.2. FEM model of cable-stayed bridge (Chen et al., 2013)

There are many publications focusing more on the vertical load effect on the track-bridge interaction and the braking and acceleration effect like (Baxter et al., 2012) as shown in Figure 3.1 and (Yan et al., 2012) The later used a simple model for a bridge carrying two tracks by modeling each rail of the tracks by a beam element as shown in Figure 3.4. (Dai and Yan., 2012) used a model assuming that the horizontal and vertical displacement did not occur between track and bridge, and they used this model to investigate the longitudinal forces of continuously welded track on high-speed railway cable-stayed bridge. (Okelo et al., 2011) investigated a model for the effect on track-structure interaction on elevated skewed steel bridge, as shown in Figure 3.3.

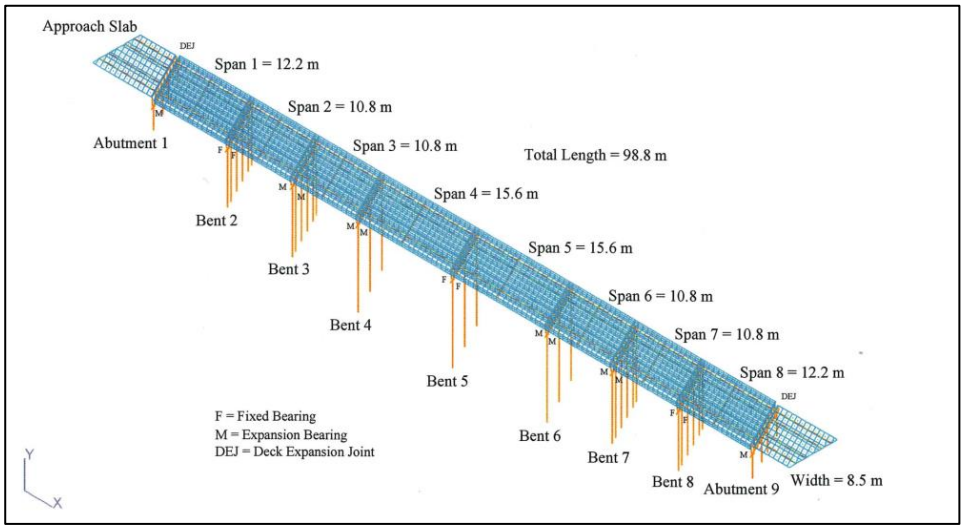

Figure 3.3. FEM model by (Okelo et al., 2011) for elevated steel bridge

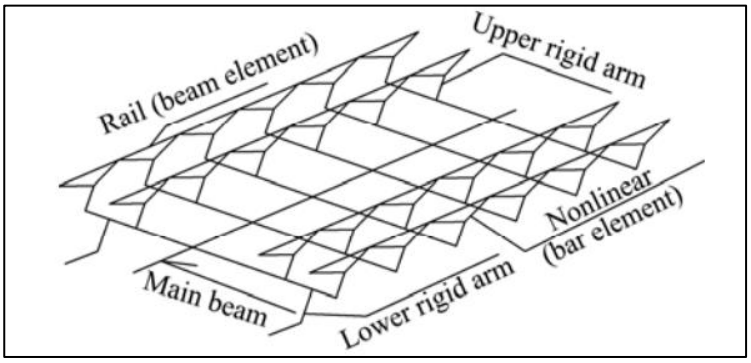

Figure 3.4. Two track carrying bridge FEM model by (Yan et al., 2012)

(Manovachirasan et al., 2018) performed a comparison between 2D and 3D modeling of track- structure interaction for a bridge structure and they concluded that stresses from 2D models were slightly greater than stresses from 3D models as shown in Figure 3.5 and 3D modeling is only needed when the CWR buckling is under investigation.

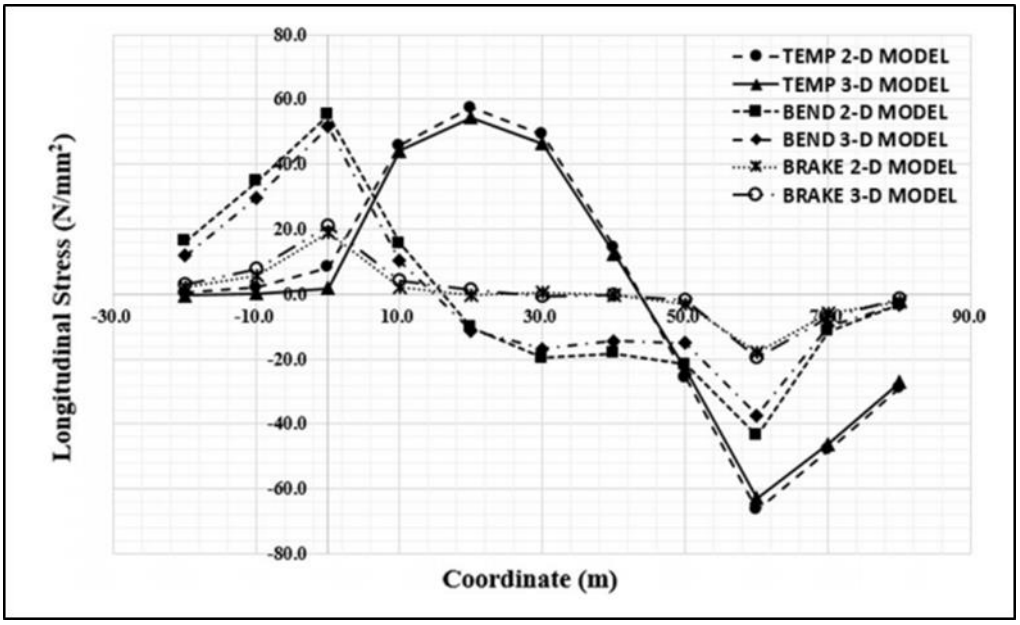

Figure 3.5. Rail Stresses from 2D and 3D models (Manovachirasan et al., 2018)

3.1.2. Bridge Modeling According to UIC

3.1.2.1. General Recommendations for The Model

The UIC (International Union of Railways) has some recommendations for the calculations of the track-structure interaction with a computer program. According to the level of accuracy, there are two types of analysis: simplified and complete analysis. The difference between the two types of analysis is discussed in Chapter 4. According to the UIC general recommendations for the interaction analysis by using a computer program, it is stated that the rail-structure interaction effect on the rail and structure should be evaluated in terms of the additional rail stresses, the absolute and relative displacement of the deck and the rails and the longitudinal force/stress carried by the fixed supporting system (supports, columns, bearings). According to UIC, the rail-structure interaction should be carried by a series of non-linear analysis to evaluate and study the system subjected to the thermal loads as well as the braking and traction force and the vertical loads coming from the traffic carried by the bridge. The UIC has

proposed a structural system for calculating the rail-structure interaction phenomena. The structural system is shown Figure 3.6.

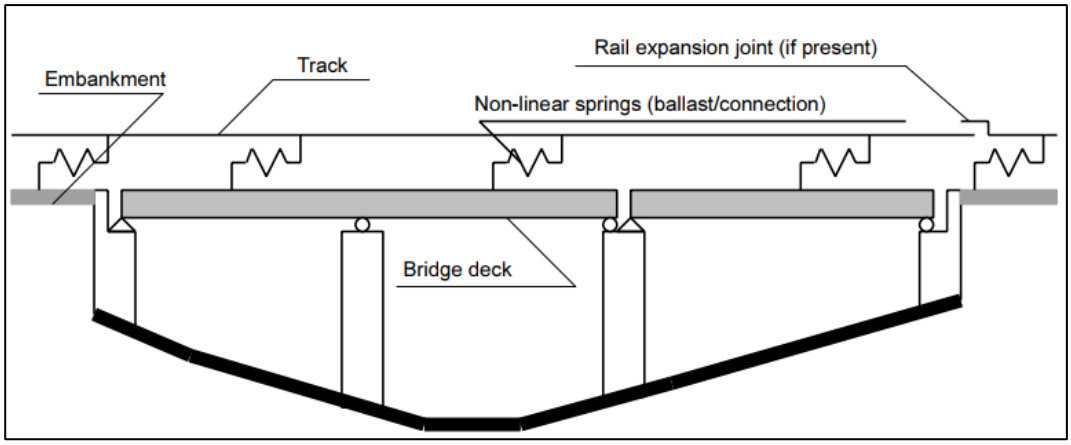

Figure 3.6. Structural System Diagram Proposed by UIC

The model should take into account the bridge structural parameters, such as the bridge arrangement from a static and geometrical point of view, bridge length, superstructure type, supporting conditions, expansion length of the bridge, deck height, bending stiffness of the deck and the longitudinal stiffness of the supports including bearings columns and foundations. The model should consider the track parameter, such as the cross-sectional area of the rails and the track stiffness. Also, the model should consider the loads applied on the bridge, such as temperature variation of the deck, braking and acceleration loads and bending of the deck due to the vertical traffic loads.

3.1.2.2. Modeling According to UIC

According to UIC, the center lines of the rails and the deck should be located in the model exactly in their actual position in the structural system, as shown in Figure 3.7. Also, the position of the boundaries like supports, columns, bearings should be located in their actual location, especially when there is a fixed bearing. The UIC modeling

approach recommends using a rigid element to connect the deck elements and the supports. The UIC has made the models simple. For example, they allow -for simplicity- the height of the track to be taken equal to the height of the deck. Moreover, for temperature effect and braking and acceleration loads, the UIC allows the bridge to be modeled without taking into account the difference of height between the track and the top of the deck and the top of the bearings/supports. The UIC doesn't require a detailed model for the substructure, including the system of bearing vertical element (Pier) foundation when normal bridges are considered. The UIC assumes that the lateral flexibility of the supporting elements (Substructure) may be evaluated while determining the stiffness of the constrains. On the contrary, for special type bridges the substructure should be accurately modeled.

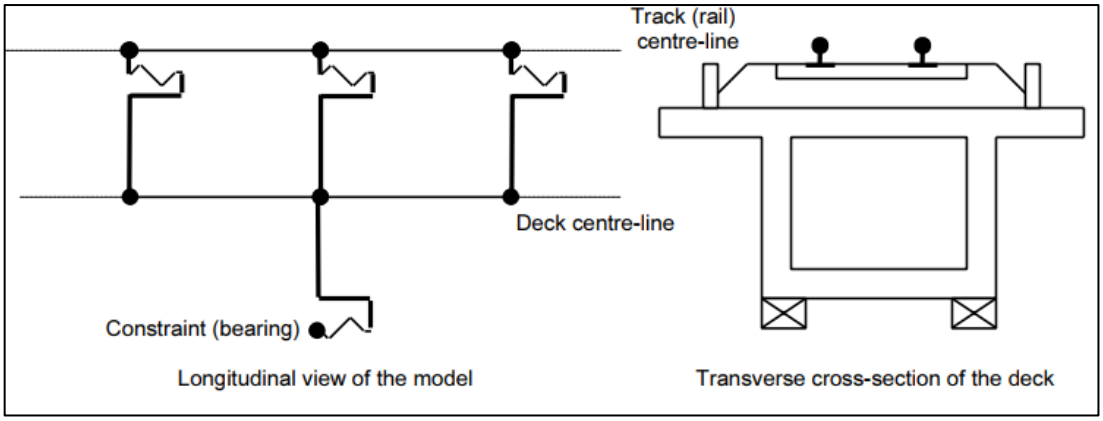

Figure 3.7. Typical Model of Rail-Deck-Bearing UIC

In general, there are some assumptions for the mathematical model shown in Figure 3.8, according to UIC:

- The behavior of the rail elements, deck elements, and the boundary elements for the fixed supports or bearings and substructure elements should be assumed as linear elastic.
- For the elements connecting the rail and the deck -for the particular case of this study ballast-, a non-linear behavior should be assumed, and the non-linear

law should reproduce the actual behavior of the ballast, taking into account the vertical load state. The element should have a resistance yield threshold depending on the state of vertical load.

- The modelling of deck and rails should be taken as discrete elements to guarantee accurate results and better evaluation of the system. For this reason, the FEM may be adopted. The element length of the deck and the rail should be modelled discretely with a maximum length of 2 m, while the model should include a part of the rail on the adjacent embankment in front of and over the bridge, at least 100 m.
- For the vertical load effects, while considering the vertical deflection of the superstructure for a single-span bridge, the vertical loads of the train should be applied to the bridge and to the embankment on one side only.
- For the complete analysis type, the assumed non-linear behavior of the ballast and the yielding threshold state should consider the dependence of lateral stiffness to the vertical load.
- The complete analysis should cover the application of the thermal load, followed by the application of the train loads (vertical and horizontal).
- For the case of CWR in which there is no rail thermal expansion device on the structure, the temperature variation in the track may be assumed to be equal to zero.
- Where there isn't any expansion device on the structure, only the maximum and minimum temperature variation applied on the deck should be considered.

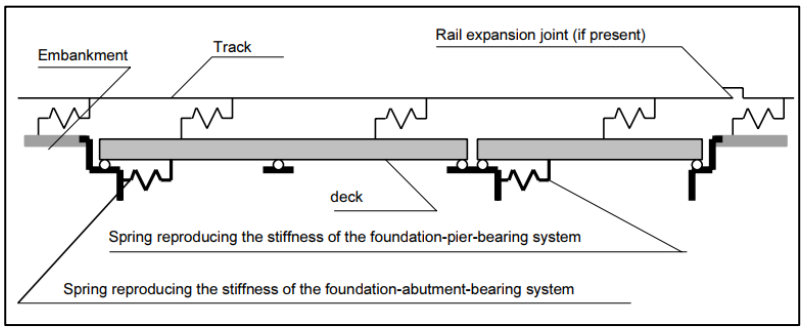

Figure 3.8. Simplified Structural Model for Interaction (UIC)

3.2. Proposed Computer Model for Track-Structure Interaction

Generally, the SAP 2000 FEM computer program is used for the evaluation of track-structure interaction analysis. Also, Midas Civil FEM computer program is used for this evaluation due to the capability of the program in performing complete analysis.

3.2.1. Bridge Components Modelling in the Program

3.2.1.1. Superstructure Components

The superstructure is modelled using a frame element, as shown in Figure 3.9; therefore, the complete deck section is concentrated in one beam element. The track, which is composed of two rails, is modeled by one beam element considering its own center of gravity location (CG). The bearings and supports are modeled in their actual locations. The bridge deck is connected to the bearings and the supports by a rigid element where the rigid element has a very high flexural and axial stiffness in comparison with the superstructure elements; thus, the high rigidity of the rigid element doesn't allow it to deform between the connected elements. The superstructure has a predefined axial and flexural stiffness, this stiffness will be discussed in Chapter 5. Since the scope of this thesis is for the CWR UIC-60 (continuous welded rail UIC type 60), only one type of rails is considered in all analyses.

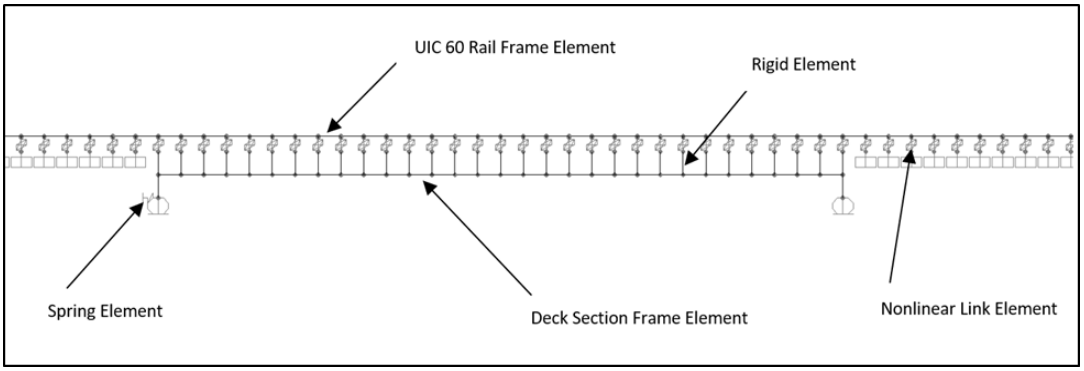

Figure 3.9. 2D FEM Model Used for the Analysis

3.2.1.2. Substructure Components

The substructure is not directly modelled in the mathematical model. Instead, support is used in the location of the substructure, as shown in Figure 3.10. Since the bridge structural arrangement is identical for all of the evaluated cases, the substructure lateral stiffness is simulated by a linear elastic spring element. The structural system is assumed to have a fixed restraint (degree of fixity is directly related to the substructure system longitudinal stiffness) in the horizontal direction (direction of the applied loads braking/acceleration) and a perfectly free-to-slide support on the other end of the bridge. Both supports have the same stiffness in the vertical direction, which were assumed to behave as fixed support. The bridge has no moment restraint and is free to rotate on both supports. Since the analysis is 2D analysis, there are no loads or boundary conditions in the direction perpendicular to the longitudinal axis of the bridge. The substructure lateral stiffnesses are accumulated in the single spring element on one side of the bridge. The spring has a predefined stiffness which is discussed in Chapter 5.

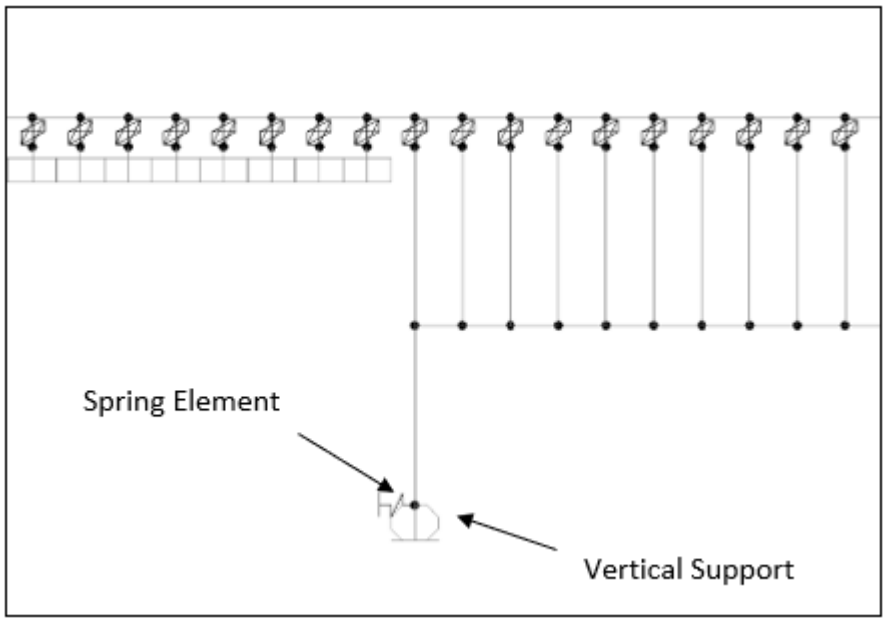

Figure 3.10. Application of Boundary Conditions on FEM Model

3.2.1.3. Ballast Element Modelling

The ballast is simulated as a link element. This element is connecting the top of the deck and the track. The distance between the track and the top of the deck is kept constant in all of the evaluated models at 60 (cm). This distance is the volume, yet in reality, it will be filled with ballast. The connecting element is a nonlinear plastic link element with two types: loaded link element and non-loaded link element.

3.2.1.3.1. Loaded Link Element

The loaded link element is used for simulating the ballast horizontal stiffness when it has a vertical load over it. As mentioned in the previous chapter, the ballast horizontal stiffness is affected by the state of vertical load shown in Figure 3.13. The link has a yielding threshold equal to 2 (mm), when the shear force in the link is equal to 60 (kN). Over the 2 (mm) the force within the link won't increase while the displacement is increasing, as shown in Figure 3.11. Thus, the link will guarantee the perfect plastic behavior. These values shown in the figure are per track.

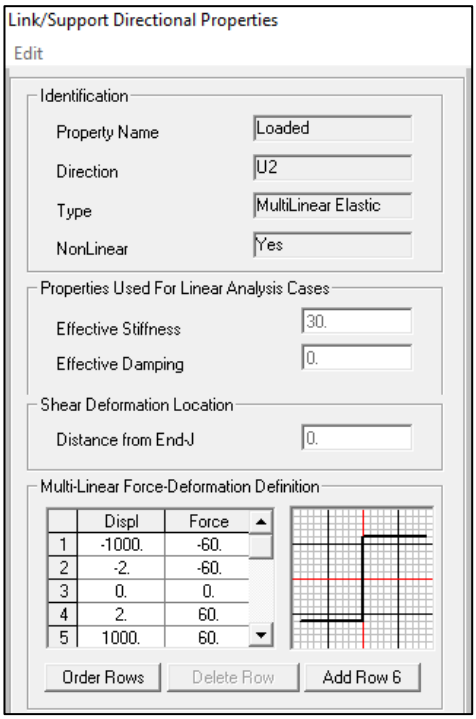

Figure 3.11. Loaded Link Element Definition in SAP 2000 (kN-mm)

3.2.1.3.2. Un-loaded Link Element

The un-loaded link element is used for simulating the ballast horizontal stiffness when there is no vertical load over it. As mentioned in the previous chapter, the ballast horizontal stiffness is affected by the state of vertical load. The link has a yielding threshold equal to 2 (mm) when the shear force in the link is equal to 20 (kN). Over the 2 (mm) the force within the link won't increase while the displacement is increasing, as shown in Figure 3.12. Thus, the link will guarantee the perfect plastic behavior. These values shown in the figure are per track.

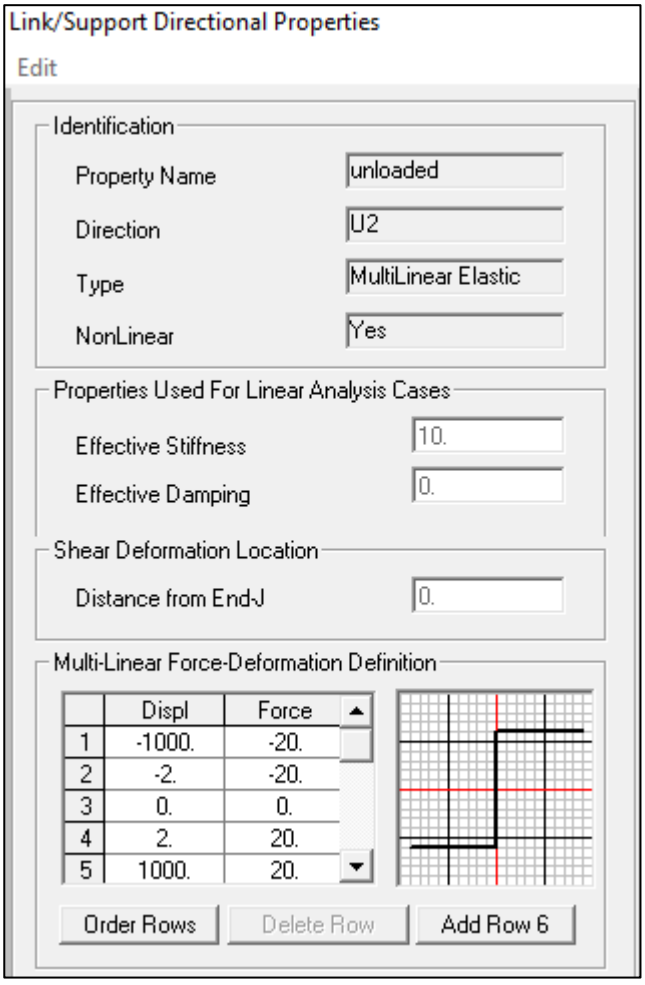

Figure 3.12. Un-Loaded Link Element Definition in SAP 2000 (kN-mm)

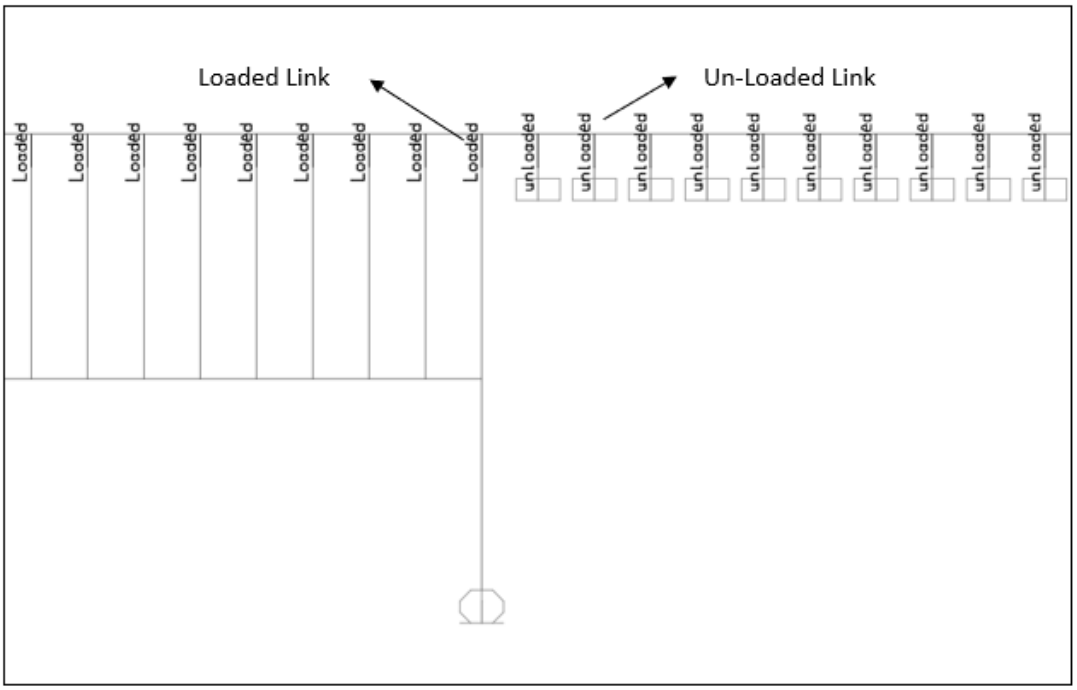

Figure 3.13. Loaded Un-Loaded Link Element Application in Model

3.2.2. Loads Application to the Bridge Model

3.2.2.1. Thermal Loads

Thermal loads are applied only to the deck elements. The deck is modeled by using a frame/beam element. The loads are applied directly to the deck by using SAP 2000 thermal load application to beam elements. Two load cases are generated thermal temperature rise (+) and thermal temperature fall (-)

3.2.2.1.1. Thermal (+) load

Thermal (+) is referred to the thermal load in the bridge deck. The thermal load is equal to +35 Kelvin, as shown in Figure 3.14 and Figure 3.15.

Load Pattern	thermal+
Temperature Load	
Temperature	35. °C
Joint Pattern	None
Load Pattern	**thermal-**
Temperature Load	
Temperature	-35. °C
Joint Pattern	None

Figure 3.14. Application of Thermal Load to the Frame Element

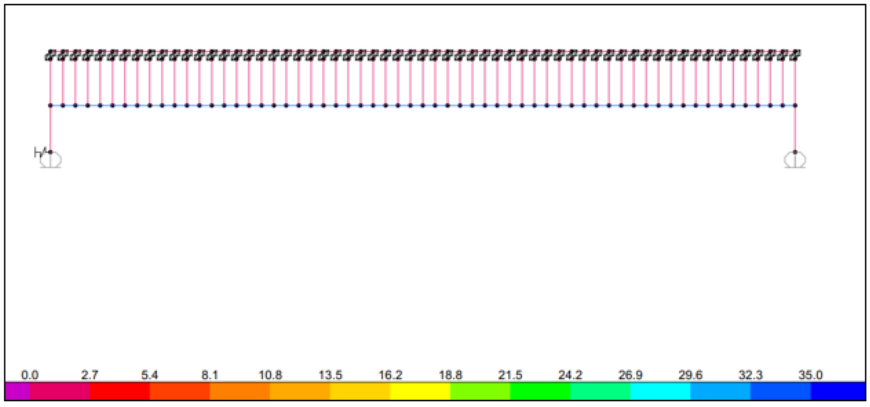

Figure 3.15. Thermal (+) load on the Frame Element ºC

3.2.2.1.2. Thermal load (-)

Thermal (-) is referred to the thermal load in the bridge deck. The thermal load is equal to -35 Kelvin, as shown in Figure 3.16.

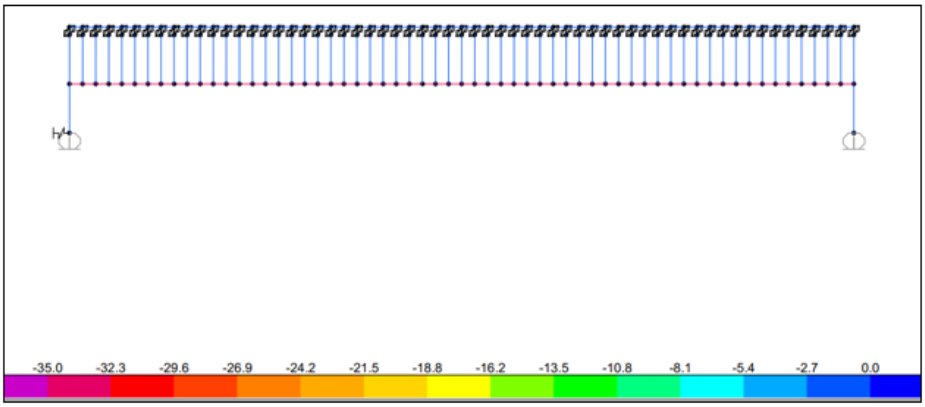

Figure 3.16. Thermal (-) load on the Frame Element ºC

3.2.2.2. Vertical Loads

The vertical load used for this study mentioned in Chapter 2 is based on the Load Model-71 (LM-71) -shown in Figure 3.17- specified in Eurocode EN 1992-2 (Eurocode 1: Action on structures-Part 2: Traffic loads on bridges). The load is applied to different locations in the bridge span to investigate the maximum response, as shown in Figure 3.20 and Figure 3.21.

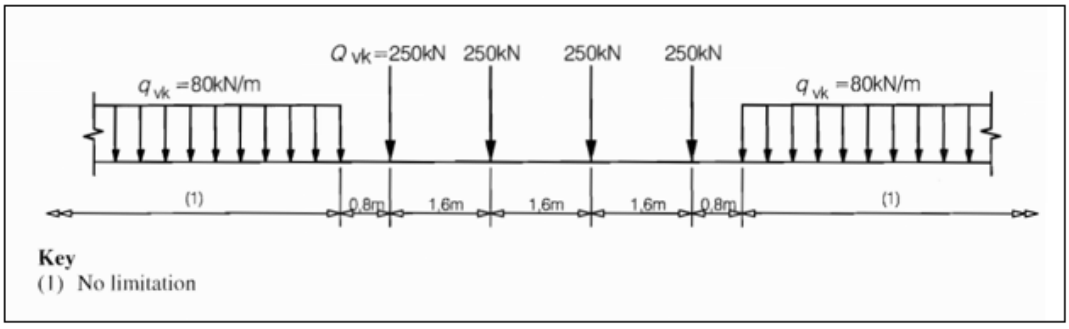

Figure 3.17. Load Model 71 according to Eurocode

According to Eurocode, Load Model 71 represents the normal rail traffic load. The load should be multiplied by α factor. The α factor is discussed in Chapter 2. According to UIC, the vertical loads should be enhanced by the dynamic factor Φ, as shown in Figure 3.18 and Figure 3.19. The vertical loads are applied to the model without any magnification. The dynamic factor Φ and the α factor will be applied to the Model accordingly by load case scale factor.

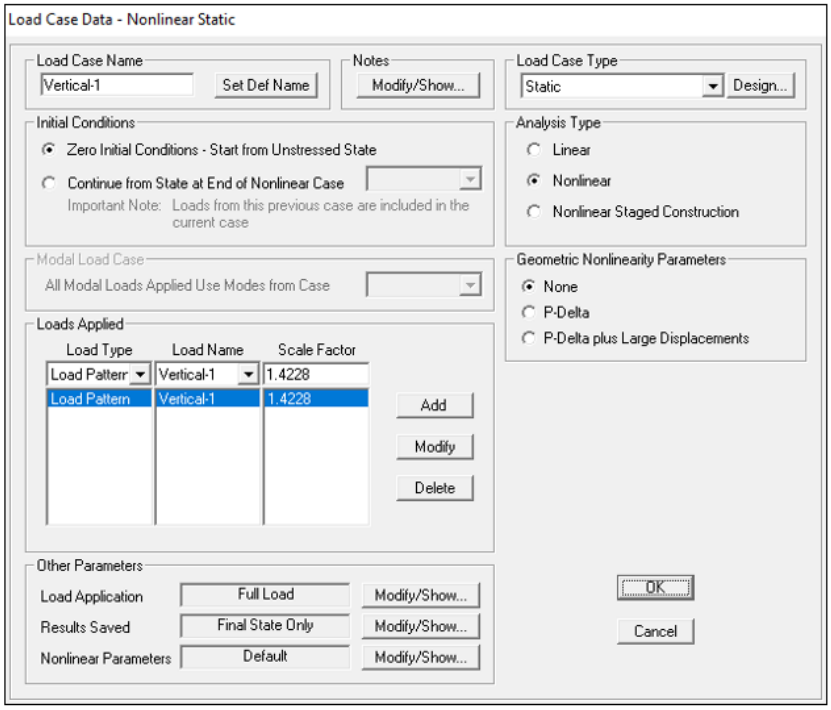

Figure 3.18. Vertical Load Case Definition in SAP 2000

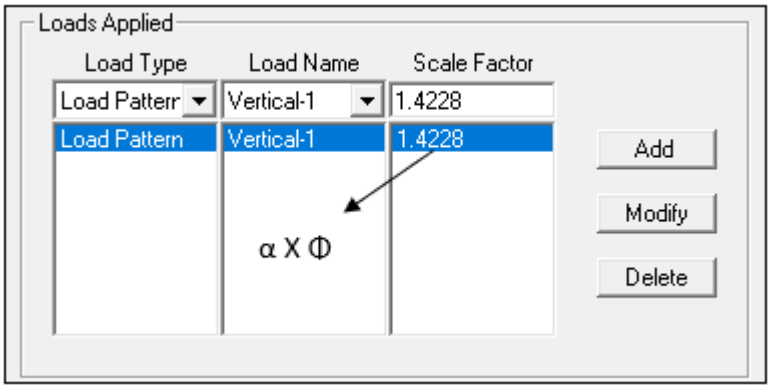

Figure 3.19. Application of α factor and Φ to the Model

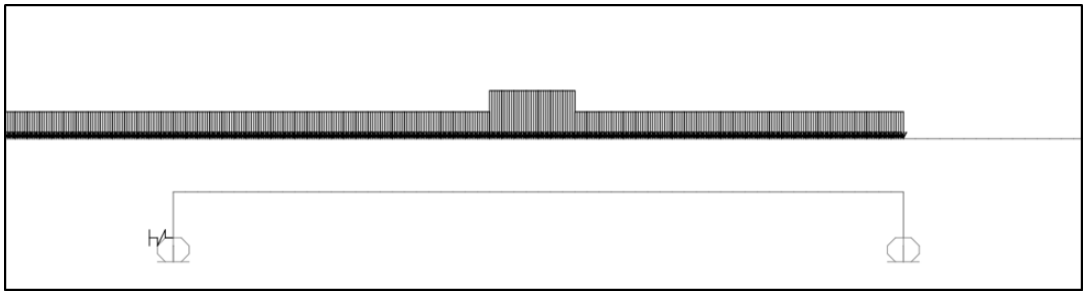

Figure 3.20. Vertical Load Application in the Model

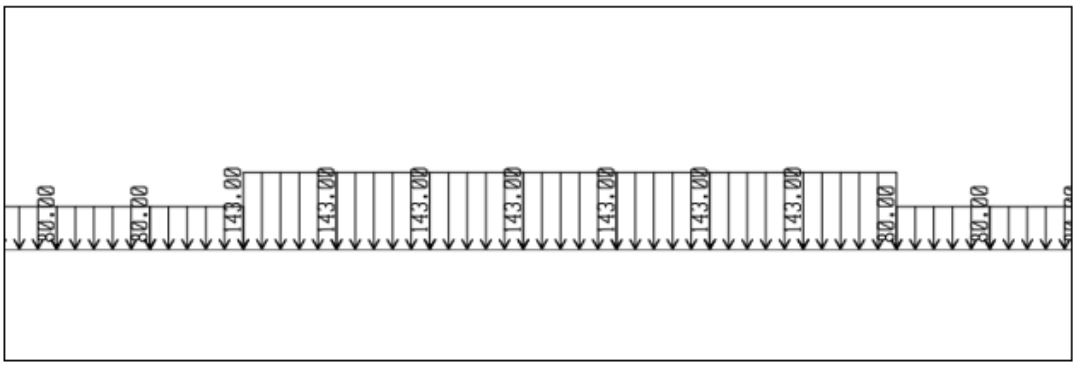

Figure 3.21. LM-71 application in the Model (kN/m)

3.2.2.3. Horizontal Forces

The horizontal forces are divided into two categories; Braking and Traction force.

3.2.2.3.1. Braking Force

The braking force is applied to the Model according to Eurocode specifications. The loads are applied to the rail elements as frame load as shown in Figure 3.22. The load is applied to different locations on the bridge and adjacent embankment to investigate the maximum response on the structure and the rail. The load for the Track- Structure interaction should not be multiplied by the dynamic factor Φ, but it should be amplified by the α factor accordingly. According to Eurocode, the load should be uniformly distributed over the investigated length with a load equal to 20 (kN/m), but

not more than 6000 (kN) in total. If an amplification factor is used, it will be applied from the load case definition, as shown in Figure 3.23. The loads are applied from the top of the rail with considering the difference in elevation between the rail center of gravity location, the deck center of gravity and top of the supports. The used approach assumes the results will be more accurate since the UIC drop this complicated modeling technique for simplicity. The effect of modeling with eccentricity is discussed in Chapter 5. Some design codes require that the model shall take into account the eccentricity between the rail level and the supports level crossing the deck level for braking and acceleration loads IAPF (2007).

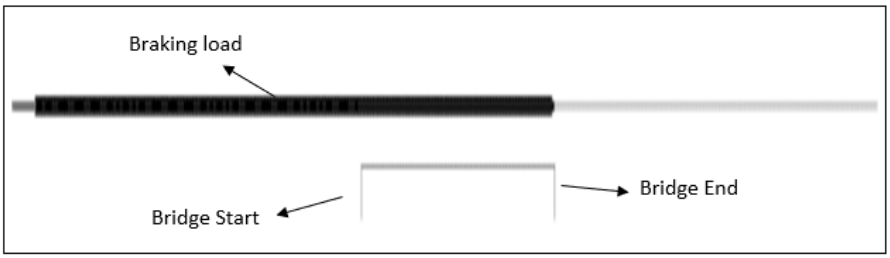

Figure 3.22. Braking Load Application on the Model

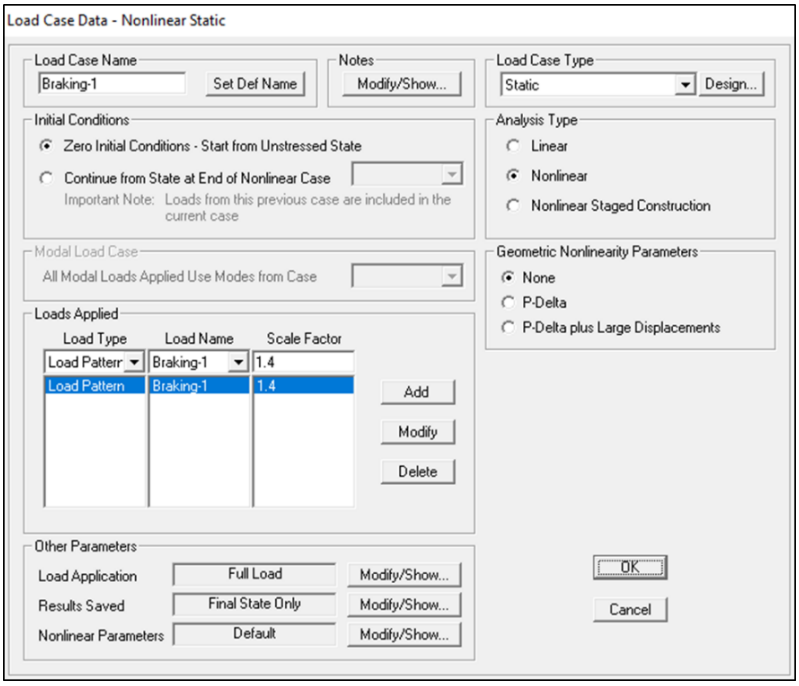

Figure 3.23. Braking Load Case Definition in SAP 2000

3.2.2.3.2. Traction Force

The Acceleration/Traction force is applied to the Model according to Eurocode specifications. The load is applied to different locations on the bridge to investigate the maximum response on the structure and rail. The load for the Track- Structure interaction should not be multiplied by the dynamic factor Φ, but it should be amplified by the α factor accordingly. According to Eurocode, the load should be uniformly distributed over the investigated length as shown in Figure 3.24 with a load equal to 33 (kN/m), but not more than 1000 (kN) in total. If an amplification factor is used, it will be applied from the load case definition, as shown in Figure 3.25. The loads are applied from the top of the rail with considering the difference in elevation between the rail center of gravity location, the deck center of gravity, and top of the supports.

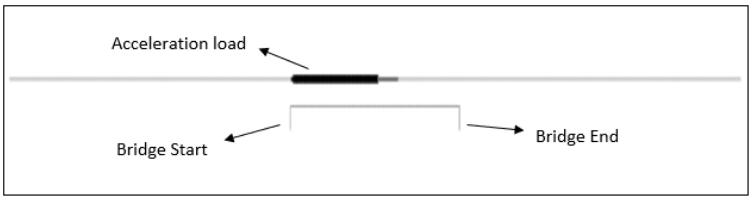

Figure 3.24. Traction Load Application on the Model

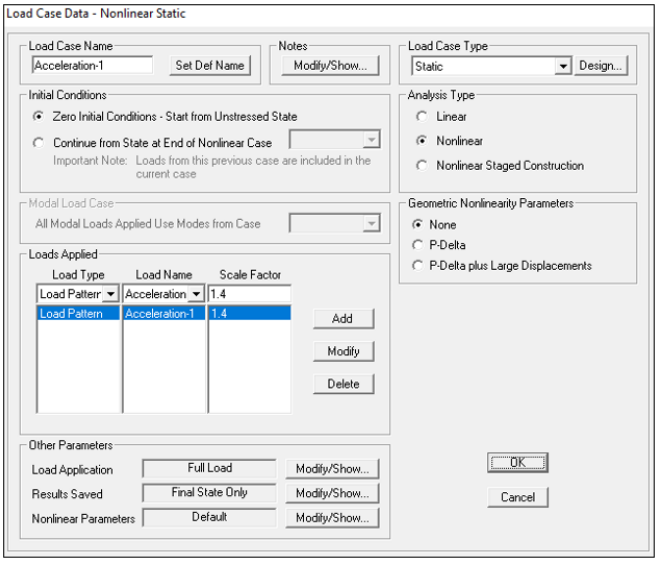

Figure 3.25. Traction Load Case Definition in SAP 2000

The horizontal loads are applied to the structure according to the state of vertical loads, where the stiffness of the ballast is the loaded stiffness. For the acceleration load case, the loads are applied to locations where the vertical load is applied, but due to the limitation of the total acceleration force, the loads are located to produce the maximum effect.

3.3. Verification of the FEM Model Used for the Analysis

The UIC requires that the computer programs for rail-bridge interaction shall be validated before using it for the analysis. The verification is carried by analyzing the cases reported in Appendix-D in UIC. The results of the analysis are given by UIC for control purposes. According to UIC, a computer program is considered as valid if the results are not deviated by more than 10% from the results given by UIC, larger tolerances up to 20% are accepted if the results are on the safe side.

3.3.1. UIC Analysis Case Parameters

The bridge used for the validation case is a single span bridge, as shown in Figure 3.27 with a deck Type-1. The deck type is shown schematically in Figure 3.26. Span lengths and longitudinal stiffness are given, and the bridge material and section properties are given in Table 3.1.

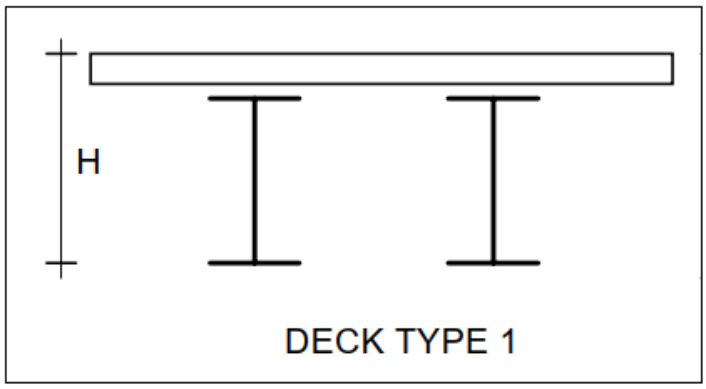

Figure 3.26. Bridge Deck Type by (UIC)

Table 3.1. *Bridge Materials and Section Properties by UIC*

Case No.	Name	Deck type	Span (m)	Long. displ. (mm)	Direct.	K long. (KN/m)	E (KN/m^2)	I (m^4)	H (m)	S (m^2)	vi (m)
A1-3	1-30-1-1	1	30	1	1	300000	2,1E+08	0,165	3,00	0,57	2,64
A4-6	1-30-1-2	1	30	1	2	300000	2,1E+08	0,165	3,00	0,57	2,64
B1-3	1-30-5-1	1	30	5	1	60000	2,1E+08	0,165	3,00	0,57	2,64
B4-6	1-30-5-2	1	30	5	2	60000	2,1E+08	0,165	3,00	0,57	2,64
C1-3	1-45-1-1	1	45	1	1	450000	2,1E+08	0,830	4,50	0,64	3,84
C4-6	1-45-1-2	1	45	1	2	450000	2,1E+08	0,830	4,50	0,64	3,84
D1-3	1-45-5-1	1	45	5	1	90000	2,1E+08	0,830	4,50	0,64	3,84
D4-6	1-45-5-2	1	45	5	2	90000	2,1E+08	0,830	4,50	0,64	3,84
E1-3	1-60-1-1	1	60	1	1	600000	2,1E+08	2,590	6,00	0,74	4,79
E4-6	1-60-1-2	1	60	1	2	600000	2,1E+08	2,590	6,00	0,74	4,79
F1-3	1-60-5-1	1	60	5	1	120000	2,1E+08	2,590	6,00	0,74	4,79
F4-6	1-60-5-2	1	60	5	2	120000	2,1E+08	2,590	6,00	0,74	4,79
G1-3	1-90-1-1	2	90	1	1	1080000	3,42E+07	80,060	9,00	7,20	5,07
G4-6	1-90-1-2	2	90	1	2	1080000	3,42E+07	80,060	9,00	7,20	5,07
H1-3	1-90-5-1	2	90	5	1	216000	3,42E+07	80,060	9,00	7,20	5,07
H4-6	1-90-5-2	2	90	5	2	216000	3,42E+07	80,060	9,00	7,20	5,07
I1-3	3-30-3-1	3	30	1	1	300000	2,1E+08	0,180	3,00	0,50	0,42
I4-6	3-30-3-2	3	30	1	2	300000	2,1E+08	0,180	3,00	0,50	0,42
J1-3	3-30-5-1	3	30	5	1	60000	2,1E+08	0,180	3,00	0,50	0,42
J4-6	3-30-5-2	3	30	5	2	60000	2,1E+08	0,180	3,00	0,50	0,42
K1-3	3-45-3-1	3	45	1	1	450000	2,1E+08	0,820	4,50	0,57	0,74
K4-6	3-45-3-2	3	45	1	2	450000	2,1E+08	0,820	4,50	0,57	0,74
L1-3	3-45-5-1	3	45	5	1	90000	2,1E+08	0,820	4,50	0,57	0,74
L4-6	3-45-5-2	3	45	5	2	90000	2,1E+08	0,820	4,50	0,57	0,74
M1-3	3-60-3-1	3	60	1	1	600000	2,1E+08	2,560	6,00	0,70	1,31
M4-6	3-60-3-2	3	60	1	2	600000	2,1E+08	2,560	6,00	0,70	1,31
N1-3	3-60-5-1	3	60	5	1	120000	2,1E+08	2,560	6,00	0,70	1,31
N4-6	3-60-5-2	3	60	5	2	120000	2,1E+08	2,560	6,00	0,70	1,31
O1-3	3-90-3-1	3	90	1	1	1080000	2,1E+08	13,340	9,00	1,30	3,18
O4-6	3-90-3-2	3	90	1	2	1080000	2,1E+08	13,340	9,00	1,30	3,18
P1-3	3-90-5-1	3	90	5	1	216000	2,1E+08	13,340	9,00	1,30	3,18
P4-6	3-90-5-2	3	90	5	2	216000	2,1E+08	13,340	9,00	1,30	3,18

Where:

- E: elastic modulus (kN/m^2)
- I: moment of inertia (m^4)
- H: bridge deck height (m)
- S: deck cross section area (m^2)

- vi: neutral axis location from the bottom of the deck (m)
- K long: longitudinal spring stiffness (kN/m)

In the UIC validation cases, for simplicity they considered the position of the center of gravity of the tracks to coincide with the top of the reinforce concrete slab. The track type is assumed to be ballasted track.

3.3.1.1. Loads Considered for the Validation Case

The loads for the validation case are as follows:

- The vertical load is assumed to be equal to 80 (kN/m)
- The horizontal forces are assumed to be braking forces and equal to 20 (kN/m)
- Thermal load variation for deck is equal to 35º C
- Thermal load variation for rail is equal to 50º C

3.3.1.2. General Considerations for the Analysis case

- The train is assumed to be 300 (m) long
- Ballasted track resistance for loaded track is assumed 60 (kN/mm/m)
- Ballasted track resistance for un-loaded track is assumed 20 (kN/mm/m)
- The braking forces, as well as the direction of travel, are considered to be acting from the fixed support towards the movable support
- The direction assumed above is recognized as direction-1 (Direct). The opposite travel direction is recognized as direction-2
- The thermal expansion coefficient for the deck is taken equal to 0.00001 $^{o}K^{-1}$

The UIC stated that the fundamental cases to be satisfied are E1-3 and E4-6 within the accepted tolerances. The other given cases are supplementary checks and should be performed if the fundamental cases are not satisfied.

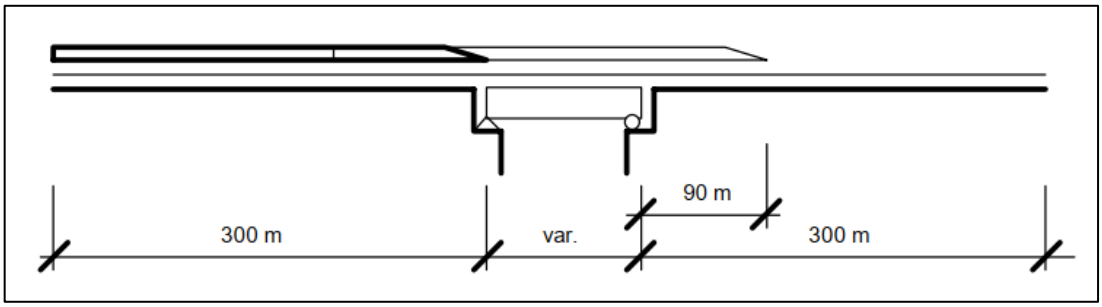

Figure 3.27. Bridge Arrangement Used by UIC for Validation

3.3.2. Validation of the Model Used for the Analysis

The validation process is applied to the proposed model by using SAP 2000 FEM computer software. The same model is used for the evaluation process in Chapter 5 with some modifications. The bending stiffness of the deck is assumed to be perfectly rigid for the thermal and the braking load cases. The braking and vertical loads will be applied without the multiplication by α factor.

3.3.2.1. Model Geometrical Configuration and Material Properties

The bridge arrangement is assumed to be identical to the bridge in the validation case, as shown in Figure 3.28 and Figure 3.29 and Figure 3.30. The bridge has one fix support with lateral stiffness simulated by elastic spring located at the support. The other end of the bridge is assumed to have a perfect sliding support. The embankment length is assumed to be equal to 300 m on both sides. The superstructure, including the bridge deck is located in the center of gravity of the deck section and the distance between the top of the supports and the bridge deck is equal to the vi (neutral axis ordinate). The distance between the top of the deck and the top of the supports is assumed to be equal to H (bridge deck height). The ballast height is assumed to be very small and could be neglected.

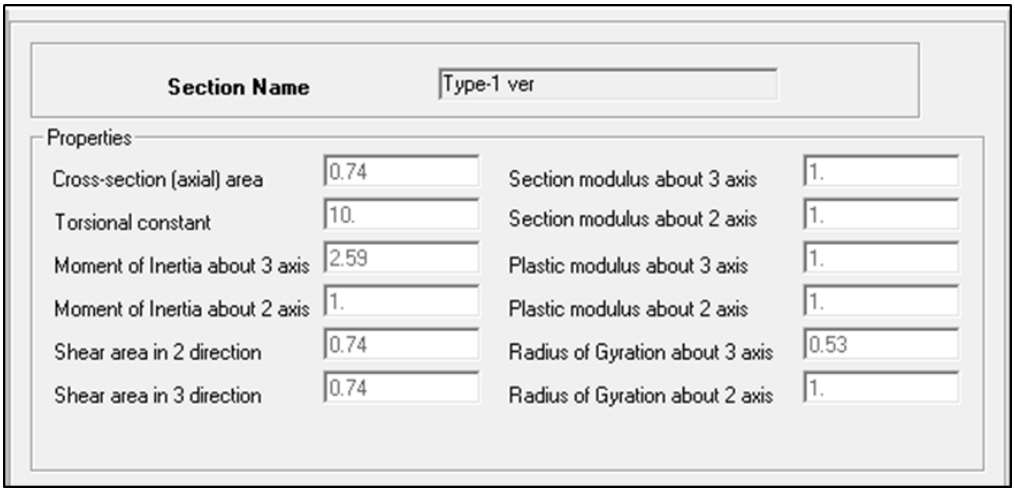

Figure 3.28. Bridge Deck Properties Used for the Validation

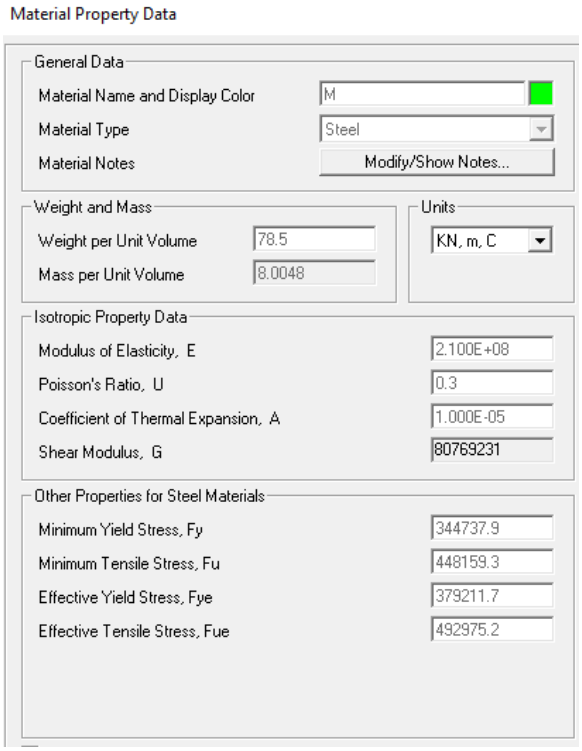

Figure 3.29. Material Property Definition Used for the Validation

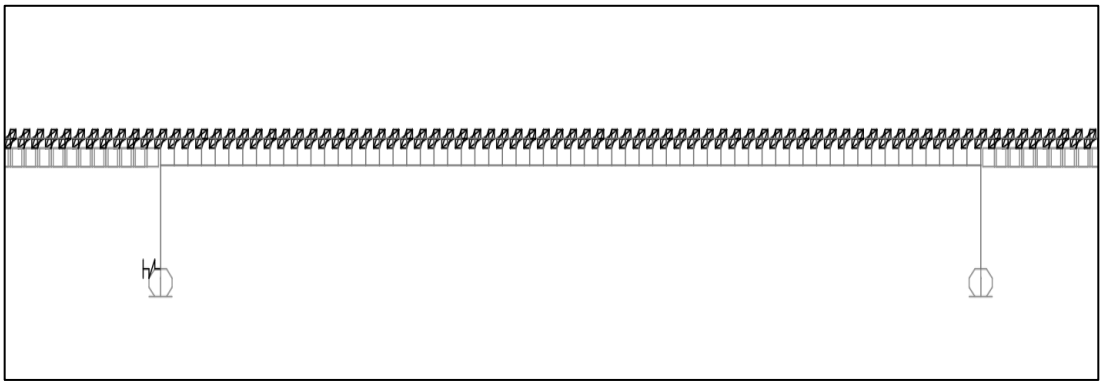

Figure 3.30. Bridge Model Used for the Validation

3.3.2.2. Loads Considered for the Validation Model

The loads applied to the Model are the same as loads considered for the Validation Case.

3.3.3. Results from the Validation Model

The results from each load case are shown and the rail axial stresses are plotted along the rail axis. Stress for each load case is summarized in the Figures below.

3.3.3.1. Thermal variation on the deck

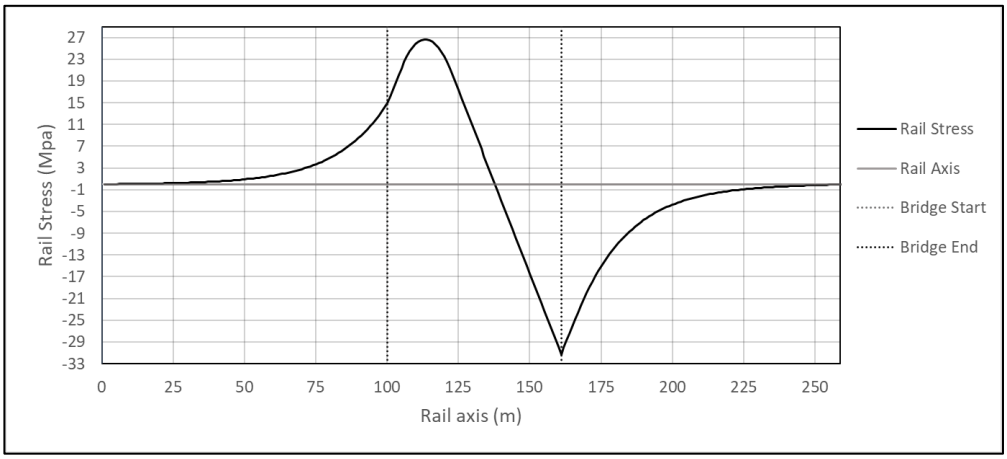

Figure 3.31. Rail Stress due to Thermal variation on the Deck

3.3.3.2. Vertical Loads

The rail stresses shown in Figure 3.32, results from vertical load in load direction-1

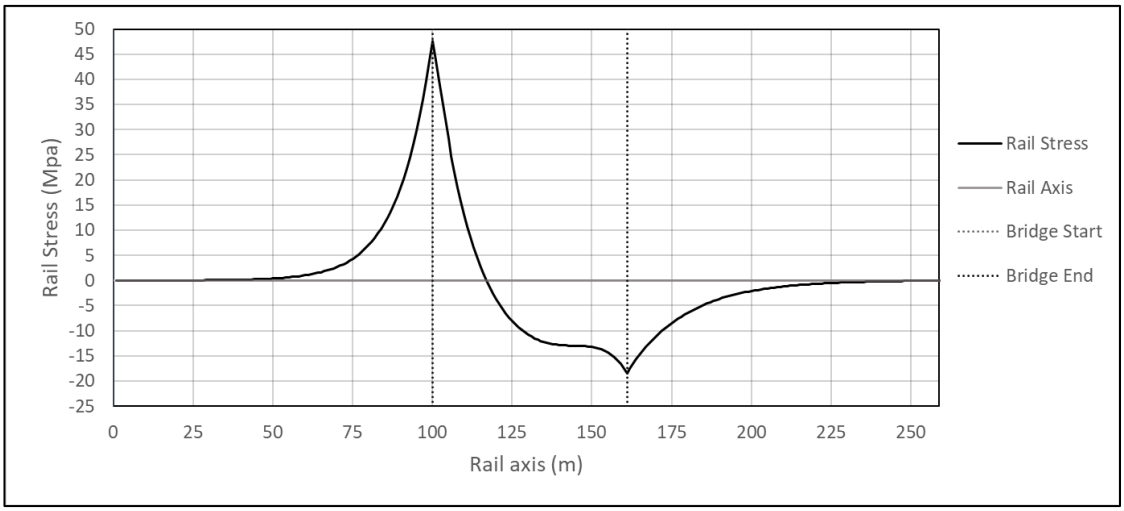

Figure 3.32. Rail Stress due to Vertical Load effect on the Deck

3.3.3.3. Horizontal Loads

The rail stresses shown in Figure 3.33, results from braking load in load direction-1

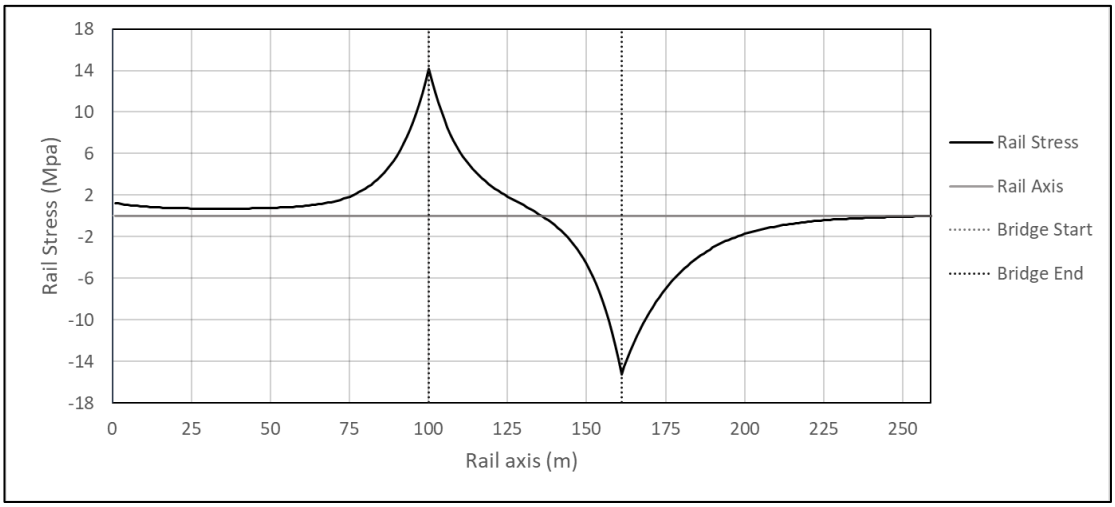

Figure 3.33. Rail Stress due to Horizontal Load Effect

3.3.4. Summary of the Results from the Validation Model

The results obtained from the validation model are summarized in the tables below.

Table 3.2. *Results summary for case E1-3*

Load Type	*Thermal*	*Vertical*	*Horizontal*
Axial Stress of Track (MPa)	-31.27	-18.52	-15.30
Absolute Displacement (mm)	-1.70	3.77	1.35
Support Reaction (kN)	708.50	1014.60	-769.00

Table 3.3. *Results summary for case E4-6*

Load Type	*Thermal*	*Vertical*	*Horizontal*
Axial Stress of Track (MPa)	-31.27	-26.81	-14.60
Absolute Displacement (mm)	-1.70	3.95	1.35
Support Reaction (kN)	708.50	955.00	765.00

3.4. Comparison between the UIC Test Case and the Model Used for Analysis

The results obtained from the validation model and the UIC test cases are compared and summarized in the tables below.

Table 3.4. *Axial Stress Comparison Case E1-3*

Load Type	*UIC (MPa)*	*Model (MPa)*	*Difference %*
Thermal	-30.67	-31.27	1.95
Vertical	-16.98	-18.52	9.07
Horizontal	-16.42	-15.30	-7.32
Total	-64.07	-65.09	1.59

Table 3.5. *Axial Stress Comparison Case E4-6*

Load Type	*UIC (MPa)*	*Model (MPa)*	*Difference %*
Thermal	-30.67	-31.27	1.95
Vertical	-28.22	-26.81	-4.99
Horizontal	-15.95	-14.60	-9.24
Total	-74.84	-72.68	-2.88

Table 3.6. *Absolute Displacement Comparison Case E1-3*

Load Type	*UIC (mm)*	*Model (mm)*	*Difference %*
Thermal	-1.69	-1.70	0.88
Vertical	3.77	3.77	0.18
Horizontal	1.36	1.35	-0.73
Total	3.43	3.42	-0.23

Table 3.7. *Absolute Displacement Comparison Case E4-6*

Load Type	*UIC (mm)*	*Model (mm)*	*Difference %*
Thermal	-1.69	-1.70	0.88
Vertical	4.16	3.95	-4.90
Horizontal	1.36	1.35	-0.73
Total	3.83	3.60	-5.98

Table 3.8. *Support Reaction Comparison Case E1-3*

Load Type	*UIC (kN)*	*Model (kN)*	*Difference %*
Thermal	700.12	708.50	1.20
Vertical	977.70	1014.60	3.77
Horizontal	-813.22	-769.00	-5.44
Total	864.60	954.10	10.35

Table 3.9. *Support Reaction Comparison Case E4-6*

Load Type	*UIC (kN)*	*Model (kN)*	*Difference %*
Thermal	700.12	708.50	1.20
Vertical	855.61	955.00	11.61
Horizontal	817.74	765.00	-6.45
Total	2373.47	2428.50	2.32

From the summary of the results, it could be found out that the minimum difference is -9.24%, which is less than 10%, and the maximum difference is +11.61, which is less than 20%. According to UIC, these results are accepted and the modelling approach used for this validation and for the evaluation process in Chapter 5 is accepted and validated. The results obtained from the sensitivity analysis in Chapter 5 are already verified and doesn't require any validation anymore.

CHAPTER 4

COMPLETE AND SEPARATE TYPE ANALYSIS

4.1. Analysis Types of Track Structure Interaction

The ballast bed, which is supporting the rail, has a non-linear behavior. This non-linear behavior changes according to the state of vertical load. Since the ballast behavior is non-linear, the analysis type that will be carried for the evaluation of the track-structure interaction should be non-linear in nature. The UIC code and Eurocode state that there are two types of analysis that could be used to evaluate the combined effect of rail structure analysis: the simplified separate analysis and the complete analysis. According to the bridge importance, type, location, arrangement, and the computer software/program capabilities, either complete analysis or the simplified separate analysis could be used.

4.1.1. Complete Type Analysis

Complete type analysis is an analysis type in which the effects from thermal variation, traction and braking forces, vertical loads are carried simultaneously. The complete type analysis joints the effects from the thermal loads and braking/traction and vertical loads in a non-liner manner. In fact, the complete analysis simulates the ballast stiffness shift from un-loaded to loaded state within the same analysis model. This behavior can be guaranteed if the computer software has a link element which is connecting the ballast and the top of the deck with a load-deformation history. Generally, as mentioned in UIC and Eurocode, first, the thermal variation should be applied to the model, and then the actions from vertical and the braking/acceleration loads will be applied. The thermal variation or the thermal load should be applied to the model with the ballast having the un-loaded stiffness. After applying the thermal load, a relative displacement will occur between the rail and the bridge deck. This

relative displacement will produce an axial deformation in the tracks, which will result in axial stress. After that, the train's horizontal and vertical loads are applied to the model and the analysis will be performed on the already deformed model where the links already have a force from the previous thermal loads. The analysis is continued from the previous stage, not performed on zero initial conditions structure. The complete analysis type is wildly used. In fact, most of the scientific researches found in the literature has adapted the complete analysis type. (Okelo et al., 2011) have used a complete type analysis for the analysis of an elevated skewed steel guideway. (Baxter et al., 2012) used the complete analysis model for the analysis of the Colfax bridge. (Ramos et al., 2019) used the complete analysis model for the evaluation of 34 railway bridges. The complete analysis type is found to be reliable for complex bridge geometries and for bridges where rail expansion joints are used.

4.1.2. Simplified Separate Analysis

the simplified separate analysis should be carried with the consideration of the non-linear behavior of the ballast, which is connecting between the bridge deck and the rail. Since the link element has a non-linear behavior superposition method should not be used, but the simplified analysis allows the separate sum of the effects from variable actions. The thermal action is analyzed in a separate model with the un-loaded ballast stiffness, then these results are algebraically summed with the results from the horizontal and vertical loads from other models. These models ballast has the loaded ballast stiffness, and the braking/acceleration loads are always applied according to the vertical load location. It is not allowed to apply a horizontal load to a location where the vertical loads are not applied. The simplified Separate analysis allows the vertical and horizontal loads to be applied simultaneously or in separate models. After the results are obtained from the different models for the variable actions, the values are algebraically sunned. The simplified separate analysis is used for the design proposes. Most designers will prefer a simple, fast way of analysis for daily problems.

4.2. Complete Versus Separate Analysis

4.2.1. Load History in the Link Element

The separate analysis allows the effects of variable actions to be super positioned. This assumption could reduce the number of computations required for the analysis, but it will yield a conservative result and will overestimate the additional rail stresses. The complete analysis is more accurate because the analyses are chained and linked into each other in a way that the effect of the thermal load will affect the state of the ballast for the train's horizontal and vertical loads and the initial conditions are changed. In contrast, the initial conditions are the same for all of the variable actions in the separate simple analysis. The behavior of the link element for both complete and separate analysis is shown in the figures below, Figure 4.1 is for Simple analysis, and Figure 4.2 is for Complete analysis.

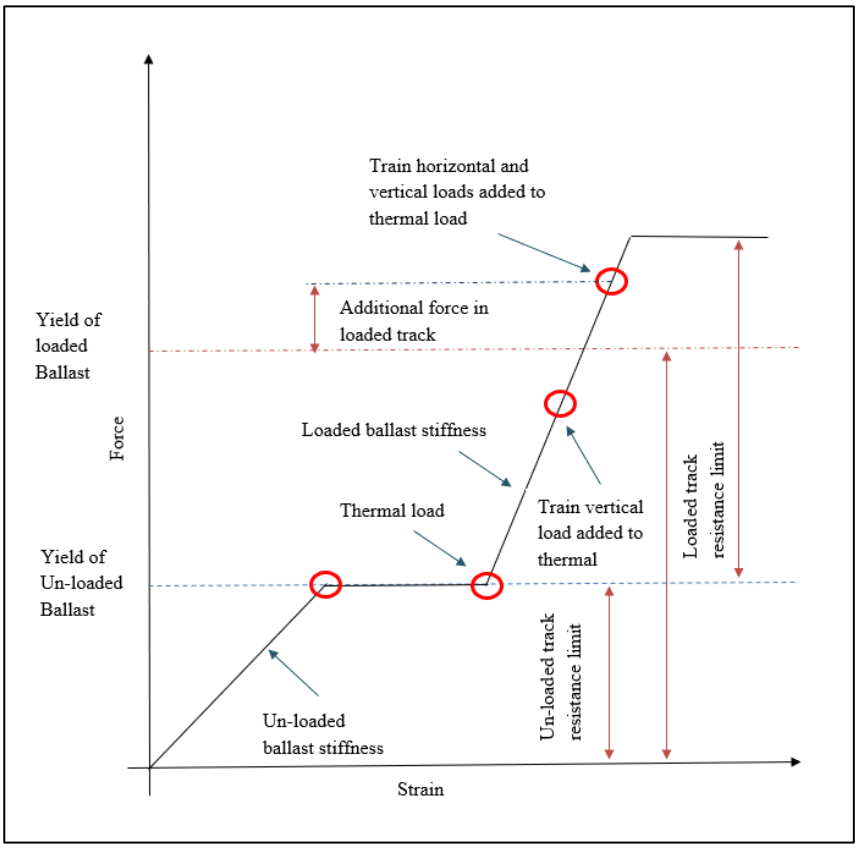

Figure 4.1. Link Element Behavior in Separate Analysis

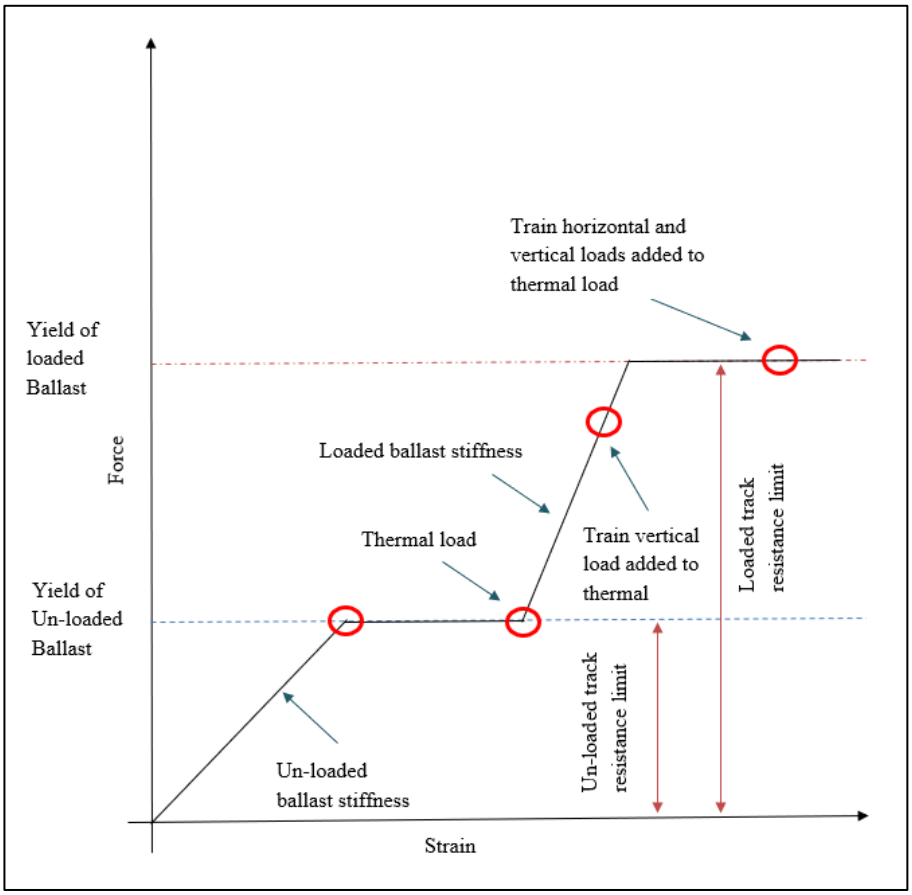

Figure 4.2. Link Element Behavior in Complete Analysis

The link element in the simple separate analysis doesn't have a load-deformation history. The loading for the train actions (horizontal and vertical) starts from zero, and it will continue to the yielding resistance without taking into account the initial strain in the link caused by thermal effect, as shown in Figure 4.2. The complete analysis considers the initial strain in the link element, and the actions due to train load won't exceed the yielding resistance of the loaded ballast. The complete analysis guarantee that the resistance after applying the variable actions on the structure won't exceed the yielding resistance of the ballast by performing a staged analysis where the initial conditions for the next step analysis are the final condition of the previous step analysis.

4.2.2. Computer Models

The track bridge interaction analysis should be performed considering the plastic behavior of the ballast, whether the complete or simple separate analysis is performed. The amount of computations required for the complete analysis is larger and longer than the amount required for the simple separate analysis. The number of models required for the complete analysis type is less than the models required for simple type. Even though the analyses will be performed in the same model, there are other requirements for the track-structure interaction analysis such as top deck displacement due to the deck rotation caused by the vertical loads, the deck horizontal displacement due to braking/acceleration forces. These effects should be evaluated separately; thus, there should be more than one model for evaluating these effects separately. The simple separate analysis is already evaluating the stresses in different models; thus, the deformations and horizontal displacements could be evaluated directly from each model.

4.2.3. Accuracy and Selection of Analysis Type

Since the Complete Analysis type could simulate the actual yielding resistance of the loaded ballast under variable actions, it should give more accurate results; thus, the complete analysis is more accurate than the separate simple analysis type. According to the bridge importance, type, arrangement, project complexity, and design standards, the analysis type could be chosen. Another important factor in selecting the analysis type is the use of rail thermal expansion device within the bridge spans or on the bridge ends. Rail expansion devices are introduced to the structure if the displacement criteria are not met or the additional rail stress from variable actions exceeds its limit. Introducing a rail thermal expansion device into the system is not favorable. In fact, the UIC and Eurocode recommend avoiding using such a device in the system because the rail expansion devices require a lot of maintenance and have some reliability issues. If an evaluation is carried by the separate simple type and the rail additional stresses exceed the allowable limits and introducing a rail expansion device will

reduce the additional stresses into an acceptable limit, the use of rail expansion device could be avoidable by carrying the evaluation according to the complete analysis type, and if the additional stresses from the variable actions on the structure are lower than the limits, there will be no need for a rail expansion device.

4.3. Computer Model for Complete and Simple Separate Analysis

The computer model required for the simple separate analysis is simple, and any FEM program with a non-linear elastic element could perform this analysis type. On the other hand, complete analysis requires a more advanced FEM computer program. The program should have the capability of performing the staged analysis. Midas Civil FEM computer program is used in this chapter for the comparison between the complete and the simple analysis. The Midas Civil program has the ability to perform the complete analysis type through its powerful tool of construction stage analysis. The program itself is designed with tools impeded in to simulate the track-structure interaction phenomena providing a link element with strain history, and a resistance could be changed through the analysis and according to the ballast state of vertical load.

4.3.1. Modeling Technique in the Computer Software

The modeling techniques used for the evaluation through this chapter are the same as in Chapter 3. The same assumptions are assumed for materials and elements where the behavior of all elements and materials apart from the connecting element between the track and the top of the deck is assumed to be linear elastic.

4.3.2. Validation of the Computer Software

The modeling technique used in Chapter 3 is validated according to UIC for the simplified separated analysis type. For Midas Civil computer program, no validation will be carried for the complete type analysis. Midas Civil computer program and the complete analysis done in it is already validated by the technical document “Rail-

Structure Interaction in accordance with UIC774-3 2012". The results of the validation will be shown in this section.

4.3.2.1. Loads Applied on the Model

4.3.2.1.1. Thermal Loads

The thermal loads considered for the verification model are the temperature variations defined by the UIC specifications. These loads are applied to the track and to the bridge deck. The load applied to the track is equal to +50 ºC and the load applied to the deck is equal to +35 ºC.

4.3.2.1.2. Braking/Traction Load

For the validation model, the braking is applied to the tracks along the train length as assumed by the UIC verification model, as shown in Figure 4.3.

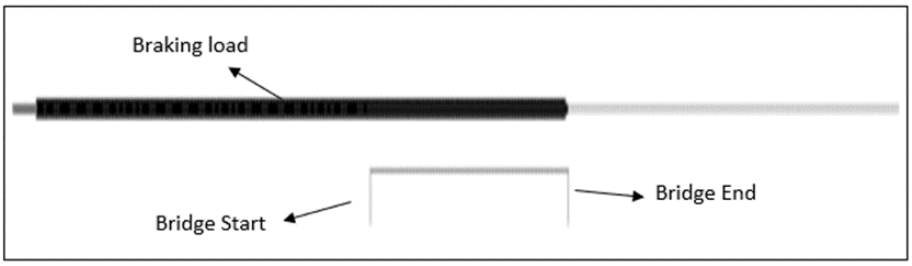

Figure 4.3. Braking Load Application on the Model

4.3.2.1.3. Train Vertical Load

The vertical load applied to the model is considered 80 (kN/m) as specified in UIC for the verification case, as shown in Figure 4.4.

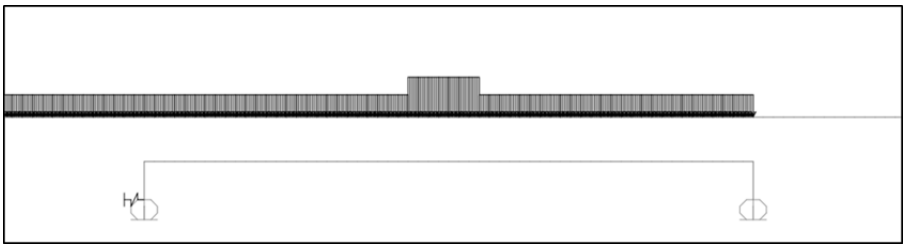

Figure 4.4. Application of Vertical Loads to the Model

4.3.2.2. Ballast Resistance Criteria

The ballast resistance used for the verification model is as per UIC specifications and shown in Table 4.1.

Table 4.1. *Ballast Resistance used for the validation per meter*

Vertical load state	*Yielding force*	*Yielding strain*
Un-Loaded	20 (kN)	2 (mm)
Loaded	60 (kN)	2 (mm)

4.3.2.3. Results Obtained from the Model

The results obtained from the verification model are summarized in the table below. The results are only reported for the thermal stress and the combined stress of thermal and train loads (through complete analysis). Table 4.2 is for case E1-3 and Table 4.3 is for case E4-6

Table 4.2. *Axial Stress Comparison Case E1-3*

Load type	*UIC (MPa)*	*Midas (MPa)*	*Difference %*
Thermal load Deck	30.67	31.87	3.90
Variable actions	182.40	188.09	3.11

Table 4.3. *Axial Stress Comparison Case E4-6*

Load type	*UIC (MPa)*	*Midas (MPa)*	*Difference %*
Thermal load Deck	30.67	31.87	3.90
Variable actions	162.06	161.37	-0.43

4.4. Comparison between Complete Simple Analysis

4.4.1. Comparison Cases Properties

In the following section, a comparison will be made between the simple separate analysis type and the complete analysis type by using the Midas Civil software. The comparison will be made through 18 different cases, each of which analyzed by using the two methods. A comparison is made between the two analyses results through the axial compression and tension rail stresses. The cases, geometrical, and section properties, are described in Table 4.4.

Table 4.4. *Analysis cases used for the comparison*

Case	*H (m)*	*N.A (m)*	K_l*(kN/mm)*	*L (m)*	*I* (m^4)	*A* (m^2)
1	1.33	1.10	100	20	0.082	4
2	2.00	2.62	150	30	0.247	4
3	2.67	2.15	200	40	0.825	5
4	3.34	2.65	250	50	3.300	6
5	4.00	3.20	300	60	6.600	10
6	4.67	3.75	350	70	13.20	8
7	5.35	4.30	400	80	26.40	10
8	6.00	4.80	450	90	41.25	12
9	1.33	1.10	100	20	0.027	4
10	2.00	2.62	150	30	0.086	4
11	2.67	2.15	200	40	0.330	5
12	3.34	2.65	250	50	0.825	6
13	4.00	3.20	300	60	1.650	10
14	4.67	3.75	350	70	5.170	8
15	5.35	4.30	400	80	6.600	10
16	6.00	4.8	450	90	10.312	12
17	4.00	3.20	120	60	6.600	10
18	4.00	3.20	120	60	1.650	10

The elastic modulus used for the bridge deck is taken as 210000 (MPa) for all cases and does not have to reflect the material property itself. In fact, it could reflect concrete material behavior because the EI product is an important factor for bending stiffness. In the UIC cases, the modulus of elasticity used for evaluation is equal to 210000 (MPa) while the thermal expansion coefficient is equal to the concrete thermal coefficient 10^{-5} K^{-1}.

Where:

H : total deck depth (m)

N.A : neutral axis ordinate measured from the deck bottom face (m)

K_l : deck support horizontal stiffness (kN/mm)

L : bridge span (m)

I : moment of inertia of the bridge deck (m^4)

A : bridge deck section cross sectional area (m^2)

It should be noted that the bridge section area has a very small effect on the track-structure interaction analysis, and this effect is negligible, as reported in Chapter 5.

4.4.2. Loads Considered for Comparison Cases

4.4.2.1. Thermal Loads

All the cases have a thermal variation load equal to ± 35 ºC. Since there is no thermal expansion device introduced to the system, the thermal variation load is only applied to the bridge deck.

4.4.2.2. Train Vertical Loads

The vertical loads considered for this particular comparison are LM-71 load model 71 with α factor equal to one. According to Eurocode, the dynamic factor Φ for enhancing the vertical load may not be used, but for this particular comparison the dynamic factor Φ is used. The vertical load is positioned in a place where it will produce the maximum deck rotation.

4.4.2.3. Train Horizontal Loads

The horizontal forces are applied according to the vertical load position. For this particular comparison only the braking effects are evaluated. The braking loads are taken equal to 20 (kN/m).

4.4.3. Ballast Resistance Criteria for Comparison Cases

The ballast resistance stiffness and the yielding strains used for this comparison are shown in Table 4.5.

Table 4.5. *Ballast Resistance Stiffness and strains for the Comparison*

Vertical load state	*Yielding force*	*Yielding strain*
Un-Loaded	20 (kN)	2 (mm)
Loaded	60 (kN)	2 (mm)

The values provided in the Table 4.5, are per one meter of track.

The horizontal stiffness of the bridge is reflected in the model through an elastic spring located at one support. The structural system adopted for the comparison cases is the simply supported system with two vertical supports and one elastic spring reflecting the horizontal support, as shown in Figure 4.5.

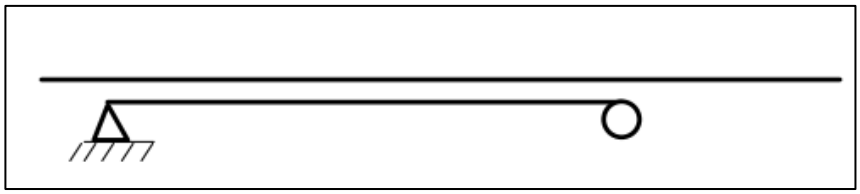

Figure 4.5. Structural System for the Comparison Cases

In the above shown system, the horizontal support is represented by the elastic spring.

4.4.4. Analysis Strategies Used for Comparison

4.4.4.1. Simplified Separated Analysis

The simplified separated analysis is performed by calculating the effects from the variable actions on the structure for each action separately. In total there will be three models for each case. The results from each analysis model are algebraically summed, and the total rail stress is calculated.

4.4.4.2. Complete Analysis

The complete analysis is performed in one model for each case. First, the thermal load is applied to the model while the ballast stiffness is considered as un-loaded, and this represents the end of the first stage. After that, the second stage is started, and the ballast stiffness is changed according to the loaded parts of the track. If there is no vertical load, the stiffness remains the same as un-loaded stiffness.

The definition of the staged analysis in Midas Civil is shown in Figure 4.6, and Figure 4.7, and Figure 4.8, and Figure 4.9. The definition of the non-linear link is shown in Figure 4.10 and Figure 4.11.

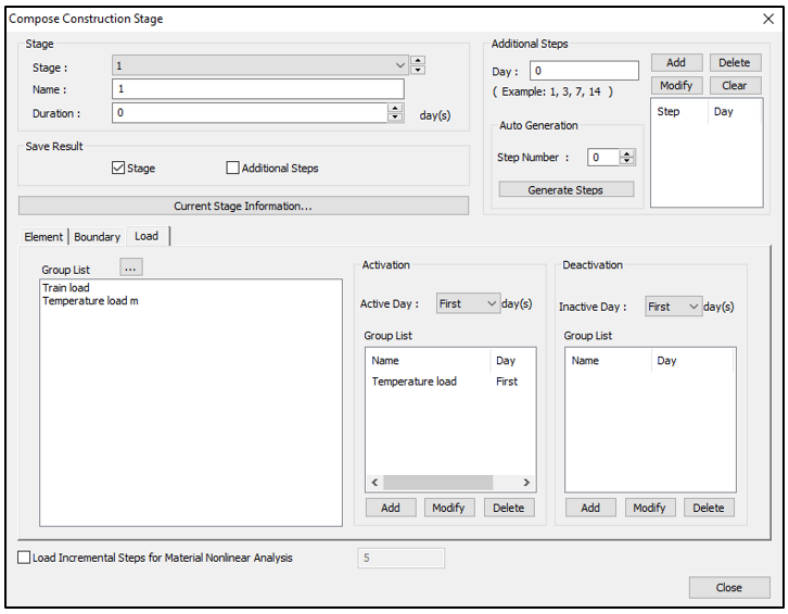

Figure 4.6. Staged Analysis Loads Definition Stage-1

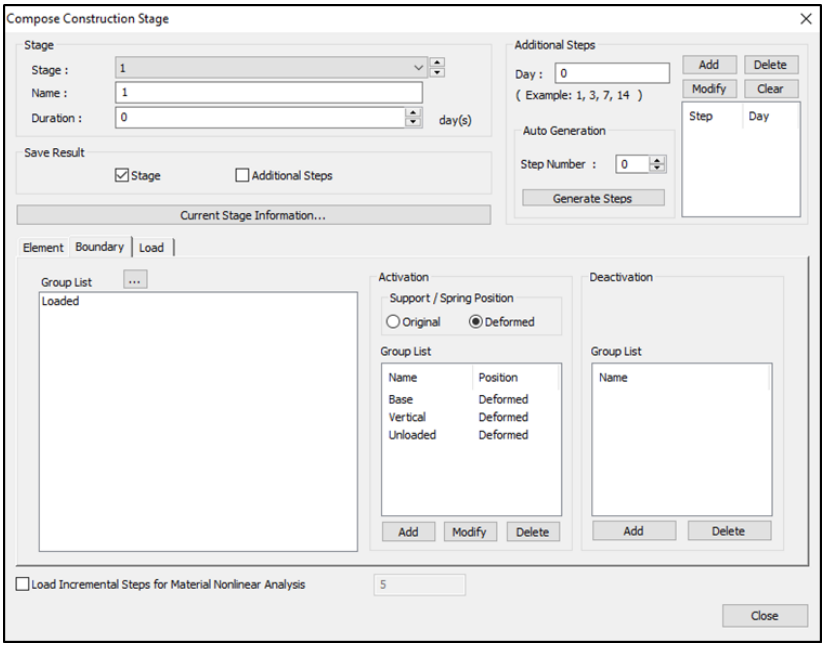

Figure 4.7. Staged Analysis Boundary Definition Stage-1

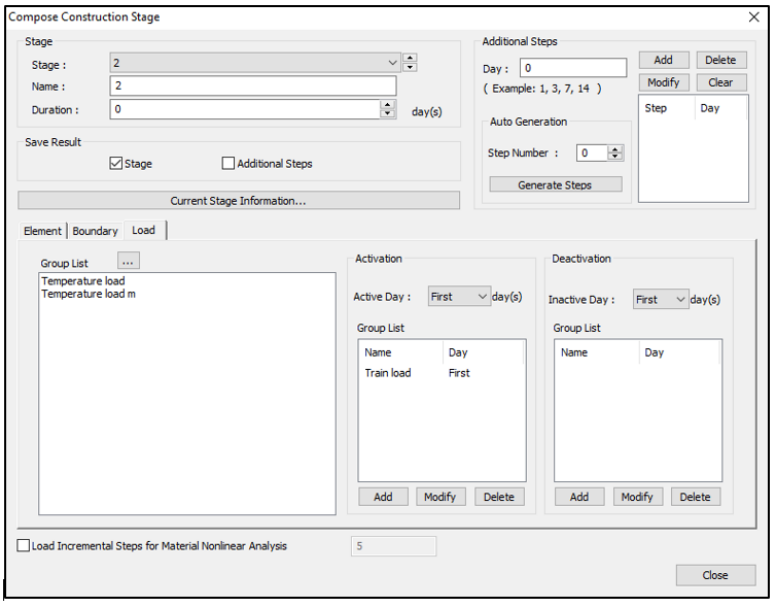

Figure 4.8. Staged Analysis Loads Definition Stage-2

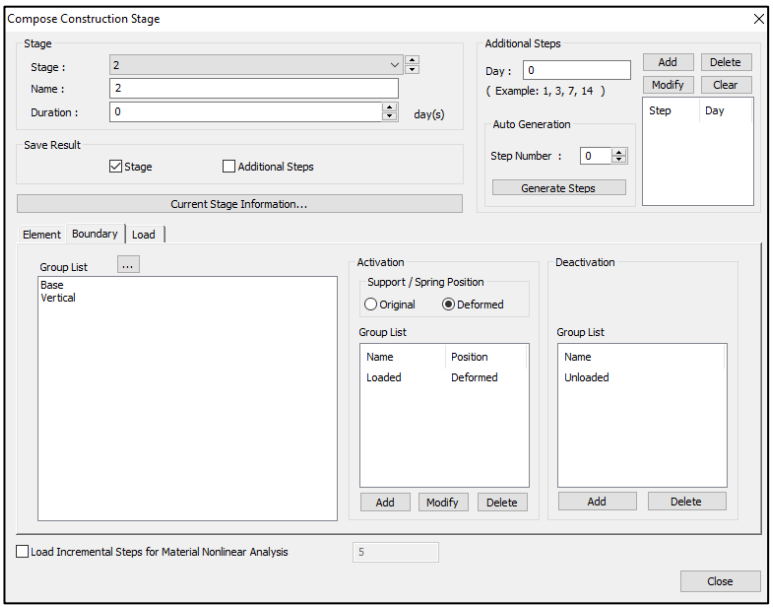

Figure 4.9. Staged Analysis Boundary Definition Stage-2

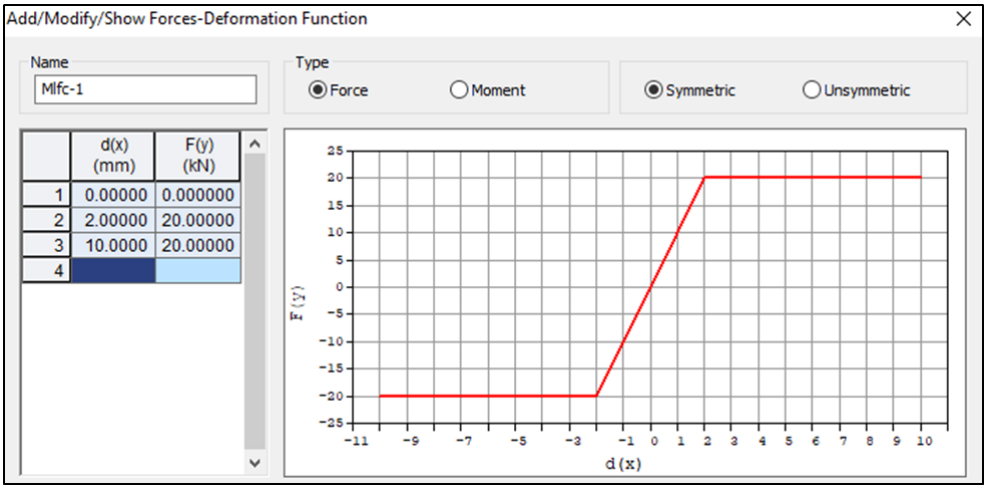

Figure 4.10. Un-loaded Link Element Definition

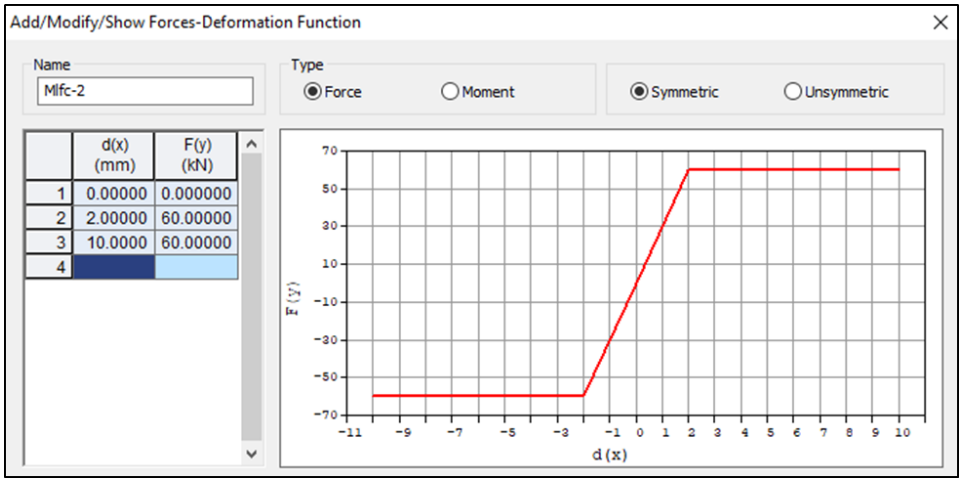

Figure 4.11. Loaded Link Element Definition

4.5. Comparison Results

The results obtained from the simple separated analysis and complete analysis for the cases 1-18 are compared. The total rail stress resulted from variable actions along the rail axis is plotted for the simple separated analysis and complete analysis on the same chart. The plots are provided for cases 1 to case 16. The comparison is provided for cases having the same bridge span length.

Rail stress for case-1 and case-9 are shown in Figure 4.12 and Figure 4.13.

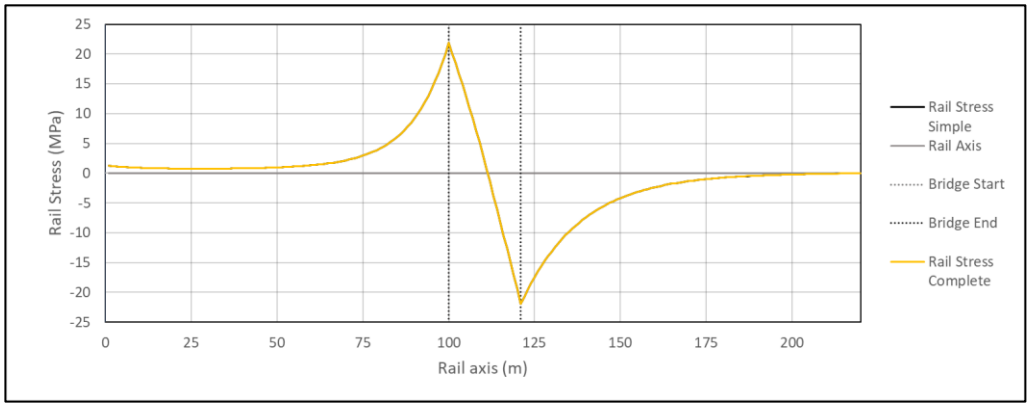

Figure 4.12. Case-1 Complete and Separate Rail Stress

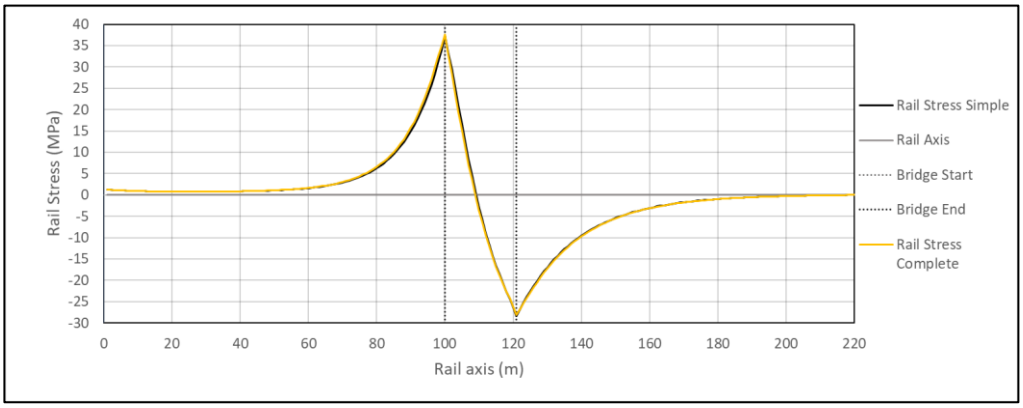

Figure 4.13. Case-9 Complete and Separate Rail Stress

Rail stress for case-2 and case-10 are shown in Figure 4.14 and Figure 4.15.

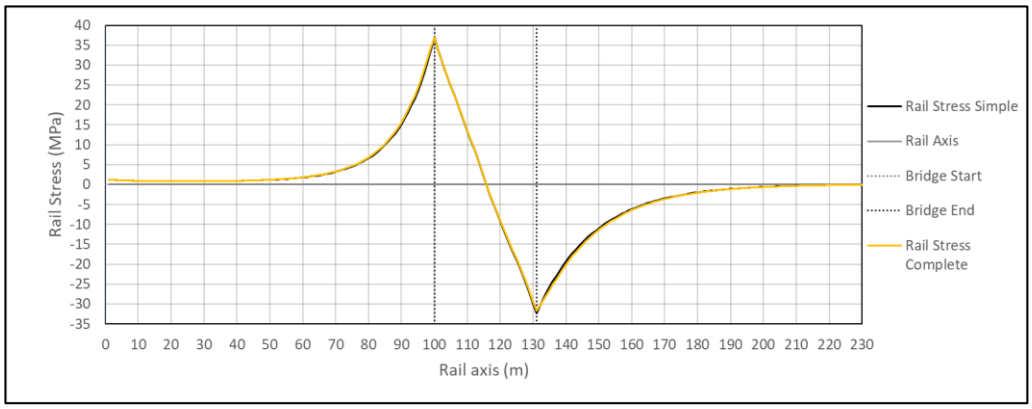

Figure 4.14. Case-2 Complete and Separate Rail Stress

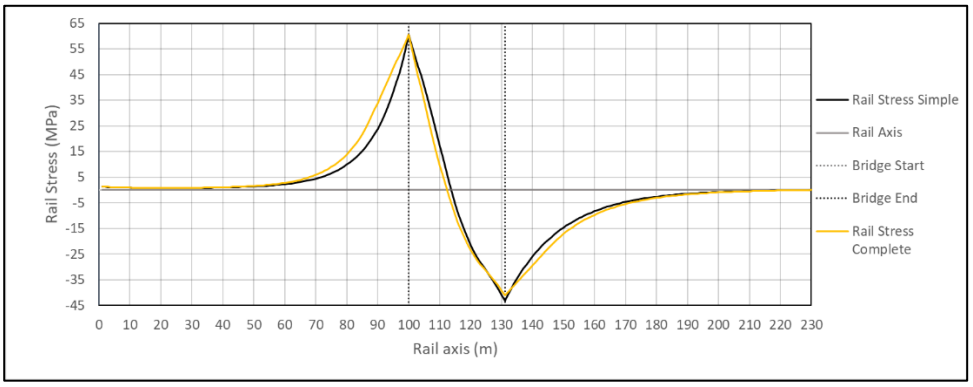

Figure 4.15. Case-10 Complete and Separate Rail Stress

Rail stress for case-3 and case-11 are shown in Figure 4.16 and Figure 4.17.

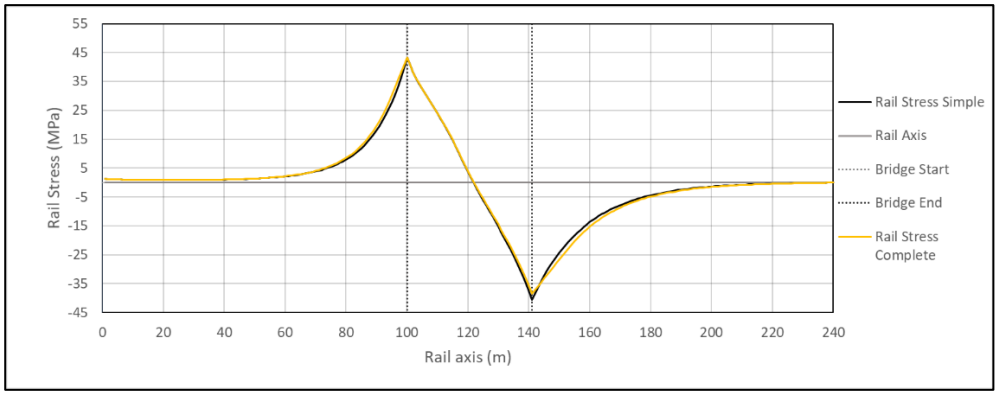

Figure 4.16. Case-3 Complete and Separate Rail Stress

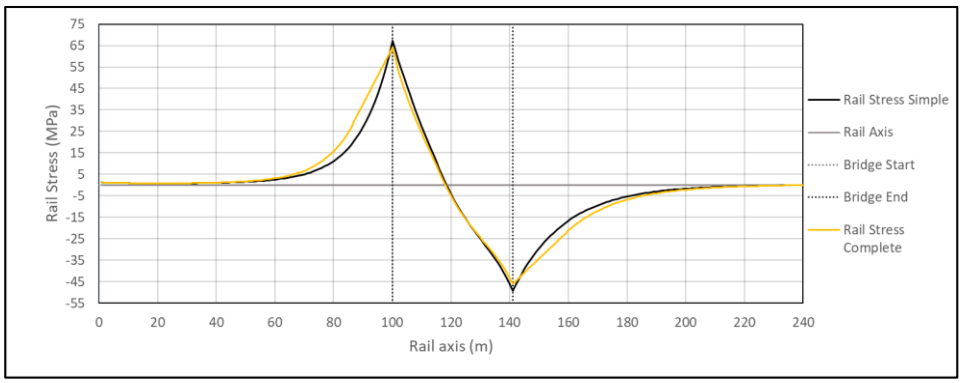

Figure 4.17. Case-11 Complete and Separate Rail Stress

Rail stress for case-4 and case-12 are shown in Figure 4.18 and Figure 4.19.

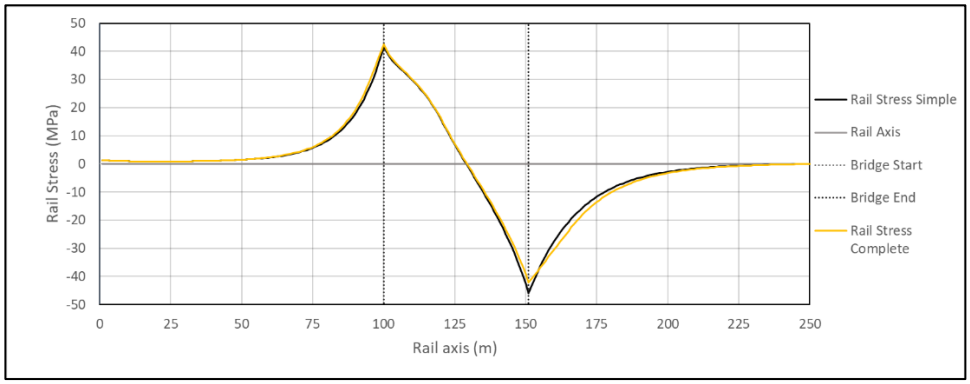

Figure 4.18. Case-4 Complete and Separate Rail Stress

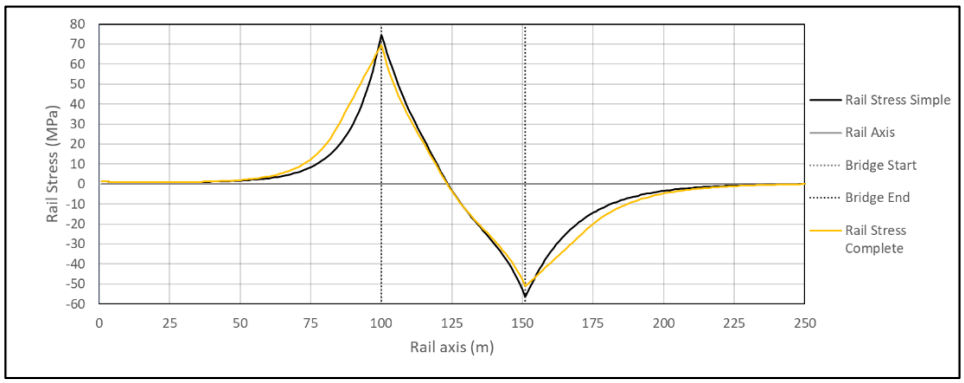

Figure 4.19. Case-12 Complete and Separate Rail Stress

Rail stress for case-5 and case-13 are shown in Figure 4.20 and Figure 4.21.

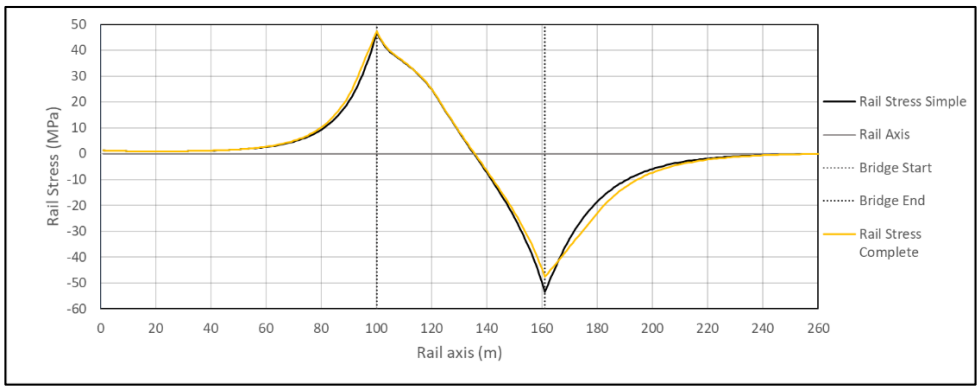

Figure 4.20. Case-5 Complete and Separate Rail Stress

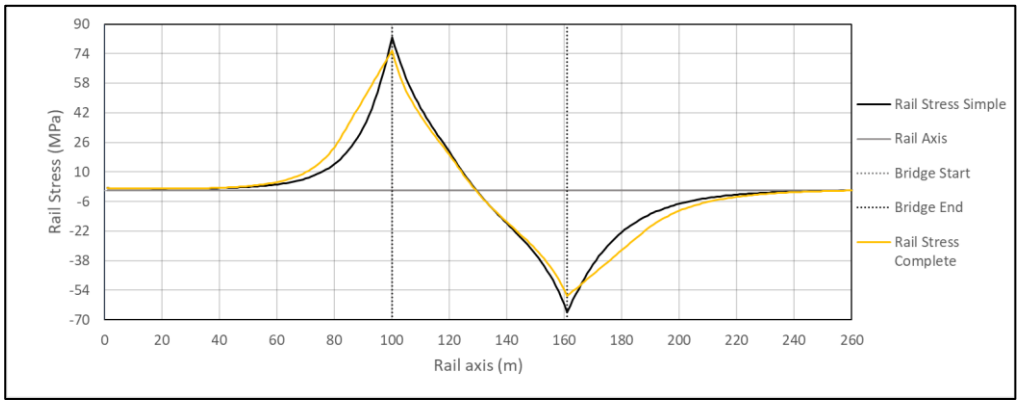

Figure 4.21. Case-13 Complete and Separate Rail Stress

Rail stress for case-6 and case-14 are shown in Figure 4.22 and Figure 4.23.

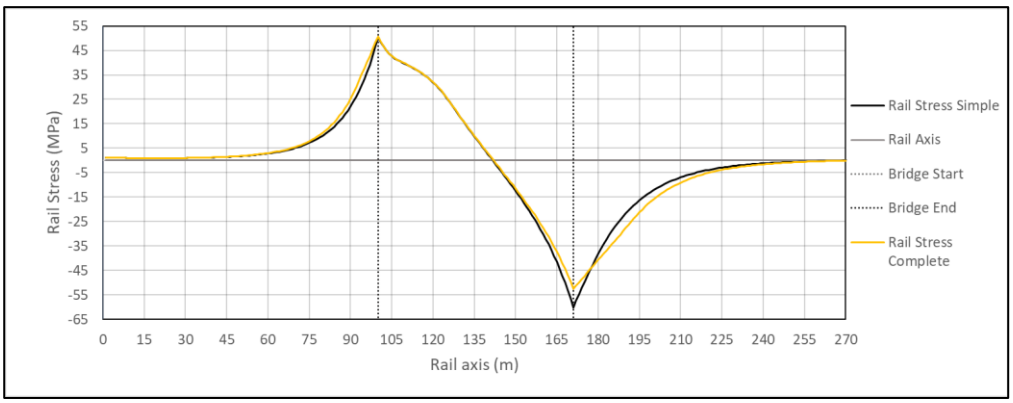

Figure 4.22. Case-6 Complete and Separate Rail Stress

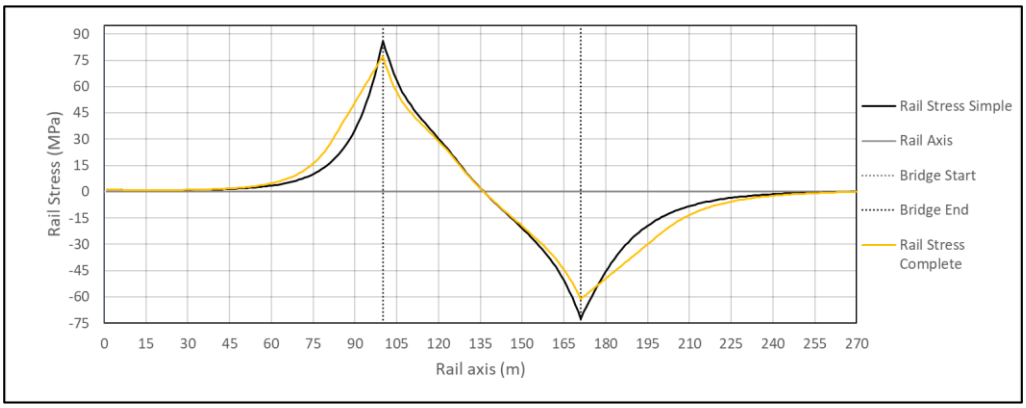

Figure 4.23. Case-14 Complete and Separate Rail Stress

Rail stress for case-7 and case-15 are shown in Figure 4.24 and Figure 4.25.

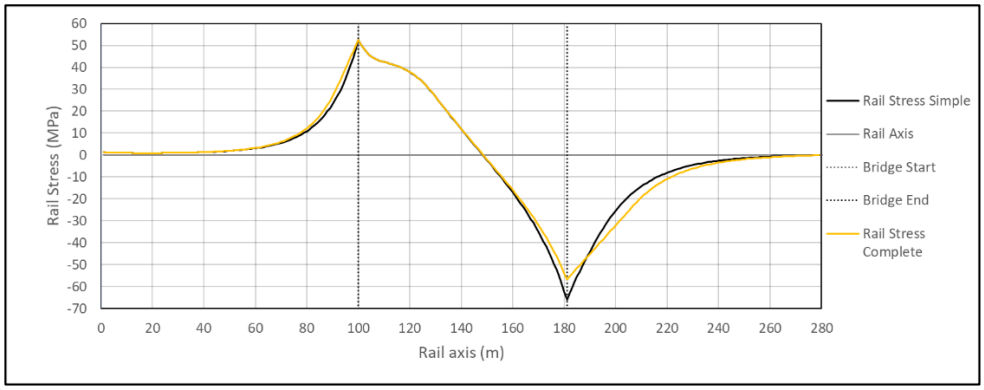

Figure 4.24. Case-7 Complete and Separate Rail Stress

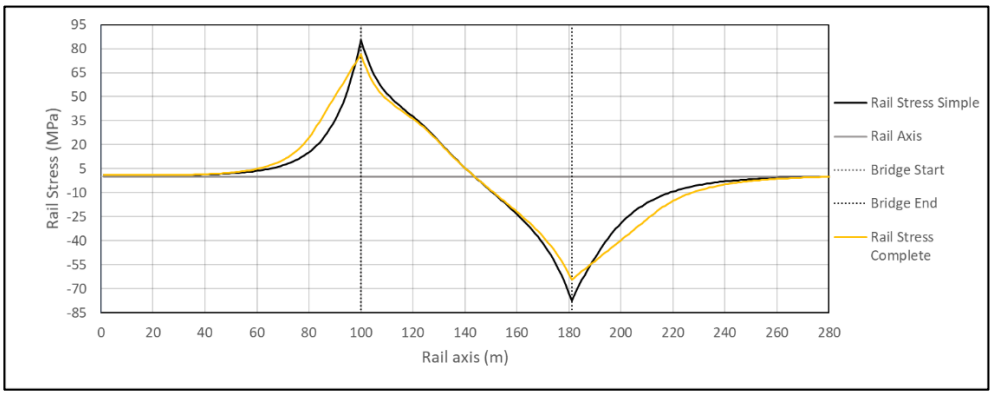

Figure 4.25. Case-15 Complete and Separate Rail Stress

Rail stress for case-8 and case-16 are shown in Figure 4.26 and Figure 4.27.

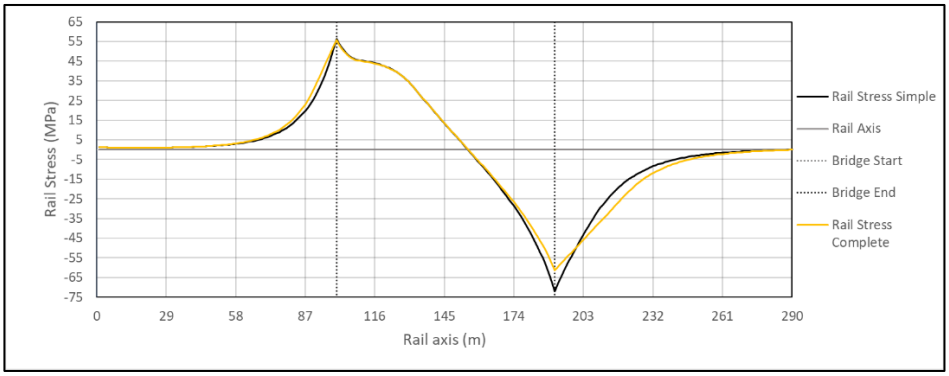

Figure 4.26. Case-8 Complete and Separate Rail Stress

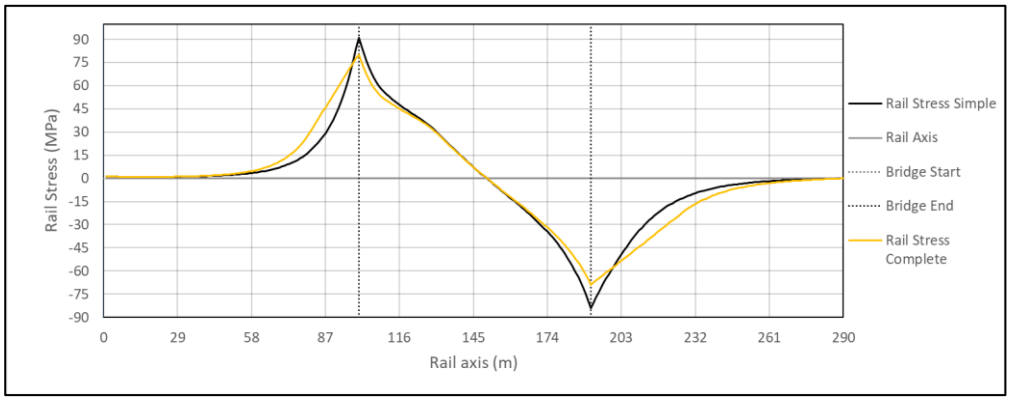

Figure 4.27. Case-16 Complete and Separate Rail Stress

Rail stress for case-5 and case-17 are shown in Figure 4.28 and Figure 4.29.

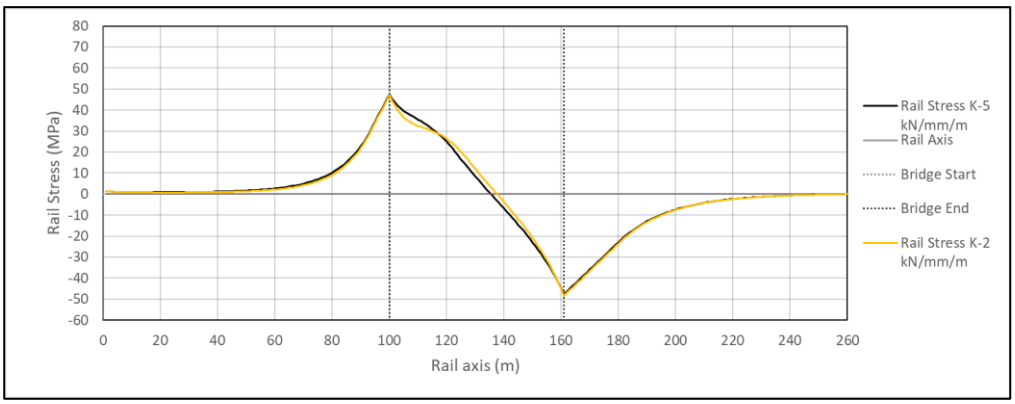

Figure 4.28. Case-5 and Case-17 Complete Rail Stress

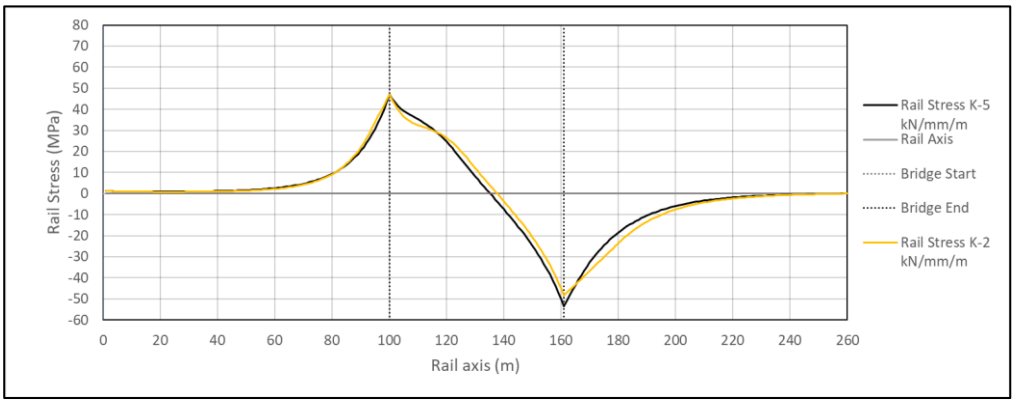

Figure 4.29. Case-5 and Case-17 Separate Rail Stress

Rail stress for case-13 and case-18 are shown in Figure 4.30 and Figure 4.31.

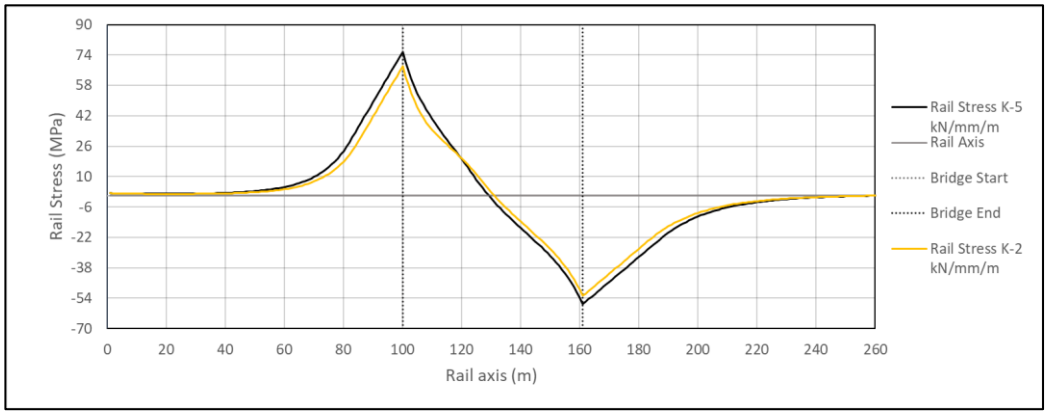

Figure 4.30. Case-13 and Case-18 Complete Rail Stress

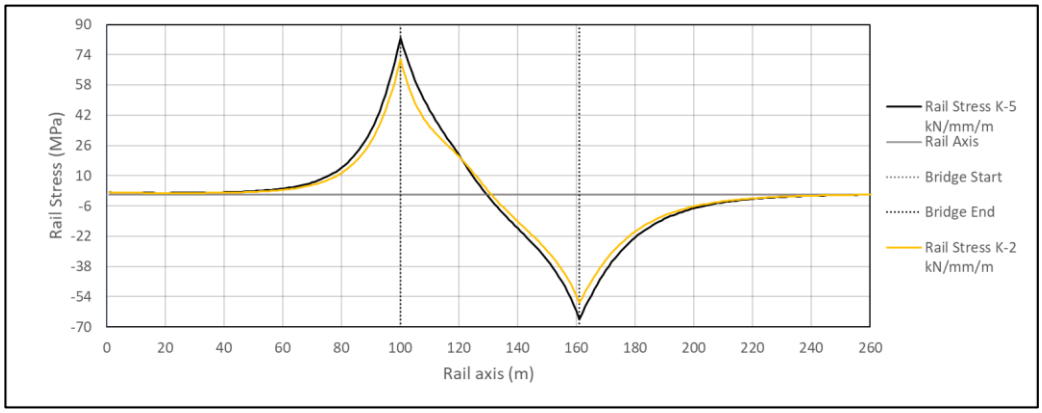

Figure 4.31. Case-13 and Case-18 Separate Rail Stress

The last two cases consider the longitudinal spring stiffness variation (cases 13-18). The effect of longitudinal stiffness is discussed in detail in Chapter 5.

The stress results from both complete and separate analyses are given in Table 4.6, and the rail stresses are shown in Figure 4.32 and Figure 4.33.

Table 4.6. *Compression Stress in Rail for the Comparison Cases*

Case	*Complete (MPa)*	*Separate (MPa)*	*Difference (%)*
1	-21.93	-21.93	0.00
2	-31.71	-32.34	1.98
3	-38.52	-40.67	5.58
4	-42.19	-45.93	8.86
5	-47.68	-53.52	12.24
6	-52.45	-60.10	14.58
7	-56.75	-65.89	16.11
8	-61.31	-72.01	17.45
9	-28.10	-28.36	0.90
10	-41.17	-43.28	5.14
11	-46.04	-49.27	7.03
12	-51.11	-56.64	10.82
13	-57.10	-65.87	15.36
14	-61.22	-72.46	18.36
15	-64.33	-77.28	20.13
16	-68.85	-84.16	22.24

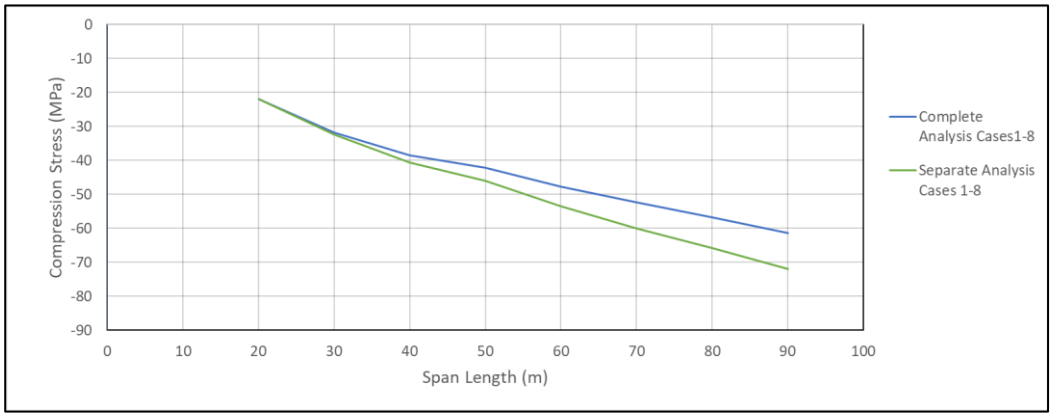

Figure 4.32. Compression Stress for Cases 1-8

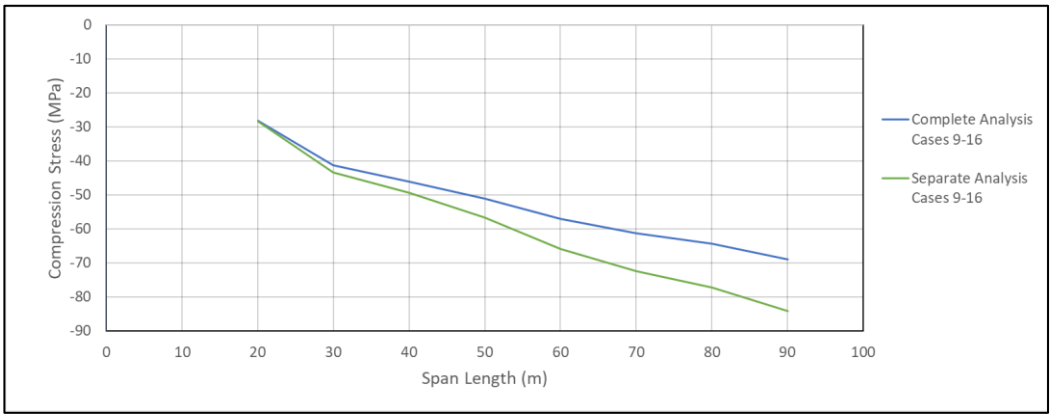

Figure 4.33. Compression Stress for Cases 9-16

According to these results, it could be found that the simple separate type analysis always gives higher stress, especially for compression stress. The difference between the Complete and the Simple Separate analysis increases by the increase in the span length. For the same span length, the difference increases when the flexural stiffness is decreased, or when the top deck displacement is higher.

The top deck displacement for each case is given in Table 4.7 and Table 4.8.

Table 4.7. *Deck top Displacement for Comparison Cases part-1*

Case	*Displacement (mm)*
1	1.38
2	2.31
3	2.18
4	1.38
5	1.44
6	1.36
7	1.19
8	1.25
9	3.88

Table 4.8. *Deck top Displacement for Comparison Cases part-2*

Case	*Displacement (mm)*
10	6.40
11	5.20
12	5.22
13	5.46
14	5.17
15	4.58
16	4.82
17	1.02
18	3.93

CHAPTER 5

SENESITIVITY ANALYSIS FOR BRIDGE DECK

In this chapter, a sensitivity analysis is performed on the bridge deck for high-speed railway bridge structure. Parameters affecting the track-bridge interaction are identified, and how changing their value will affect the overall response of the bridge-track interaction is explained. The methodology followed for this particular study is as follows; apart from the parameter under consideration, all other parameters are held constant, then changing the value of the parameter under consideration will show the effect of this parameter on the interaction, then another parameter is chosen and its effect is observed till finishing all the parameters affecting the interaction phenomena.

5.1. Bridge Deck Types for High-Speed Railway Bridges

For this study, the bridge deck type is not directly selected, some deck types covered by this study are shown in Figure 5.1, and Figure 5.2, and Figure 5.3. Since the maximum allowable length is limited by the top deck displacement under vertical loads, any bridge deck satisfying the top deck displacement is covered with some limitations as follows:

- The track center of gravity lies above the section neutral axis
- The total deck height H lies between the values of (L/8 – L/35) (m)
- The neutral axis location is between 0.5 H to 0.95 H of the deck height from the bottom surface of the deck
- The deck cross-section area is physically achievable

The bridge bending stiffness is limited by the bridge top deck displacement.

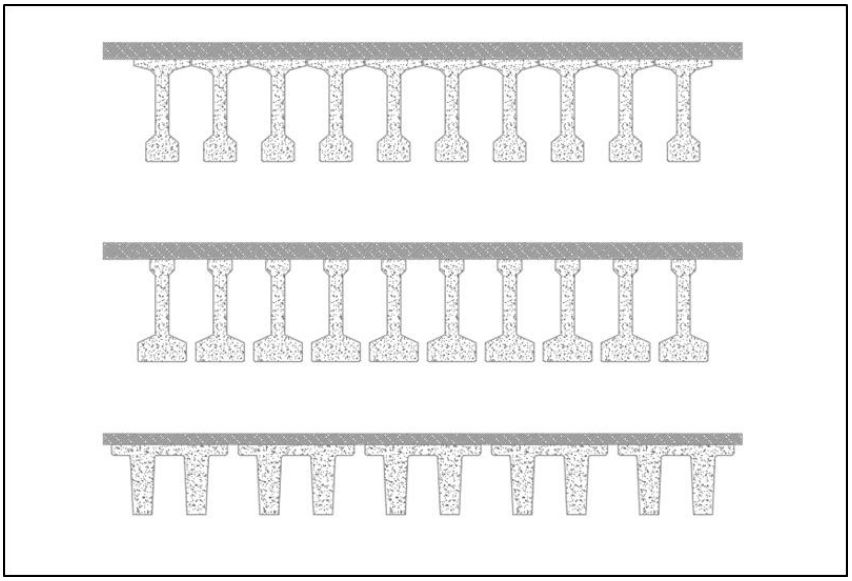

Figure 5.1. Ordinary High-speed Railway Deck, Precast Sections

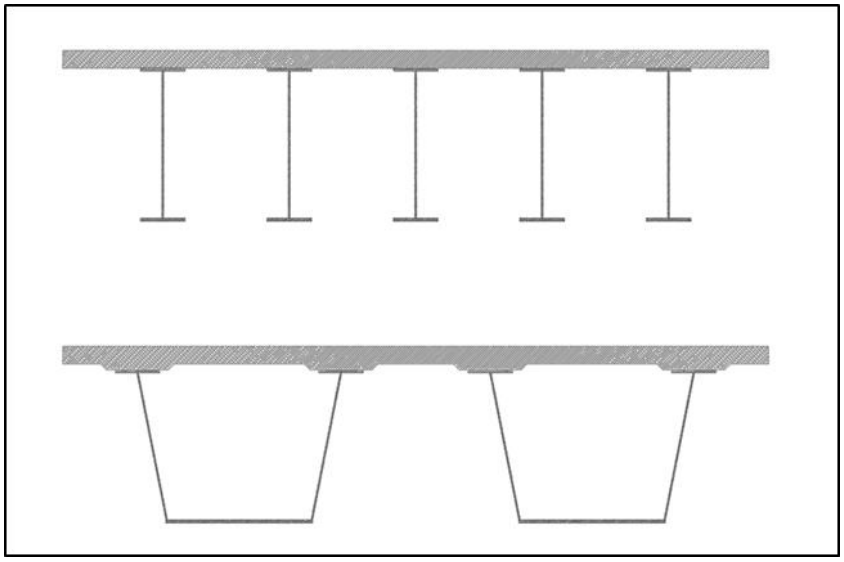

Figure 5.2. Ordinary High-speed Railway Deck, Composite Sections

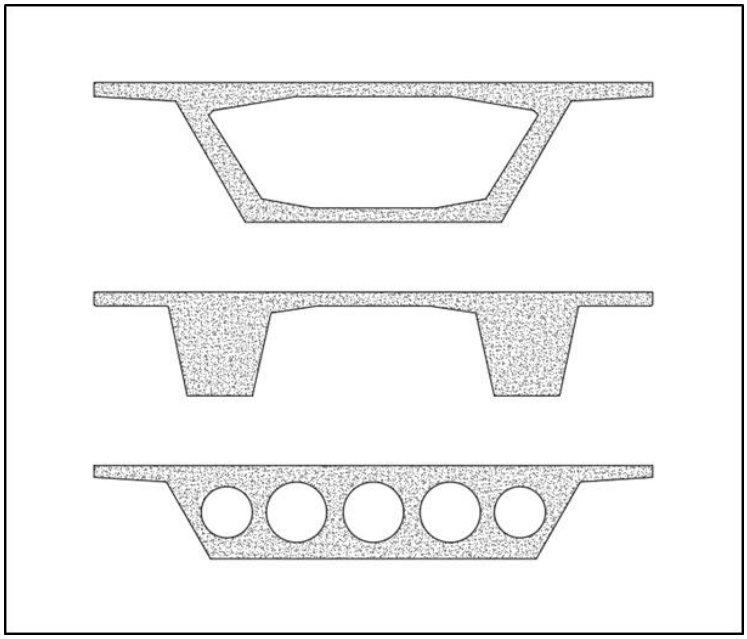

Figure 5.3. Ordinary High-speed Railway Deck, Cast in Place Sections

5.2. Parameters Affecting Track-Bridge Interaction

Train movement over the bridge will induce horizontal and vertical forces. The rails are positioned on the ballast above the bridge deck. Due to vertical loads, the bridge deck will bend, and due to horizontal forces bridge deck will sway, and also, due to thermal actions bridge will expand or contract. It should be noted from the previously mentioned actions the bridge parameters affecting the deck behavior are:

- Longitudinal stiffness of substructure (1)
- Expansion length of the bridge deck (2)
- Deck bending stiffness (3)
- The total depth of bridge deck (4)
- Neutral-axis ordinate (5)
- The axial stiffness of bridge deck (6)
- Track configuration (7)
- Rail type and longitudinal stiffness (8)

- Rail thermal expansion device (9)

For this particular study, the effect from 7,8, and 9, is kept constant. Since the track configuration is assumed as ballast bed with a minimum thickness of 30 (cm) and no rail thermal expansion device is used on the bridge deck or 100 (m) away from the bridge start and end, and a fixed rail type is used UIC-60 with standard track gauge according to European standards. Other parameters are discussed in detail.

5.2.1. Longitudinal Stiffness of Substructure

Bridge decks for high-speed railways have factors affecting the track-bridge interaction. The bridge deck longitudinal movement -as shown in Figure 5.4- is prevented by a restraint. This resistance could be provided by guided bearing or integrated column with the superstructure. Bearings are supported by pier or abutment which they are supported by the foundation, substructure under lateral forces will induce extra deformations due to:

- Pier bending will induce extra lateral movement (1)
- Rotation of the foundation will induce lateral movement (2)
- Displacement of the foundation (3)
- All of these displacements will result in total extra lateral movement (4)

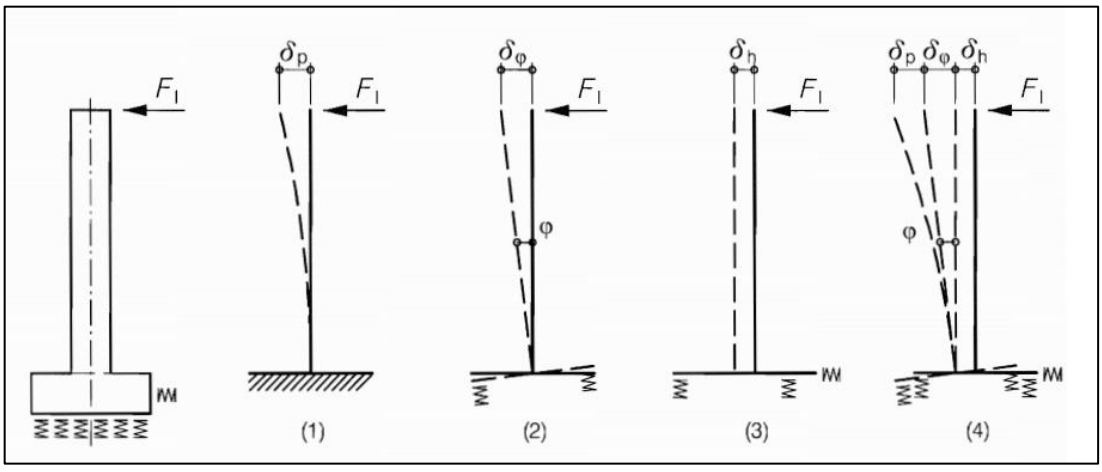

Figure 5.4. Equivalent Lateral Displacement of the Support

In this parametric study, the lateral stiffness of the complete substructure, including the foundation system, is simulated by a linear spring at the bearing location reflecting the equivalent longitudinal stiffness of the substructure.

5.2.2. Expansion Length of Bridge Deck

Bridge expansion length will directly affect the deck movement under temperature rise or fall. Bridge expansion length is determined according to the total deck length and to the support's configuration. In this particular study, only one type of bridge decks is considered, the simply supported bridge deck. The bridge deck is assumed to have a free-to-slide bearing on one end and horizontal support on the other end as shown in Figure 5.5. This support is simulated by the linear spring.

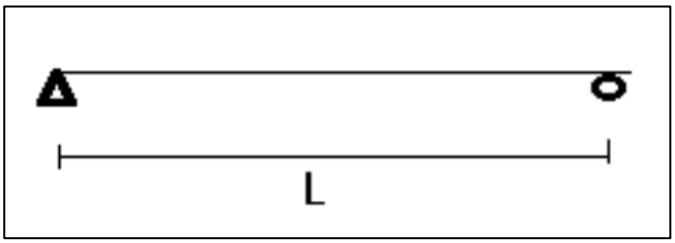

Figure 5.5. Simply Supported Bridge Deck with Expansion Length (L)

5.2.3. Deck Mechanical Properties

The bridge deck mechanical properties include the deck inertia, deck height, neutral axis location relative to the top surface of the deck, and cross-sectional area of the deck section. Deck material will affect the bending stiffness and the axial rigidity of the bridge deck through Young's Modulus of Elasticity E (MPa). In this particular study, the deck inertia and material will be treated as one parameter through the product EI. This assumption will make this parametric study cover a wide range of deck types, concrete and, steel bridge decks. Concrete modulus of elasticity is related to concrete grade e.g. C35, C40, C50, C60. Using the product of EI will overcome the variation of the modulus of elasticity according to the material used. Vertical loads will make the deck bend and bending of the deck will cause the top surface to deform

laterally, as shown in Figure 5.6. This movement is affected by the deck total height, neutral axis location, and bending stiffness.

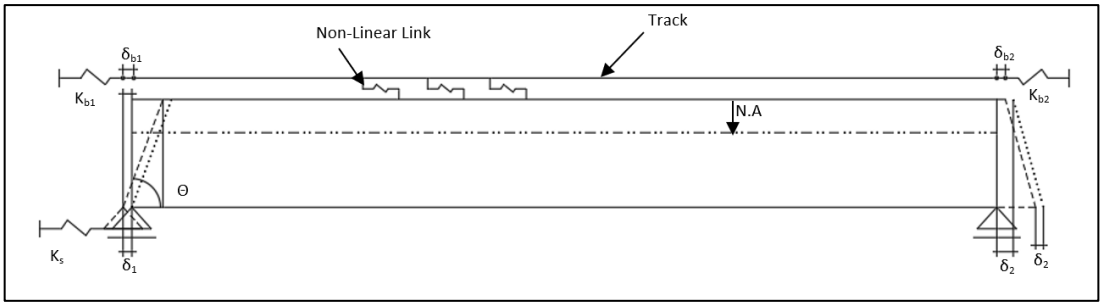

Figure 5.6. Deck Bending Components

Where:

- K_s : the substructure horizontal stiffness
- N.A: the Neutral axis distance from the top
- δ_{b1}: the displacement in the track due to the interaction in the behind fill
- δ_{b2}: the displacement in the track due to the interaction in the front fill
- δ_1: the displacement due to the horizontal stiffness of the supporting system at the point of support
- δ2: the displacement due to the horizontal stiffness of the supporting system on the other end
- K_{b1}: the track horizontal stiffness due to the interaction in the behind fill
- K_{b1}: the track horizontal stiffness due to the interaction in the front fill
- Θ: the rotation of the deck system due to vertical loads

5.2.4. Track Configuration

Track configuration used for this study is based on ballasted bed with a minimum thickness of 30 (cm) and concrete sleepers spaced not more than 65 (cm). The plastic

low of ballast behavior adapted in Eurocode and UIC shown in Figure 5.7 is used, with a dynamic factor assumed for standard maintenance condition.

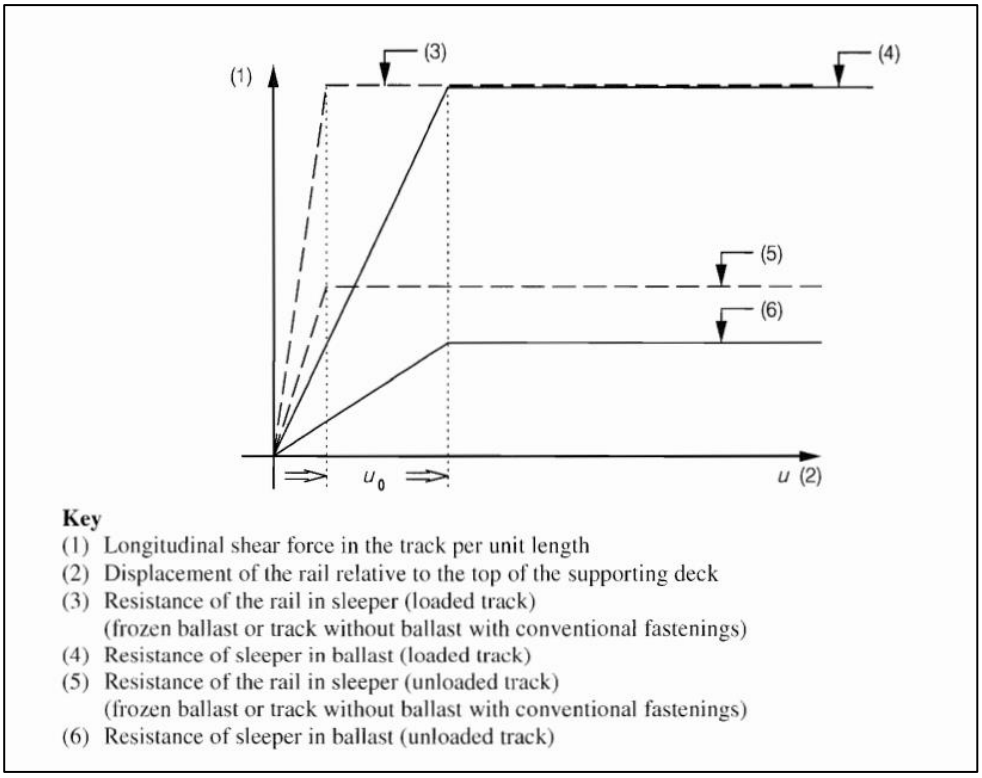

Figure 5.7. Ballast Resistance for Parametric Study

The track ballast resistance force and yielding displacement are similar to the values assumed in Table 2.2.

5.2.5. Rail Type

For this particular study, only one rail type is used UIC-60. The mechanical properties of the rail are shown in Table 5.1.

Table 5.1. *Mechanical Properties of UIC-60*

Property	*Value*	*Unite*
Area	76.70	cm^2
Moment of inertia	3038.30	cm^4
Total depth	172	mm
Bending axis from bottom	76.25	mm
Thermal expansion coefficient	1.2E-6	K^{-1}
E Young's Modulus	210000	MPa

5.3. Loads for the Parametric Study

For this particular study, thermal and traffic loads are considered. Traffic consist of vertical load and horizontal loads.

5.3.1. Thermal loads

Thermal load is applied to the bridge deck structure as a temperature variation from reference temperature, which is assumed as 0 ºC and the thermal variation is taken as ±35 ºC with two load cases temperature rise and temperature fall. Since there is no rail thermal expansion device used, the thermal load is not applied to the rail.

5.3.2. Vertical Loads

Vertical loads are based on Load Model -71 (LM-71) train load defined in Eurocode and enhanced by the dynamic factor for moderate maintenance shown in Figure 2.19. The value of the alpha factor (α) is taken equal to 1 for the parametric study.

5.3.3. Horizontal Forces

Horizontal forces due to train traffic consist of two separate loads; braking and traction/acceleration load.

5.3.3.1. Braking Force

Braking force is considered as uniformly distributed force accompanied by vertical load location. Braking load magnitude is 20 (kN/m). The braking loads are not enhanced with dynamic factor, but they are multiplied by α factor accordingly. The maximum braking force is limited according to the loaded, length not by a fixed value. The maximum allowed loading length of the braking force for this study is taken equal to 300 (m).

5.3.3.2. Traction/Acceleration Force

Traction/Acceleration force is considered as uniformly distributed force accompanied by vertical load location. acceleration load magnitude is 33 (kN/m). The acceleration loads are not enhanced with dynamic factor, but they are multiplied by α factor accordingly. The maximum acceleration force is limited according to the loaded length, not by a fixed value. The maximum allowed loading length of the acceleration force for this study is taken equal to 30 (m).

5.3.4. Modeling Approach and Load Application on the Model

For the parametric study, finite element models are created, and the analysis is performed using SAP 2000 FEM computer program. The modeling approach is the same validate modeling approach used in Chapter-3. Loads applied to the model are applied in a way to produce the maximum effect. Vertical loads are positioned to produce the maximum top displacement and maximum stress in the rails. Horizontal loads are placed to produce the maximum deck sway displacement and maximum rail stresses. The maximum response is also related to ballast condition (loaded/unloaded). For considering the maximum effect, many analyses are run for vertical and horizontal loads with different portions of deck span loaded, and the case producing the maximum result is considered. For each bridge deck case four different models are created

5.3.4.1. Type-1 Model

For this model, all ballast loading state are unloaded, and the resistance of the ballasted is the unloaded resistance. This model type is used for investigating the thermal load effect on the bridge deck.

5.3.4.2. Type-2 Model

For this model, the embankment behind the bridge and the bridge structure ballast state is loaded and unloaded for the embankment front of the bridge is unloaded, as shown in Figure 5.8. This model according to analysis results, found to be the model producing the maximum rail stresses under vertical and horizontal forces.

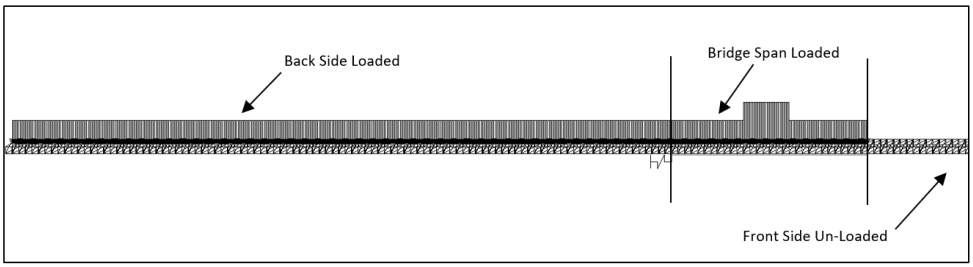

Figure 5.8. Bridge Model Loading for Type-2 Model

5.3.4.3. Type-3 Model

In this model, only the bridge deck is loaded, and the ballast state is loaded. For the embankment in front of and behind the bridge, the ballast state is unloaded. This model is found to produce the maximum deck top displacement and deck absolute displacement under traction forces.

5.3.4.4. Type-4 Model

This model is only valid for braking force application. For all bridge deck and embankment, the ballast state is loaded. This model, in some cases produces the maximum absolute deck sway displacement under braking force.

5.4. Limits for Parametric Study

The limits used for the additional rail stresses and relative and absolute displacement for this study are shown in Table 5.2.

Table 5.2. *Enter the Table Caption here*

Limit Type	*Action*	*Value*	*Unite*
Compression Stress	Variable	72	MPa
Tension Stress	Variable	92	MPa
Absolute Displacement	Braking/Traction	5	mm
Relative Displacement	Braking/Traction	5	mm
Relative Displacement	Vertical Loads	8	mm

5.5. Bridge Deck Parameters Effect on the Response to Interaction

Bridge parameters effect on the track-structure interaction is investigated according to the applied loads. How each parameter affects the bridge response to a specific load will be shown. There might be some parameters that do not have any effects. These parameters are defined for each load.

5.5.1. Thermal Load

Thermal load is primarily affected by the expansion length of the bridge (bridge deck span), and the stiffness of the longitudinal supporting system, the deck area, bending stiffness, deck height and neutral axis ordinate are found to have no effect on the thermal load stresses.

Different cross-section area affects the rail stress are shown in Figure 5.9, Figure 5.10, Figure 5.11 and Figure 5.12 of bridge decks with the same span length and longitudinal stiffness. Bridge deck properties are shown in Table 5.3.

Temperature rise case:

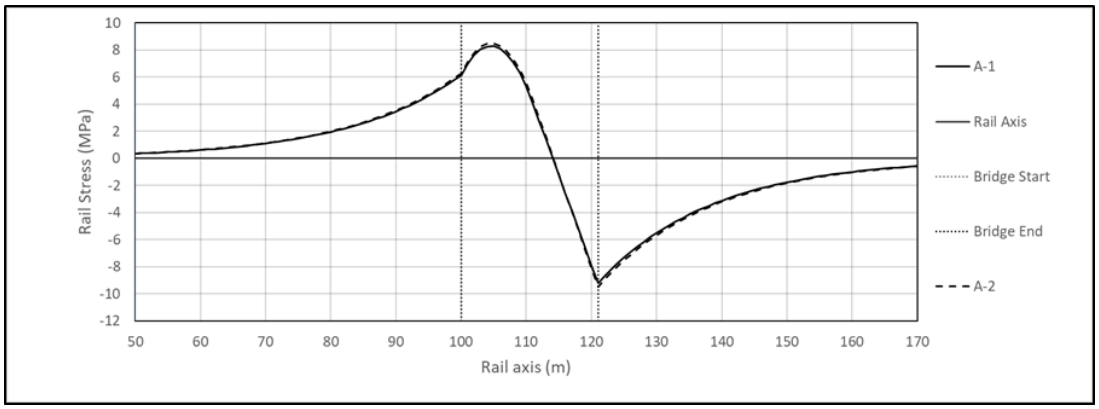

Figure 5.9. Deck with 20 (m) Span Length and Longitudinal Stiffness k-2 T(+)

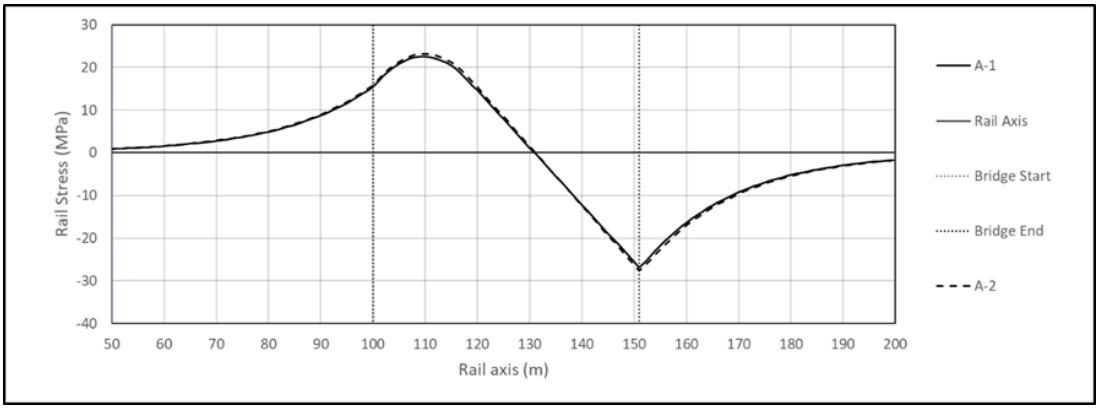

Figure 5.10. Deck with 50 (m) Span Length and Longitudinal Stiffness k-20 T(+)

Temperature fall case:

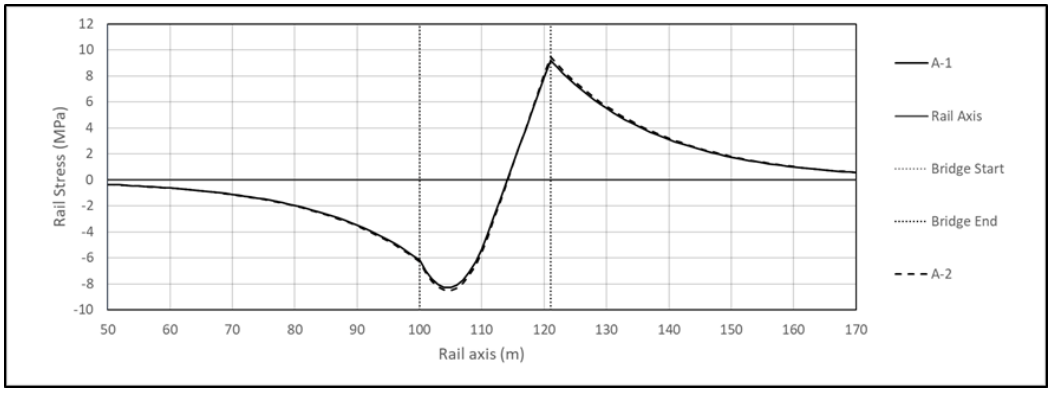

Figure 5.11. Deck with 20 (m) Span Length and Longitudinal Stiffness k-2 T(-)

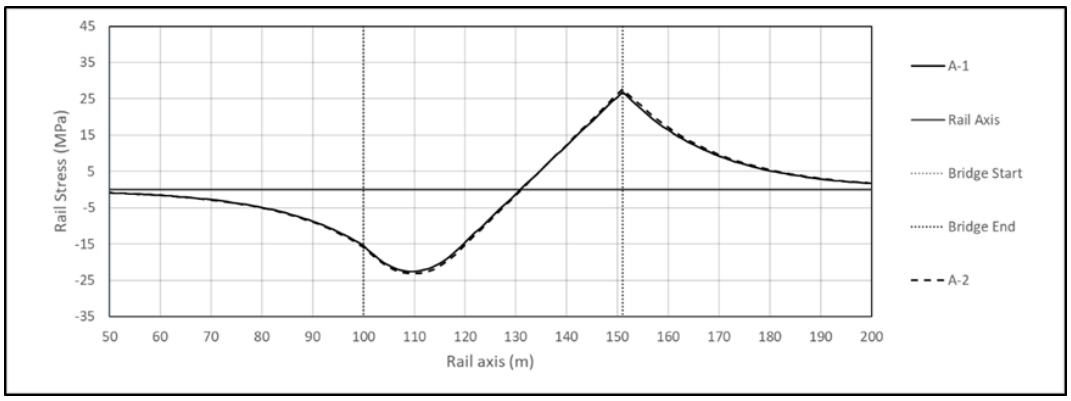

Figure 5.12. Deck with 50 (m) Span Length and Longitudinal Stiffness k-20 T(-)

Table 5.3. *Deck Properties for Area Effect under Thermal Loads*

Span Length (m)	*Area Type*	*Area (m^2)*	*Stiffness per (m/track) (kN/mm)*	*Total Longitudinal Stiffness (kN/mm)*
20	A-1	2	2	40
20	A-2	8	2	40
50	A-1	3	20	1000
50	A-2	9	20	1000

Rail stresses under thermal load for fixed and free longitudinal stiffness of the support are shown in Figure 5.13, Figure 5.14, Figure 5.15 and Figure 5.16.

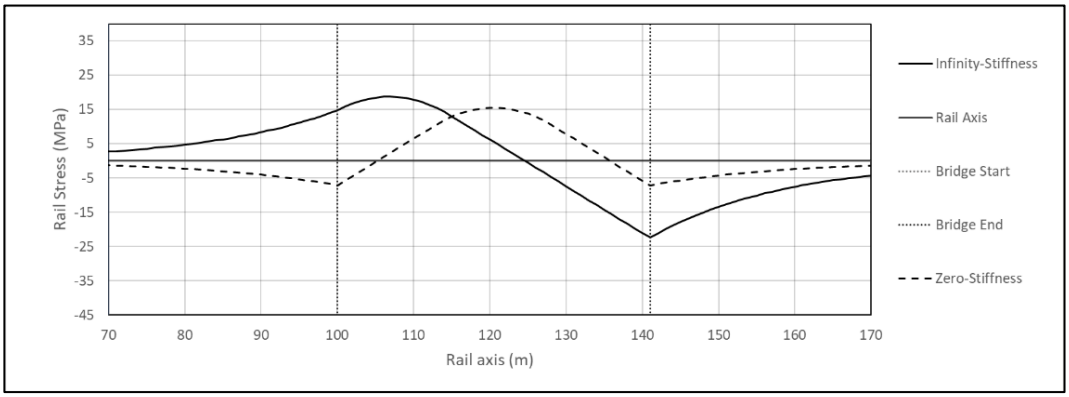

Figure 5.13. Temperature Rise Rail Stresses for 40 (m) Deck Span

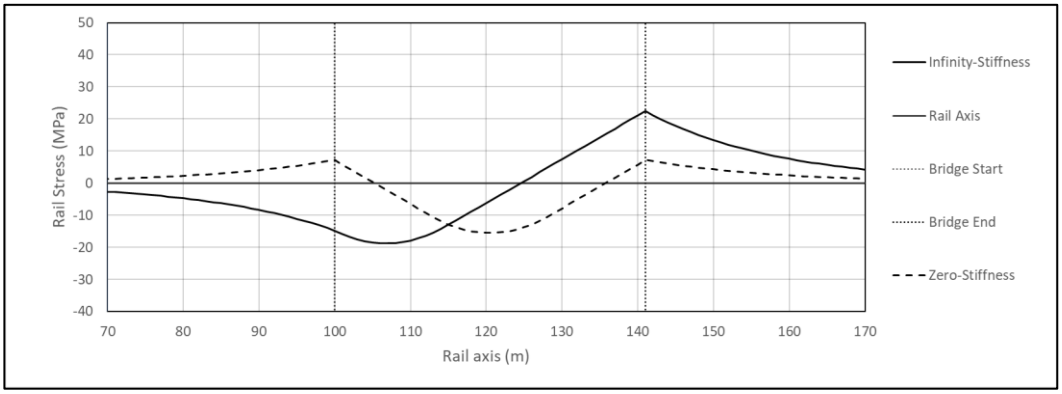

Figure 5.14. Temperature Fall Rail Stresses for 40 (m) Deck Span

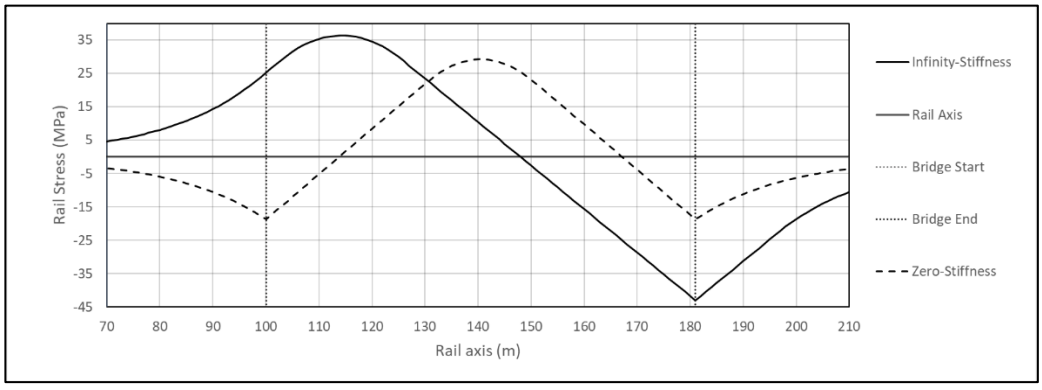

Figure 5.15. Temperature Rise Rail Stresses for 80 (m) Deck Span

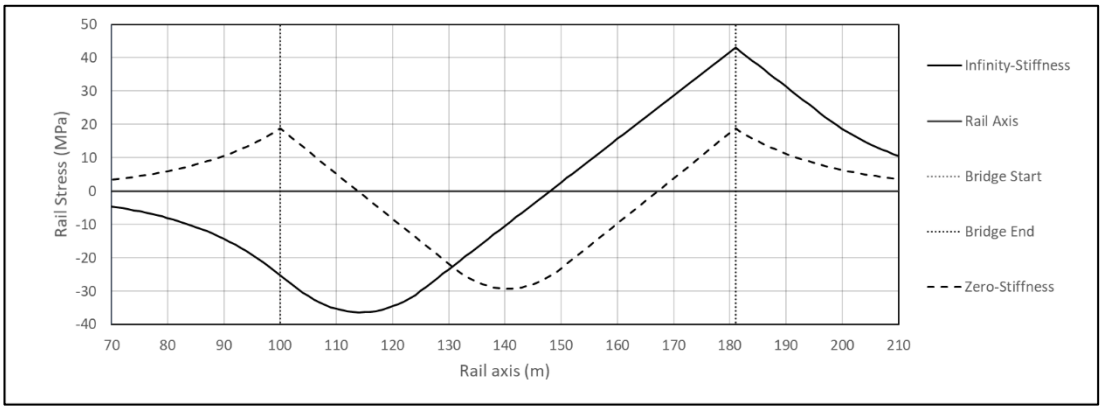

Figure 5.16. Temperature Fall Rail Stresses for 80 (m) Deck Span

Rail stress for different longitudinal stiffness with the same bridge deck span are shown in Figure 5.17, Figure 5.18, Figure 5.19 and Figure 5.20.

Temperature rise case:

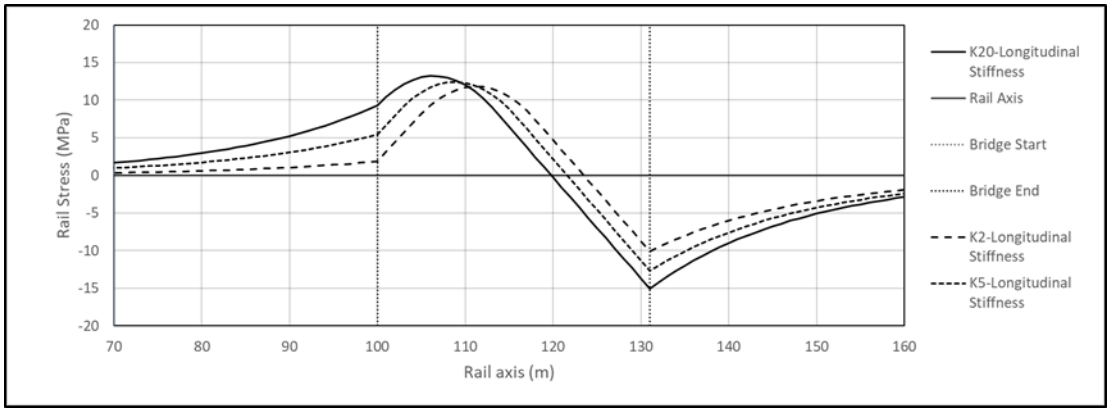

Figure 5.17. Rail Stress for 30 (m) bridge span with different longitudinal stiffness T(+)

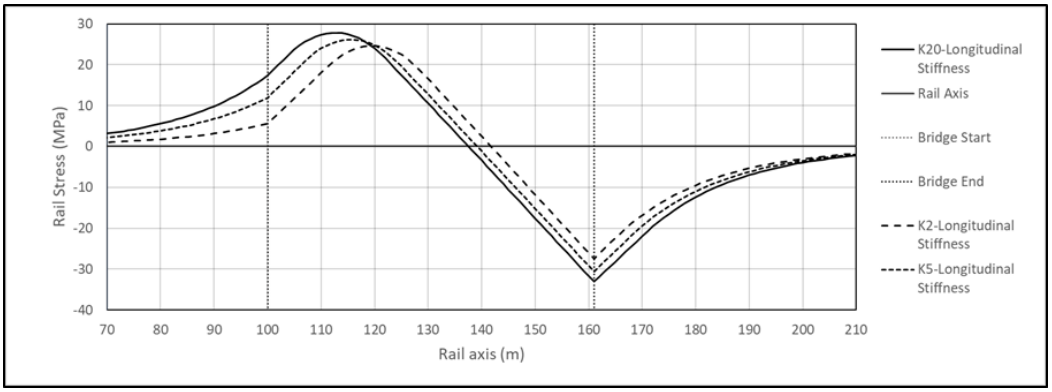

Figure 5.18. Rail Stress for 60 (m) bridge span with different longitudinal stiffness T(+)

Temperature fall case:

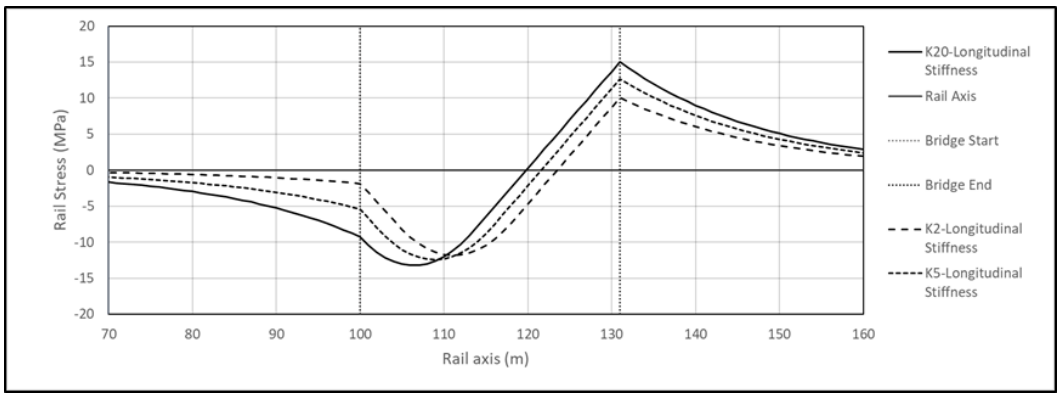

Figure 5.19. Rail Stress for 30 (m) bridge span with different longitudinal stiffness T(-)

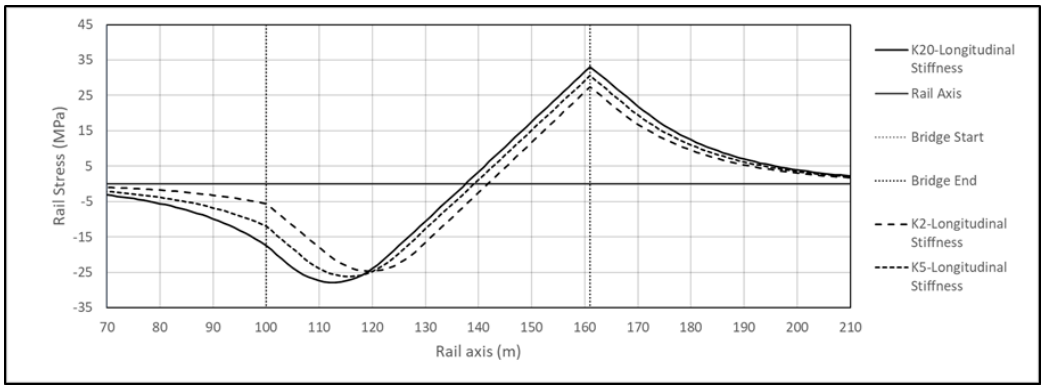

Figure 5.20. Rail Stress for 60 (m) bridge span with different longitudinal stiffness T(-)

Rail stress for the same longitudinal stiffness and different span length are shown in Figure 5.21, Figure 5.22, Figure 5.23, Figure 5.24, Figure 2.25 and Figure 5.26.

Temperature rise case:

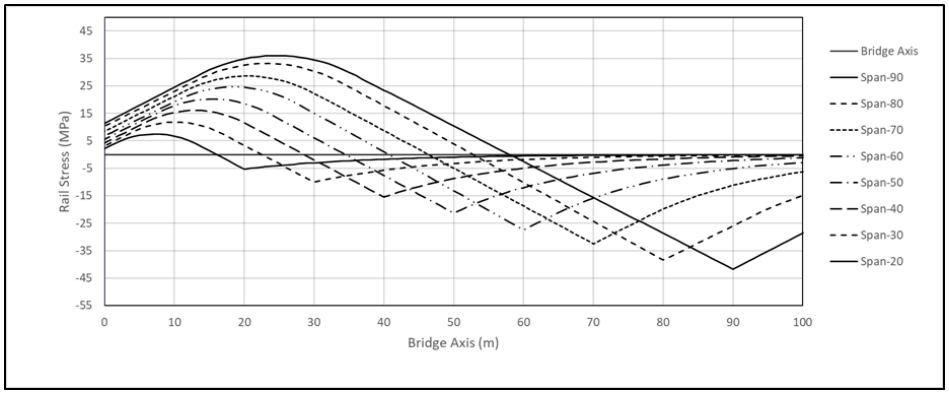

Figure 5.21. Rail Stress for Longitudinal Stiffness equal to 2 (kN/mm) per meter per track T (+)

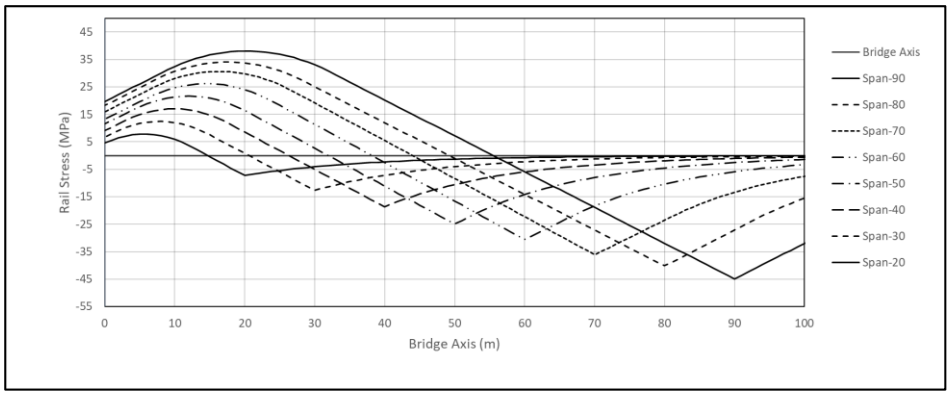

Figure 5.22. Rail Stress for Longitudinal Stiffness equal to 5 (kN/mm) per meter per track T (+)

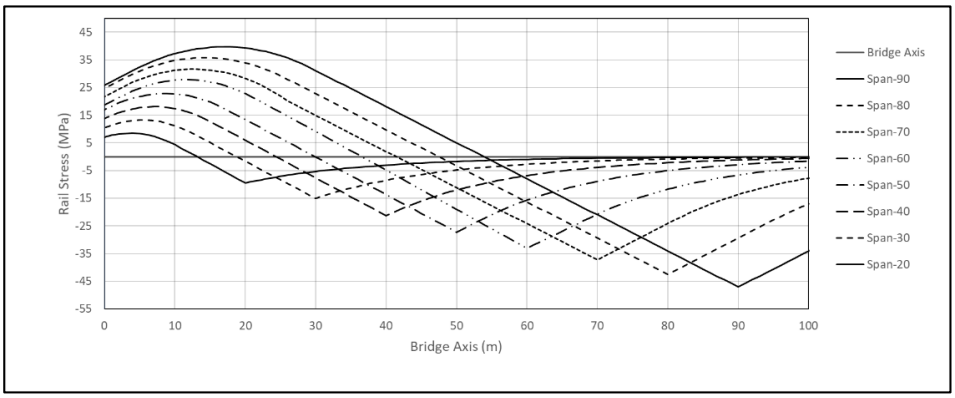

Figure 5.23. Rail Stress for Longitudinal Stiffness equal to 20 (kN/mm) per meter per track T (+)

Temperature fall case:

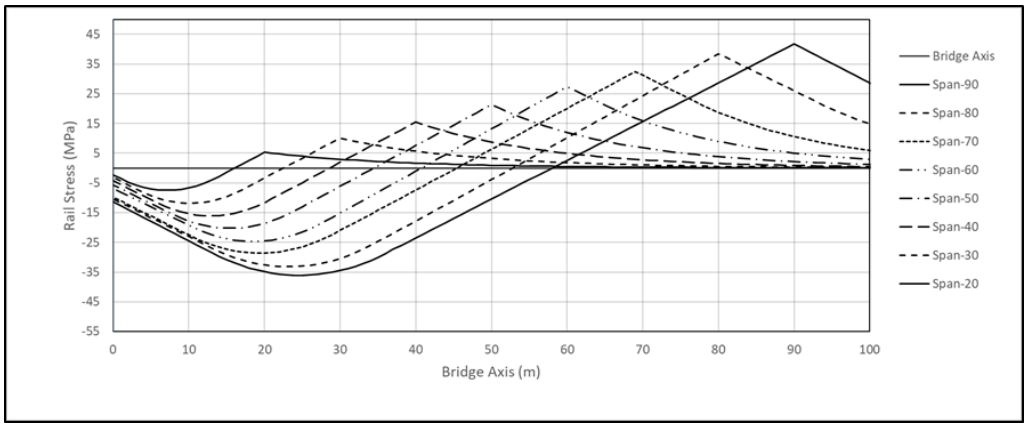

Figure 5.24. Rail Stress for Longitudinal Stiffness equal to 2 (kN/mm) per meter per track T (-)

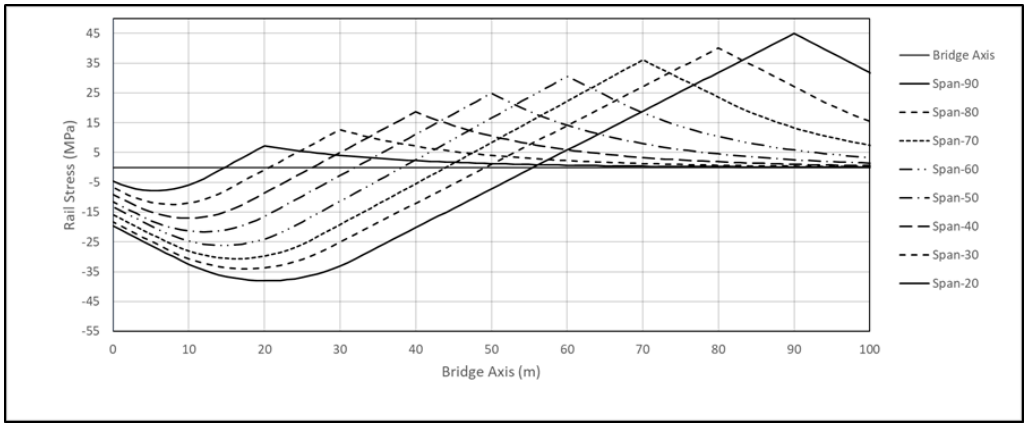

Figure 5.25. Rail Stress for Longitudinal Stiffness equal to 5 (kN/mm) per meter per track T (-)

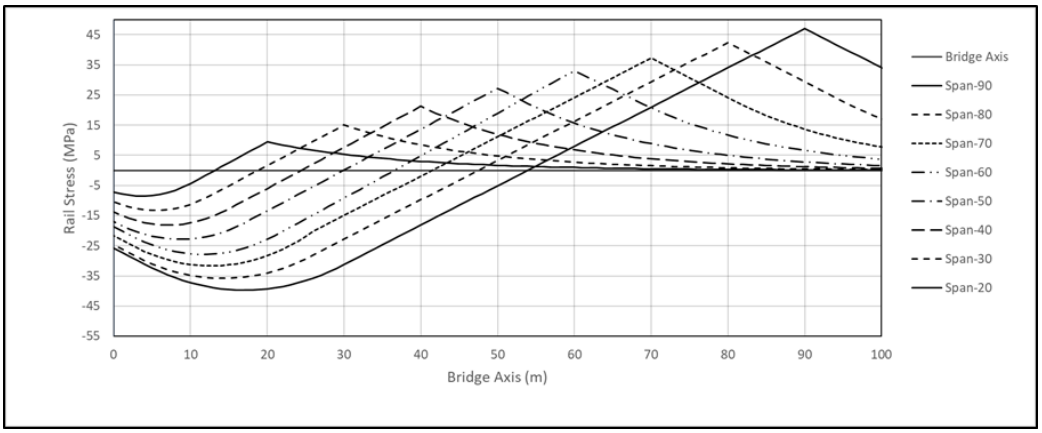

Figure 5.26. Rail Stress for Longitudinal Stiffness equal to 20 (kN/mm) per meter per track T (-)

5.5.2. Horizontal loads

The braking and acceleration forces are found to be directly affected by the bridge span length and the longitudinal stiffness of the system. Deck mechanical properties are found to have limited effect. The effect magnitude changes according to the longitudinal stiffness of the substructure system. The effect of the longitudinal stiffness of the substructure is directly affected by the bending stiffness of the system. For low longitudinal stiffness with both high and low bending stiffness, there is not any effect from deck height and neutral axis location. The rail stress is directly related to the deck span length and longitudinal stiffness. For high longitudinal stiffness with high bending stiffness, there is not any effect from deck height, and neutral axis rail stress is directly affected by bridge deck span, and longitudinal stiffness for high longitudinal stiffness with low bending stiffness, deck height and neutral axis location has an effect on rail stress. The effect magnitude is related to the bending stiffness of the bridge deck. Rail stresses are directly affected by span length bending stiffness and marginally by bridge deck height and neutral axis location. It is found that the deeper the deck, the higher the stress will result in rail; the closer the neutral axis to the top of the deck, the higher the rail stress is. Rail stresses along the rail axis are plotted for each case under the longitudinal force applied to all rail sections.

Rail stresses for bridge decks with 20 (m) span and different bending stiffness, deck height and neutral axis location are shown in Figure 2.27, Figure 2.28, Figure 2.29 and Figure 2.30.

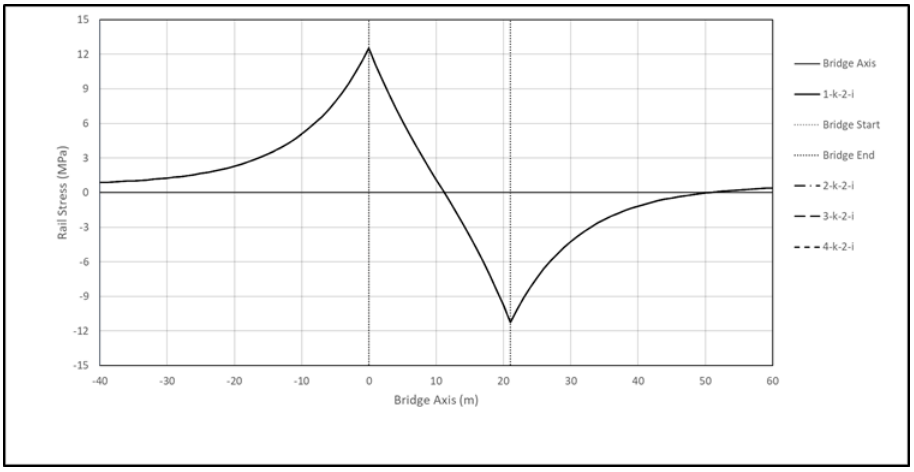

Figure 5.27. Rail Stress 20 (m) Span, k-2 Stiffness and High Bending Stiffness

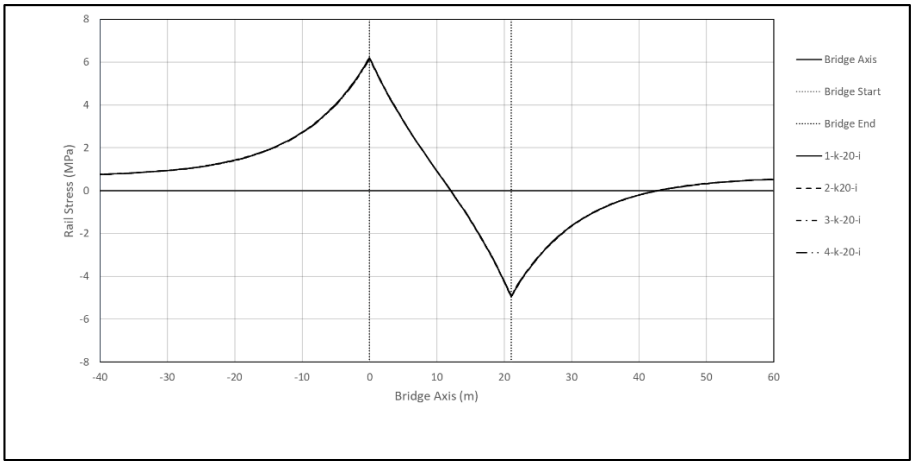

Figure 5.28. Rail Stress 20 (m) Span, k-20 Stiffness and High Bending Stiffness

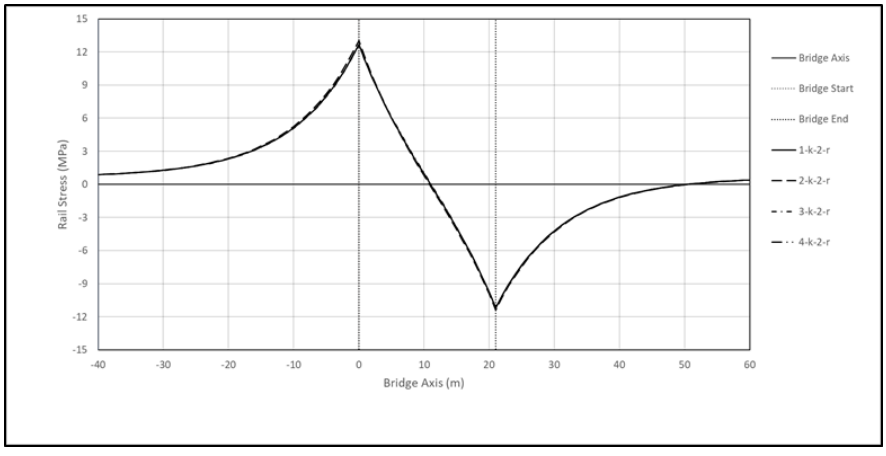

Figure 5.29. Rail Stress 20 (m) Span, k-2 Stiffness and Low Bending Stiffness

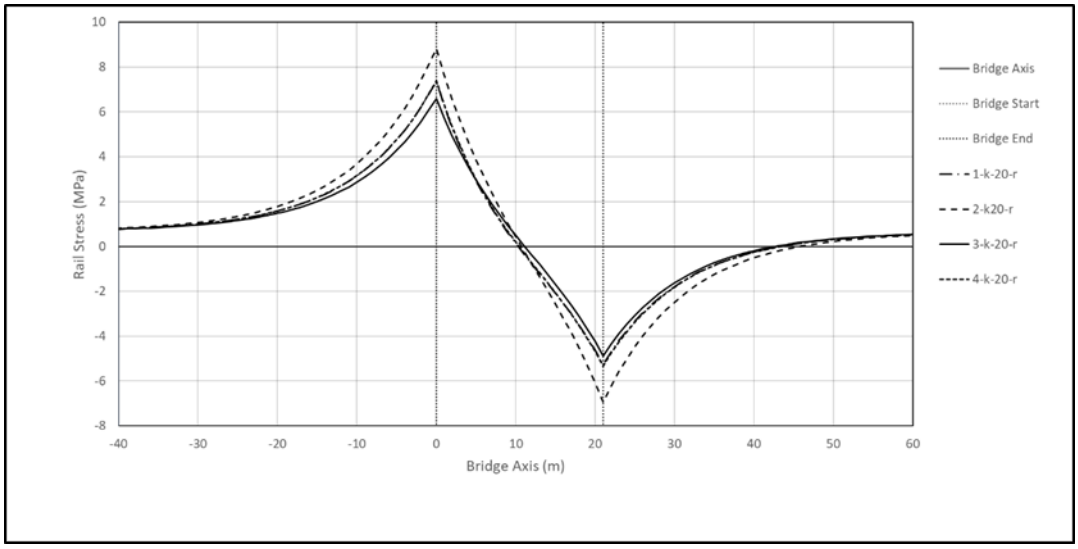

Figure 5.30. Rail Stress 20 (m) Span, k-20 Stiffness and Low Bending Stiffness

Rail stresses for bridge decks with 60 (m) span and different bending stiffness, deck height and neutral axis location are shown in Figure 5.31, Figure 5.32, Figure 5.33 and Figure 5.34.

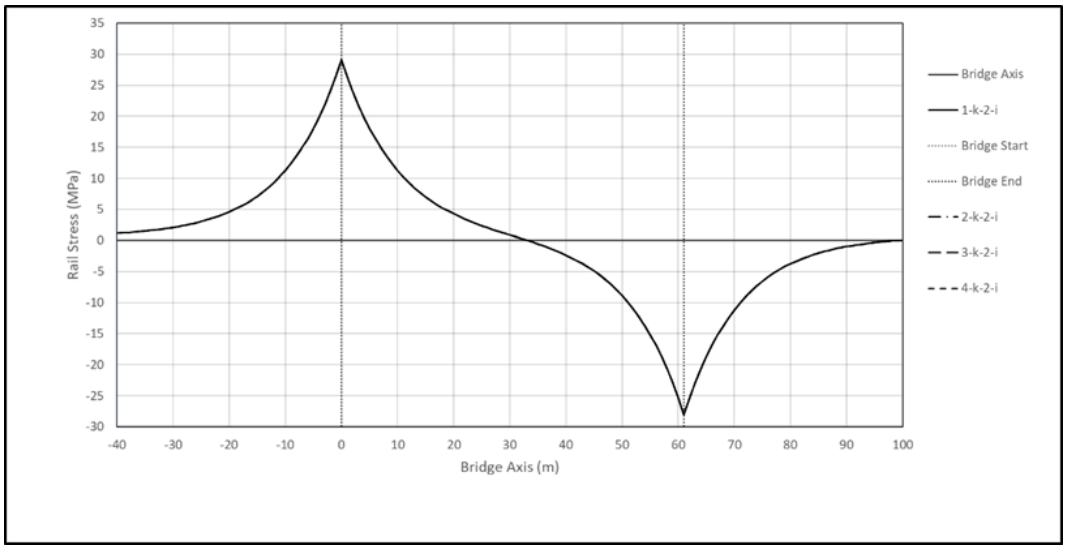

Figure 5.31. Rail Stress 60 (m) Span, k-2 Stiffness and High Bending Stiffness

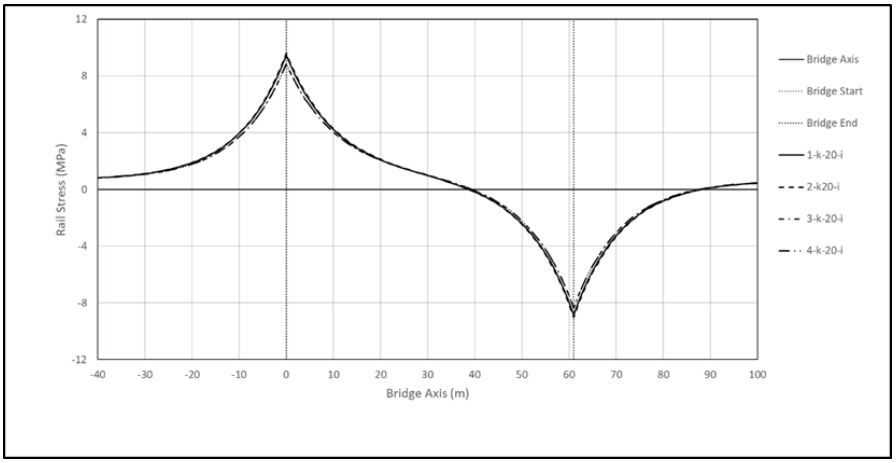

Figure 5.32. Rail Stress 60 (m) Span, k-20 Stiffness and High Bending Stiffness

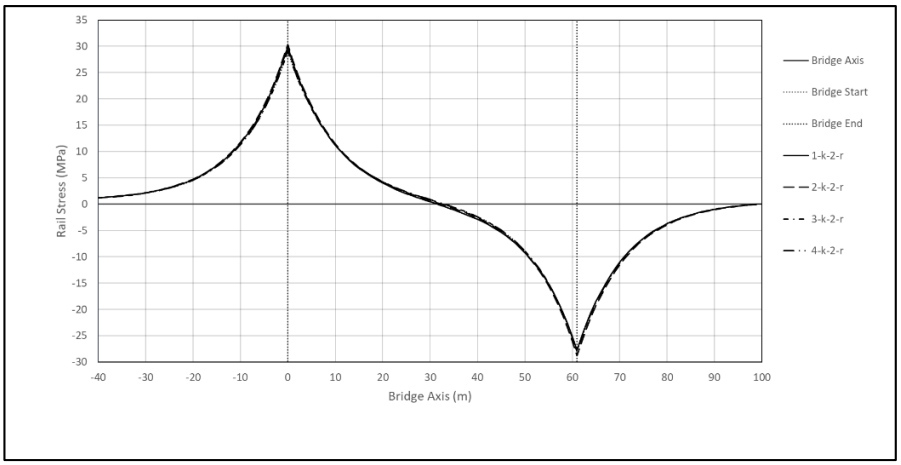

Figure 5.33. Rail Stress 60 (m) Span, k-2 Stiffness and Low Bending Stiffness

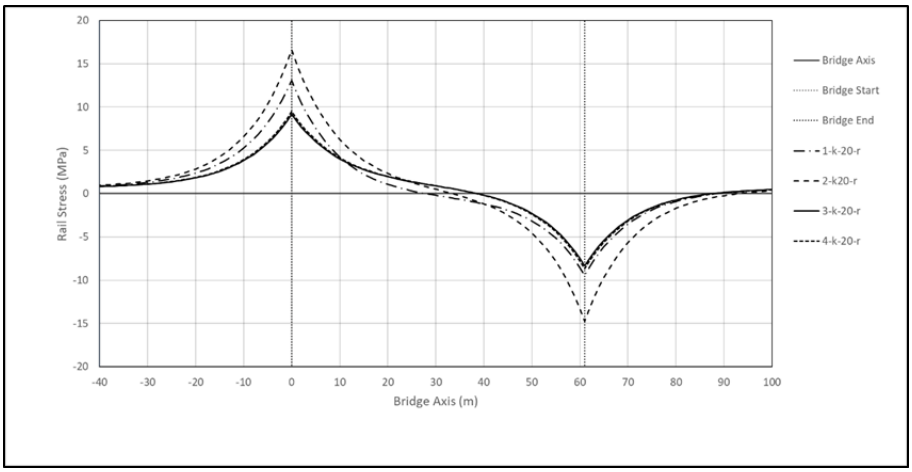

Figure 5.34. Rail Stress 60 (m) Span, k-20 Stiffness and Low Bending Stiffness

Rail stresses for bridge decks with 80 (m) span and different bending stiffness, deck height and neutral axis location are shown in Figure 5.35, Figure 5.36, Figure 5.37 and Figure 5.38.

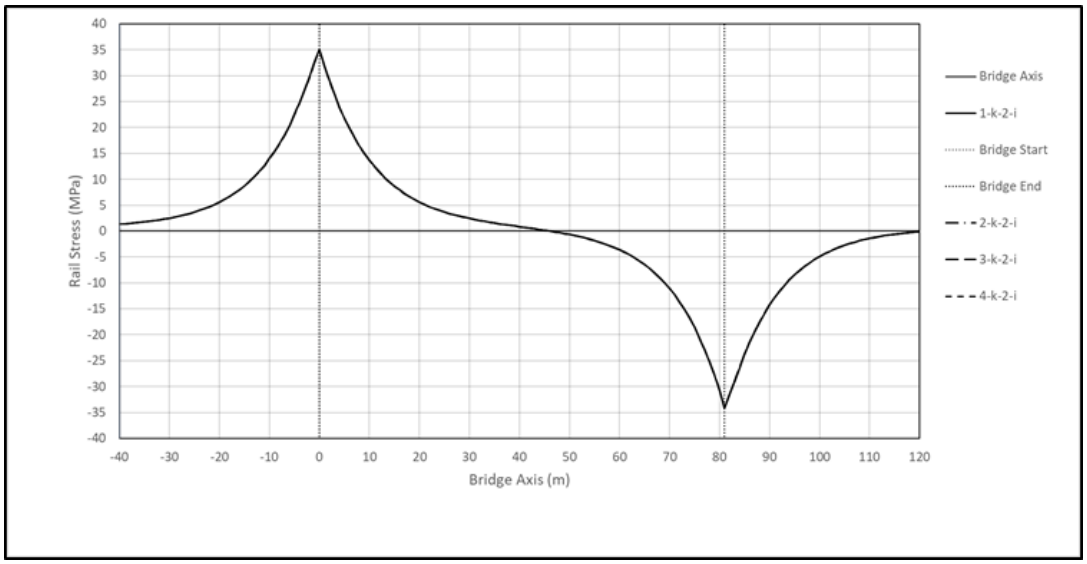

Figure 5.35. Rail Stress 80 (m) Span, k-2 Stiffness and High Bending Stiffness

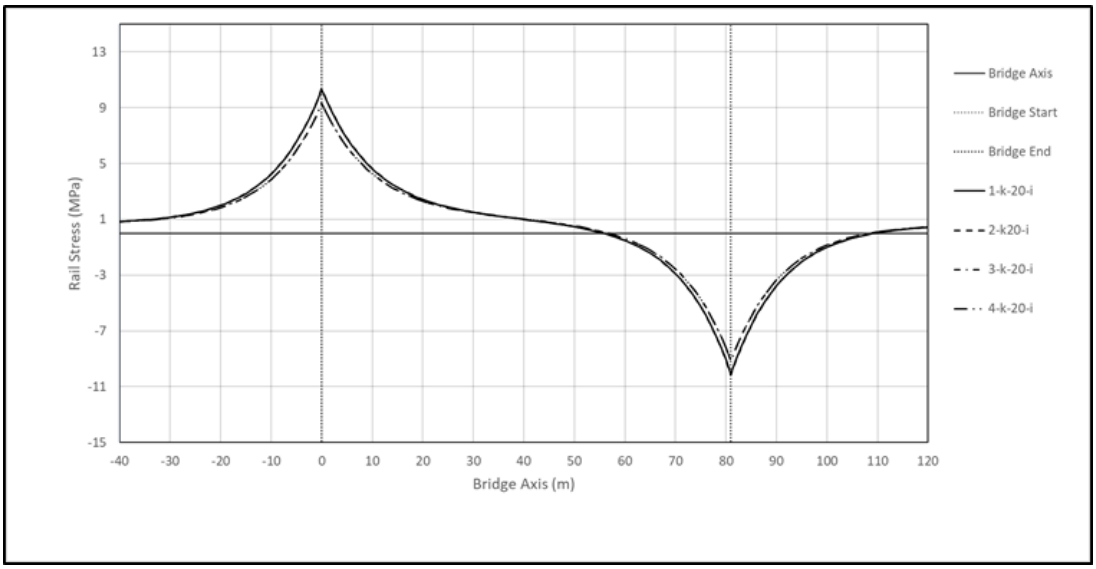

Figure 5.36. Rail Stress 80 (m) Span, k-20 Stiffness and High Bending Stiffness

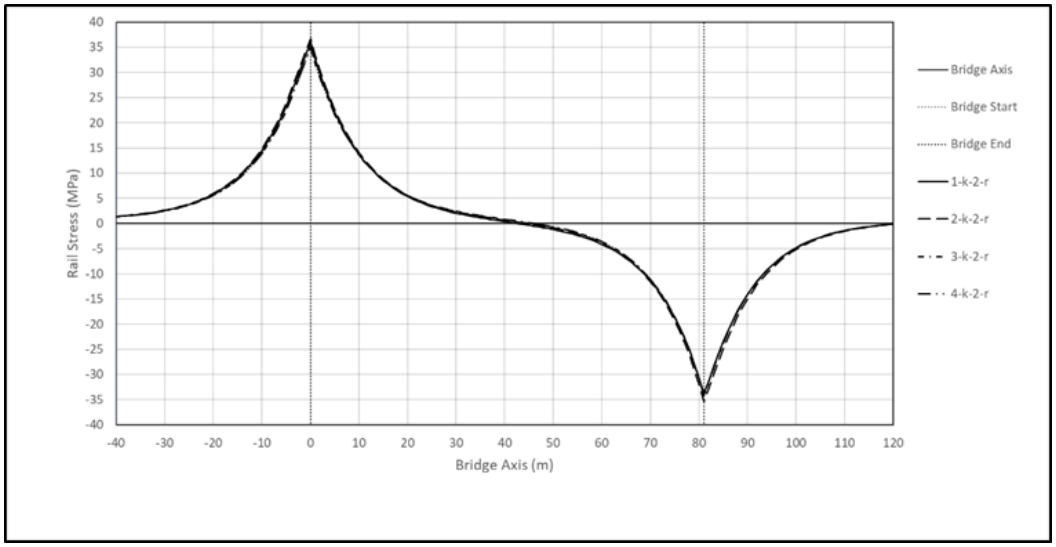

Figure 5.37. Rail Stress 80 (m) Span, k-2 Stiffness and Low Bending Stiffness

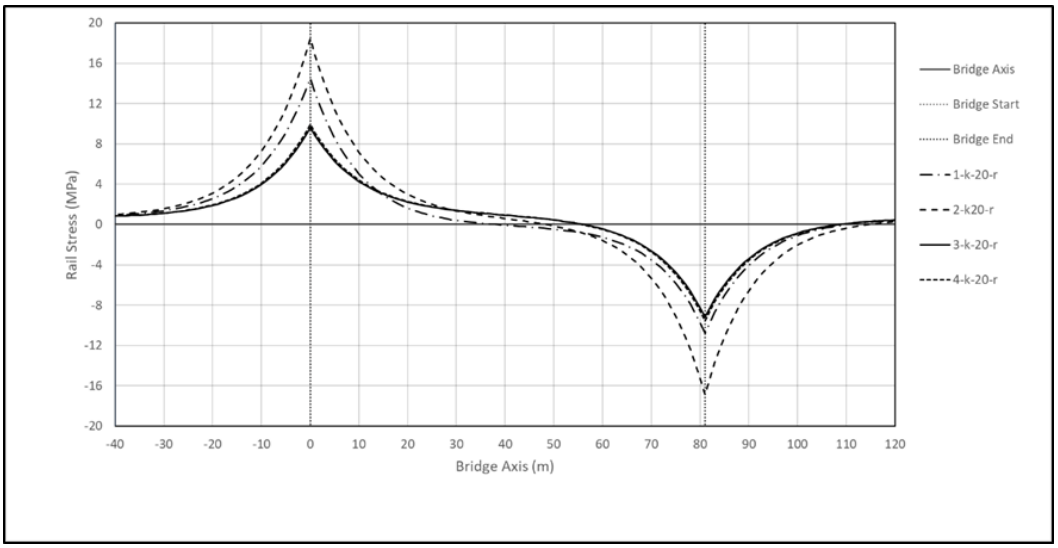

Figure 5.38. Rail Stress 80 (m) Span, k-20 Stiffness and Low Bending Stiffness

Section properties for bridge decks with spans equal to 20, 60 ,80 (m) are shown in Table 5.4 and Table 5.5 and Table 5.6.

Table 5.4. *Section Properties for Horizontal Load Rail Stresses 20 (m) span*

Span length (m)	*Case*	*I (m^4)*	*E (MPa)*	*H (m)*	*N.A from top (m)*	*k (kN/mm/m)*	*K (kN/mm)*
20	1	0.16	35000	2.5	1.25	2	40
20	2	0.16	35000	2.5	0.12	2	40
20	3	0.16	35000	0.6	0.30	2	40
20	4	0.16	35000	0.6	0.03	2	40
20	1	41.25	35000	2.5	1.25	2	40
20	2	41.25	35000	2.5	0.12	2	40
20	3	41.25	35000	0.6	0.30	2	40
20	4	41.25	35000	0.6	0.03	2	40
20	1	0.16	35000	2.5	1.25	20	400
20	2	0.16	35000	2.5	0.12	20	400
20	3	0.16	35000	0.6	0.30	20	400
20	4	0.16	35000	0.6	0.03	20	400
20	1	41.25	35000	2.5	1.25	20	400
20	2	41.25	35000	2.5	0.12	20	400
20	3	41.25	35000	0.6	0.30	20	400
20	4	41.25	35000	0.6	0.03	20	400

Table 5.5. *Section Properties for Horizontal Load Rail Stresses 60 (m) span part-1*

Span length (m)	*Case*	*I (m^4)*	*E (MPa)*	*H (m)*	*N.A from top (m)*	*k (kN/mm/m)*	*K (kN/mm)*
60	1	25	35000	7.50	3.75	2	120
60	2	25	35000	7.50	0.37	2	120
60	3	25	35000	1.75	0.87	2	120
60	4	25	35000	1.75	0.08	2	120
60	1	2500	35000	7.50	3.75	2	120
60	2	2500	35000	7.50	0.37	2	120
60	3	2500	35000	1.75	0.87	2	120
60	4	2500	35000	1.75	0.08	2	120

Table 5.6. *Section Properties for Horizontal Load Rail Stresses 60 (m) span part-2*

Span length (m)	*Case*	*I (m^4)*	*E (MPa)*	*H (m)*	*N.A from top (m)*	*k (kN/mm/m)*	*K (kN/mm)*
60	1	25	35000	7.50	3.75	20	1200
60	2	25	35000	7.50	0.37	20	1200
60	3	25	35000	1.75	0.87	20	1200
60	4	25	35000	1.75	0.08	20	1200
60	1	2500	35000	7.50	3.75	20	1200
60	2	2500	35000	7.50	0.37	20	1200
60	3	2500	35000	1.75	0.87	20	1200
60	4	2500	35000	1.75	0.08	20	1200

Table 5.7. *Section Properties for Horizontal Load Rail Stresses 80 (m) span*

Span length (m)	*Case*	*I (m^4)*	*E (MPa)*	*H (m)*	*N.A from top (m)*	*k (kN/mm/m)*	*K (kN/mm)*
80	1	79.2	35000	10.0	5.00	2	160
80	2	79.2	35000	10.0	0.50	2	160
80	3	79.2	35000	2.3	1.15	2	160
80	4	79.2	35000	2.3	0.11	2	160
80	1	7920	35000	10.0	5.00	2	160
80	2	7920	35000	10.0	0.50	2	160
80	3	7920	35000	2.3	1.15	2	160
80	4	7920	35000	2.3	0.11	2	160
80	1	79.2	35000	10.0	5.00	20	1600
80	2	79.2	35000	10.0	0.50	20	1600
80	3	79.2	35000	2.3	1.15	20	1600
80	4	79.2	35000	2.3	0.11	20	1600
80	1	7920	35000	10.0	5.00	20	1600
80	2	7920	35000	10.0	0.50	20	1600
80	3	7920	35000	2.3	1.15	20	1600
80	4	7920	35000	2.3	0.11	20	1600

Rail Stresses of bridges with the same bridge deck span length and high bending stiffness with different longitudinal stiffness are shown in Figure 5.39 and Figure 5.40.

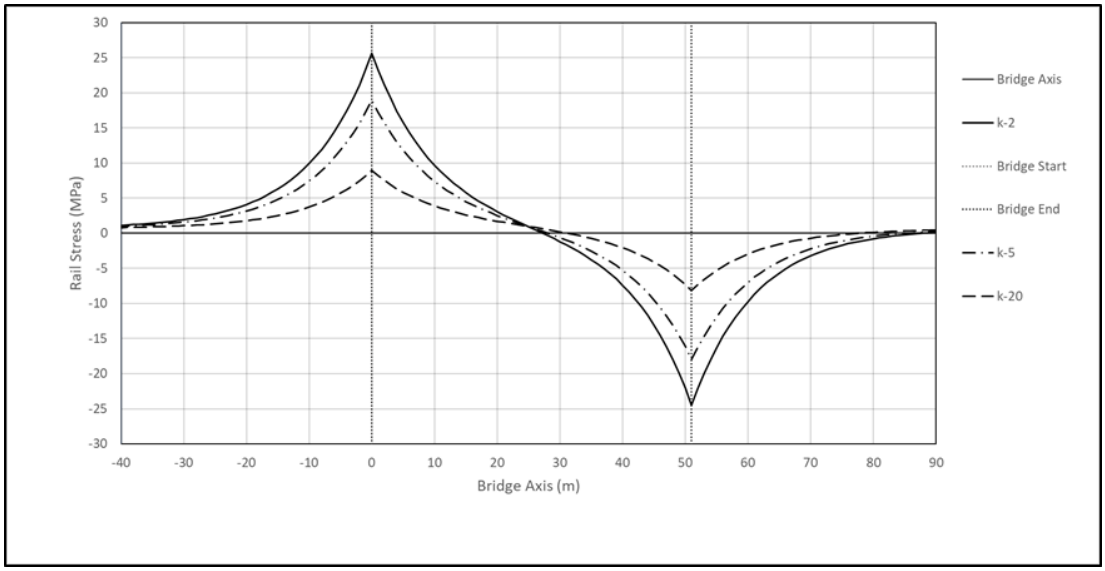

Figure 5.39. Rail Stress for 50 (m) Span with Different Longitudinal Stiffness

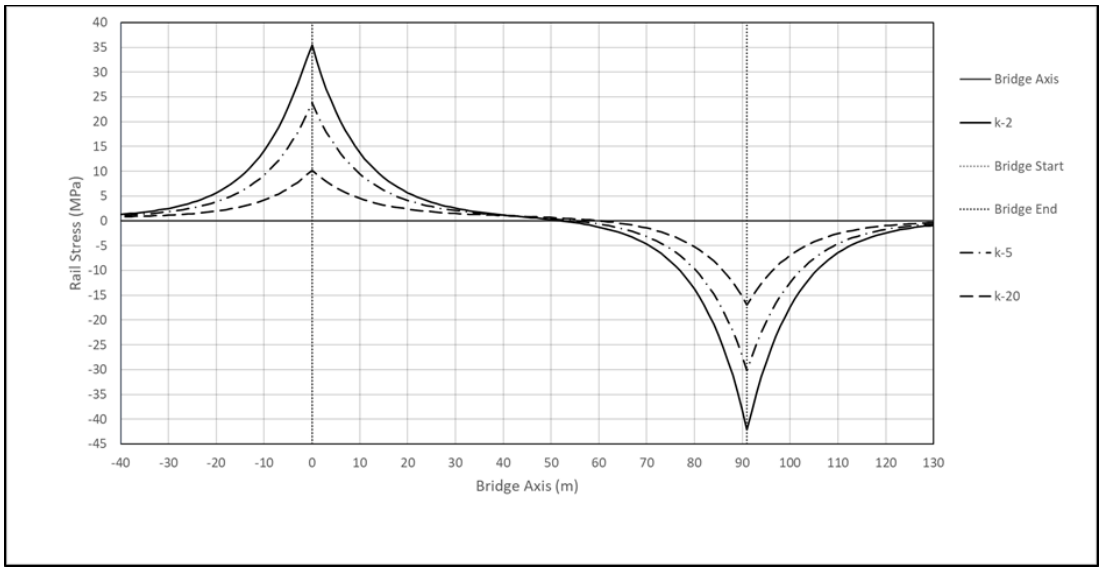

Figure 5.40. Rail Stress for 90 (m) Span with Different Longitudinal Stiffness

Rail stresses of bridge decks under horizontal loads with high bending stiffness and same longitudinal stiffness with different span length are shown in Figure 5.41, Figure 5.42 and Figure 5.43:

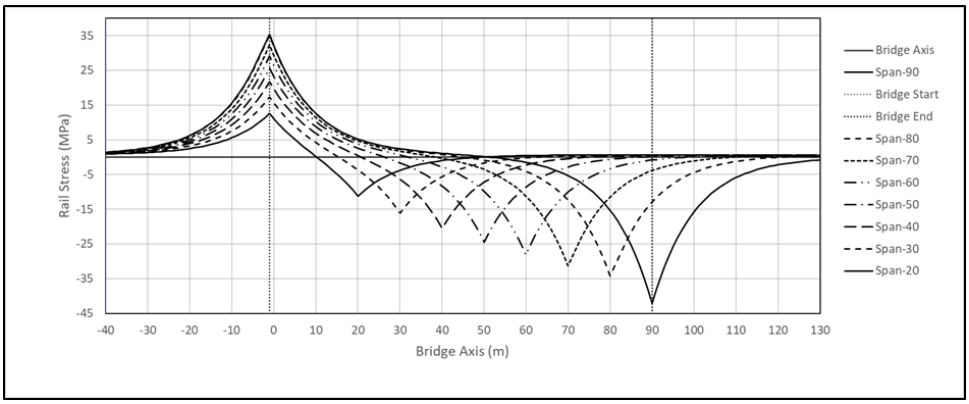

Figure 5.41. Rail Stress k-2 stiffness with high bending stiffness, different deck span length

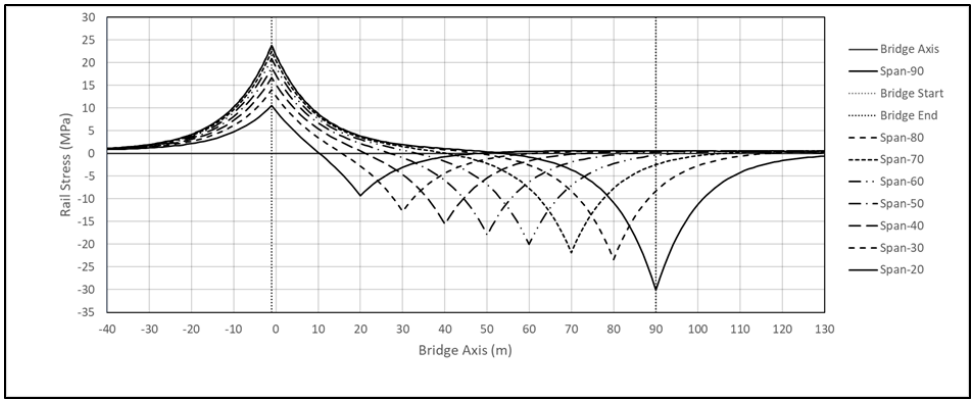

Figure 5.42. Rail Stress k-5 stiffness with high bending stiffness, different deck span length

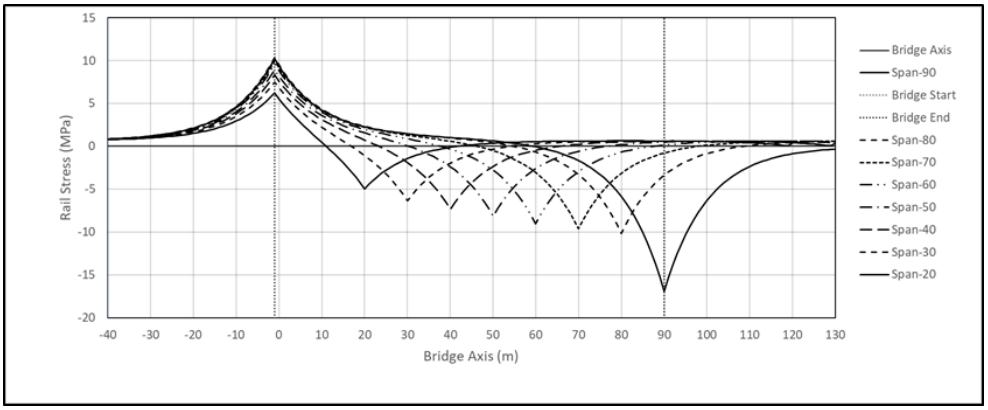

Figure 5.43. Rail Stress k-20 stiffness with high bending stiffness, different deck span length

5.5.3. Vertical loads

Vertical loads are found to be affected directly by the bridge span length mechanical properties of the bridge deck and longitudinal stiffness of the supporting system. The bridge deck cross-section area is found to have no effect on the response to vertical loads.

For bridges with bending stiffness results in 2 (mm) in top deck displacement at longitudinal stiffness equal to 2 (kN/mm/m), the rail stresses are given with different longitudinal stiffness values in Figure 5.44 and Figure 5.45 and Figure 5.46.

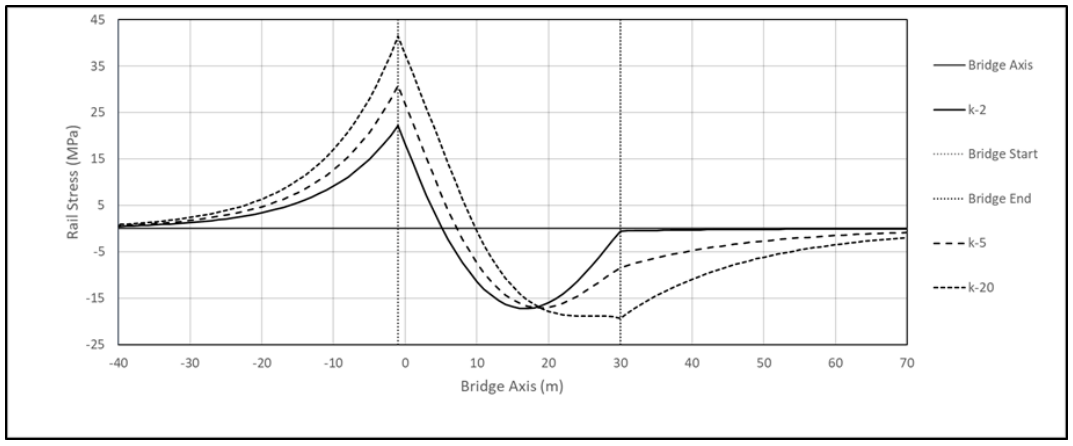

Figure 5.44. Rail Stress for 30 (m) span H = 3.75 (m) N.A = 3.375 (m)

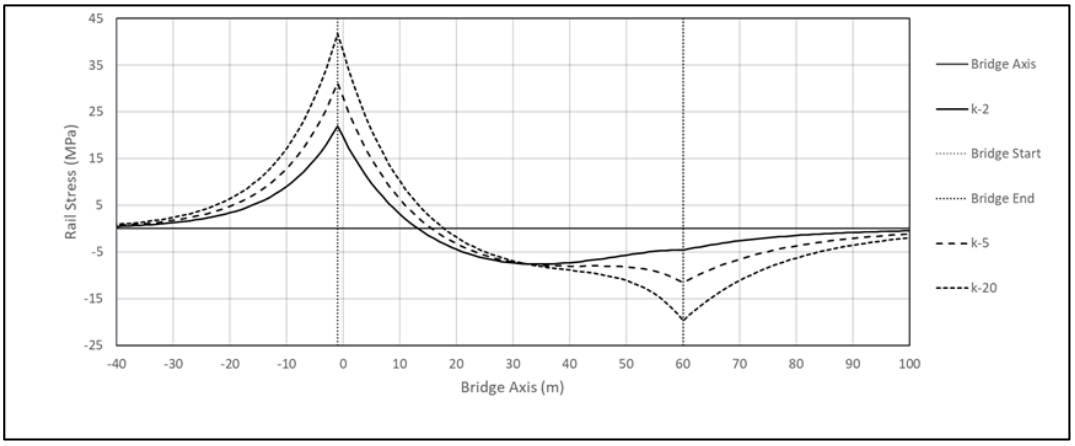

Figure 5.45. Rail Stress for 60 (m) span H = 7.5 (m) N.A = (m)

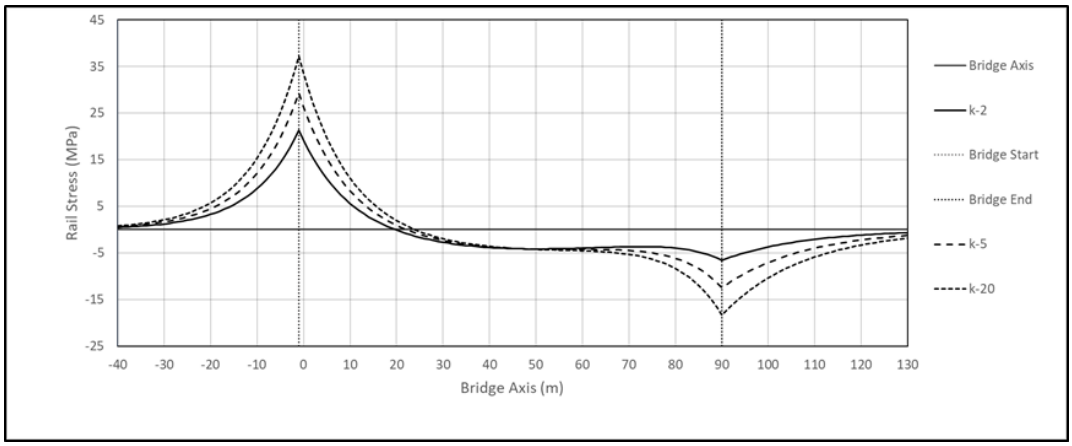

Figure 5.46. Rail Stress for 60 (m) span H = 11.25 (m) N.A = 10.125 (m)

For bridges with bending stiffness results in 2 (mm) in top deck displacement at longitudinal stiffness equal to 2 (kN/mm/m), the rail stresses are given for bridges with different spans in Figure 5.47 and Figure 5.48 and Figure 5.49.

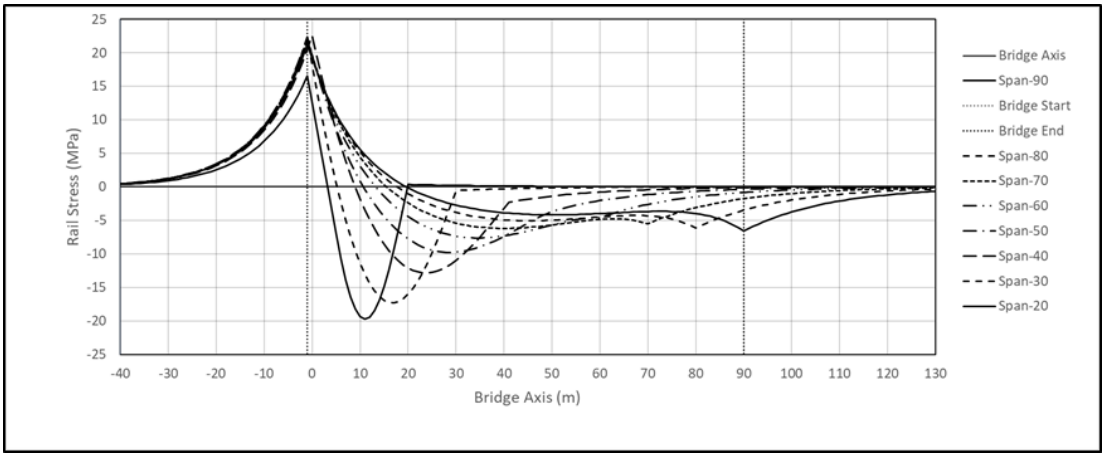

Figure 5.47. Rail Stress, k= 2 (kN/mm/m), H = L/8 (m), N.A = 0.9 x H (m)

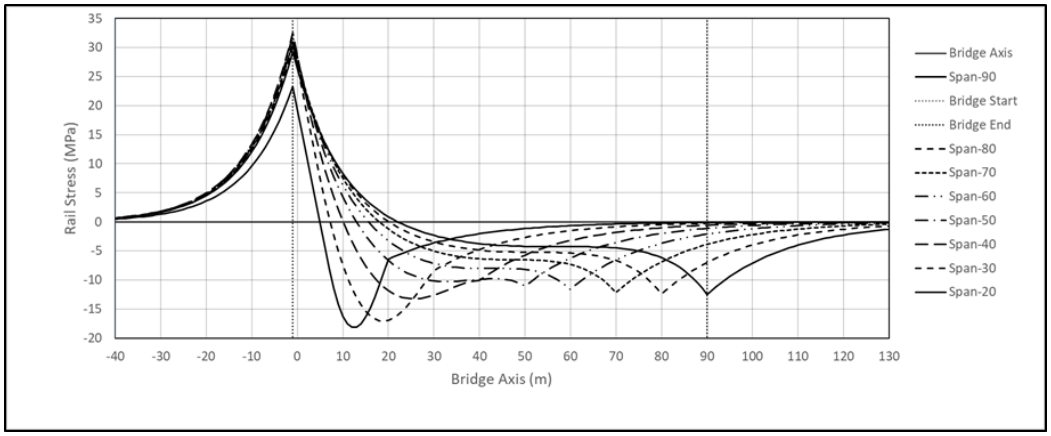

Figure 5.48. Rail Stress, k= 5 (kN/mm/m), H = L/8 (m), N.A = 0.9 x H (m)

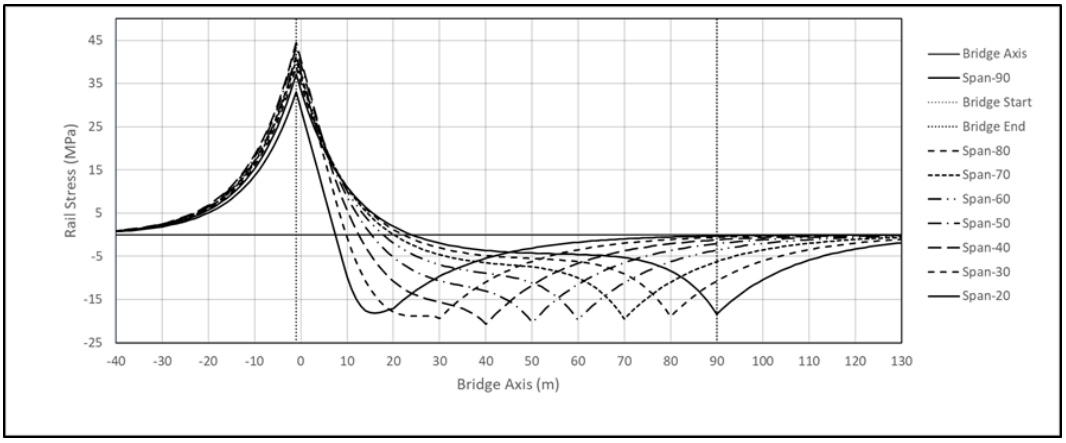

Figure 5.49. Rail Stress, k= 20 (kN/mm/m), H = L/8 (m), N.A = 0.9 x H (m)

For bridge deck with 60 (m) span and H = 7.5 (m), N.A = 6.75 (m), the rail stresses are given with different top deck displacement in Figure 5.50.

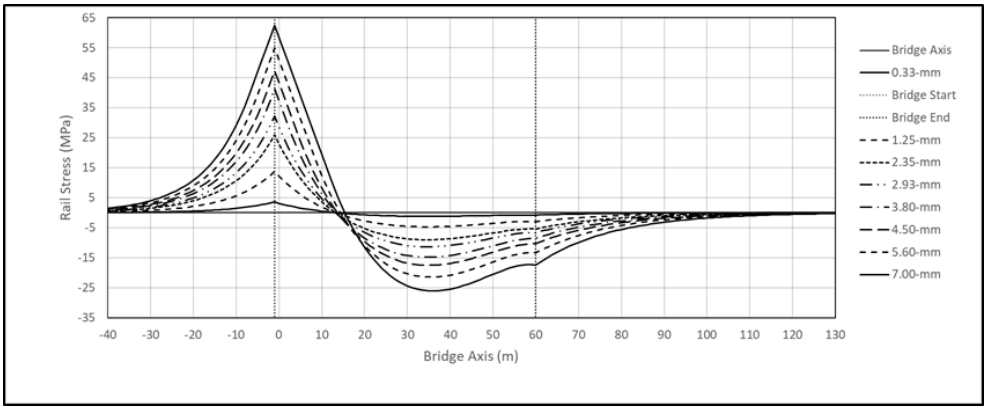

Figure 5.50. Enter the Figure Caption here

For bridge deck with 60 (m) span and N.A = 0.9 x H (m), the rail stresses are given for different deck height according to top deck displacement are shown in Figure 5.51 and Figure 5.52. Bridge top deck displacement, according to deck inertia, is shown in Figure 5.53.

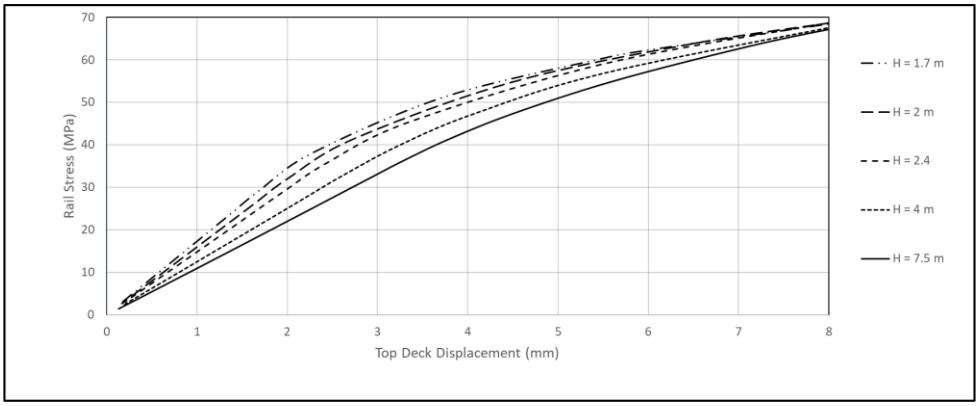

Figure 5.51. Rail Maximum Tension Stress for Different H

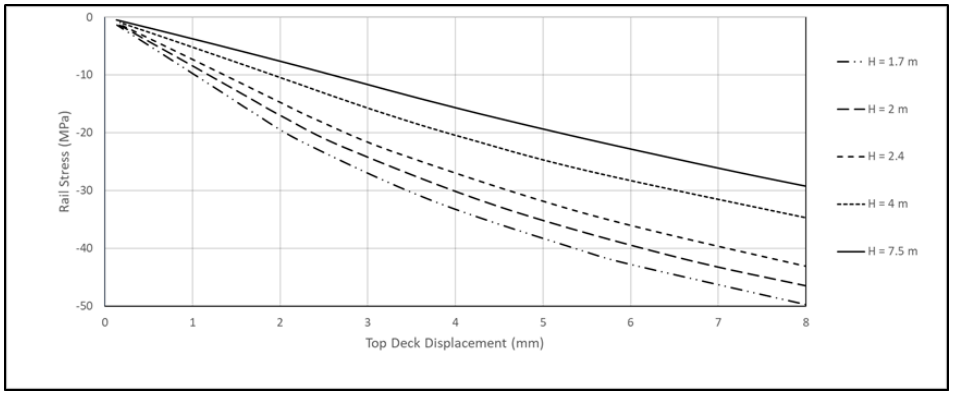

Figure 5.52. Rail Maximum Compression Stress for Different H

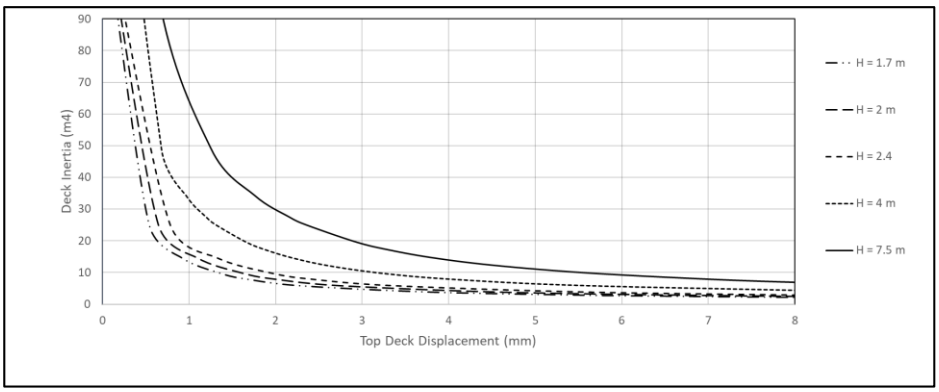

Figure 5.53. Top Deck Displacement According to Deck Inertia Different H, E = 35 (GPa)

For bridge deck with 60 (m) span and H = 7.5 (m), the rail stresses are given for neutral axis location according to top deck displacement are shown in Figure 5.54 and Figure 5.55. Bridge top deck displacement, according to deck inertia, is shown in Figure 5.56.

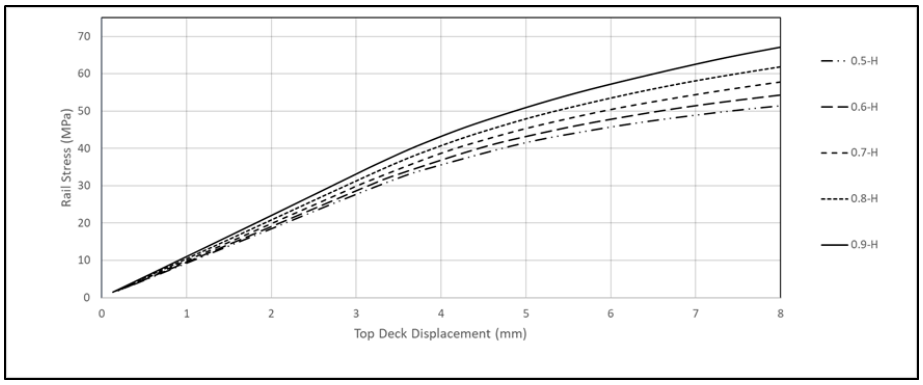

Figure 5.54. Rail Maximum Tension Stress for Different Neutral-Axis Location (m)

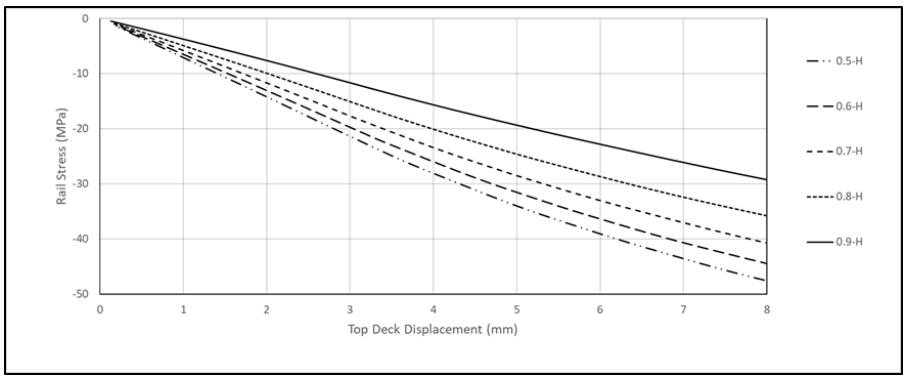

Figure 5.55. Rail Maximum Compression Stress for Different Neutral-Axis Location (m)

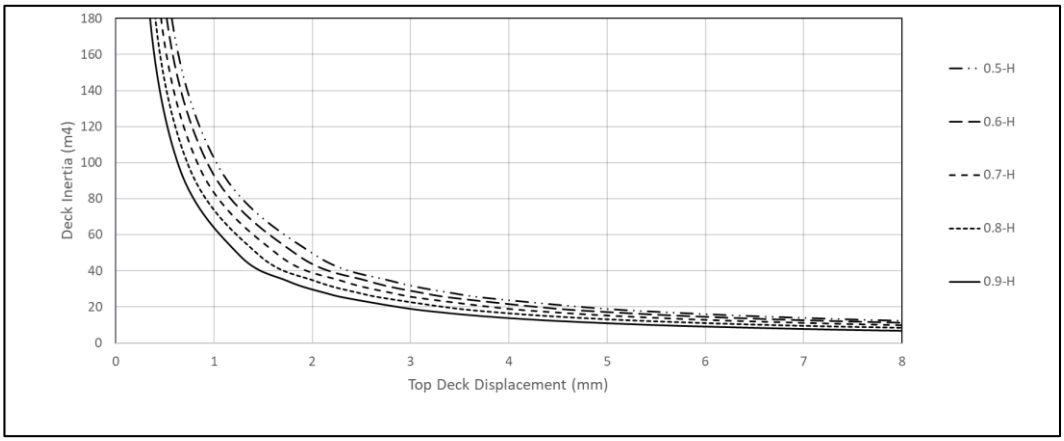

Figure 5.56. Top Deck Displacement According to Deck Inertia Different N.A, E = 35 (GPa)

5.6. Method for Determining the Combined Response of Track-Bridge to Variable Actions

In this section, a method is given for determining the combined response of the bridge and track to variable actions. This method is valid for a single bridge deck, whether it is a single simply supported deck or a single deck continuous bridge. This method could be reflected on bridges consisting of a succession of a simply supported bridge deck and succession of a continuous one-piece bridge deck.

5.6.1. Method Limitations

This method is valid for high-speed railway bridges with continuous welded rail with the UIC-60 Rail type. The rail should have steel material with at least 900 (MPa) tensile strength. The track should be supported by a ballast bed with at least 30 (cm) thickness, and the track should be attached to concrete heavy sleepers with maximum spacing 65 (cm). Track geometry should be straight or radius mores than 1500 (m).

5.6.2. Track Configuration

This method is only valid for ballasted tracks. The ballast longitudinal plastic shear resistance values used for this study are 20 (kN) per meter per track for un-loaded ballast case and 60 (kN) per meter per track for loaded ballast case.

5.6.3. Loads for Combined Response

- Vertical load: the vertical load is LM-71 with α factor = 1.4.
- Horizontal loads: the horizontal loads are 20 (kN/m) for braking force with α alpha factor = 1.4 and Acceleration force 33 (kN/m) with alpha factor = 1.4.
- Temperature action: Temperature variation applied to the bridge deck ±35 ºC.

5.6.4. Design Criteria

The rail allowable additional stresses and the allowable relative displacement are the same as used by Eurocode.

5.6.5. Evaluation Method for Combined Action

For this study, the validated modeling approach used in Chapter 3 is used with the Separated Simple method described in Chapter-4 for combining the variable actions. Bridge decks with span to depth ratio varying from L/8 to L/35 with neutral axis location varying from 0.5xH to 0.95xH from the bottom surface of the deck are evaluated. The bending stiffness for this specific study is not defined directly, but it is related to bridge top deck displacement. The bending stiffness is chosen to satisfy the 8 (mm) top deck displacement condition. If the rail stresses exceed the allowable stress, the bending stiffness is increased to satisfy the additional rail stress condition. Three different longitudinal stiffness are defined. Linear interpolation is allowed between the stiffnesses. Evaluated bridge deck properties are shown in Table 5.8.

Table 5.8. *Section and Deck Properties for Evaluation Cases part-1*

Case	*Span (m)*	*H (m)*	*N.A (m)*	*A (m^2)*	*k/m (kN/mm)*	*T ᾱ (1/ºK)*	*E (GPa)*	*I (m^4)*	*K (kN/mm)*	*D*
1	20	2.50	1.25	4.0	2	1E-6	35	0.34	40	1
2	30	3.75	1.87	4.0	2	1E-6	35	0.99	60	1
3	40	5.00	2.50	5.0	2	1E-6	35	5.77	80	1
4	50	6.25	3.12	6.0	2	1E-6	35	39.60	100	1
5	60	7.50	3.75	7.0	2	1E-6	35	24.99	120	1
6	70	8.75	4.37	8.0	2	1E-6	35	39.50	140	1
7	80	10.00	5.00	10.0	2	1E-6	35	79.20	160	1
8	90	11.25	5.62	12.0	2	1E-6	35	123.70	180	1
9	20	2.50	2.37	4.0	2	1E-6	35	0.16	40	1
10	30	3.75	3.56	4.0	2	1E-6	35	0.99	60	1
11	40	5.00	4.75	5.0	2	1E-6	35	5.77	80	1
12	50	6.25	5.93	6.0	2	1E-6	35	39.60	100	1
13	60	7.50	7.12	7.0	2	1E-6	35	245.00	120	1
14	70	8.75	8.31	8.0	2	1E-6	35	39.50	140	1
15	80	10.00	9.50	10.0	2	1E-6	35	79.20	160	1
16	90	11.25	10.68	12.0	2	1E-6	35	123.70	180	1

Table 5.9. *Section and Deck Properties for Evaluation Cases part-2*

Case	*Span (m)*	*H (m)*	*N.A (m)*	*A (m^2)*	*k/m (kN/mm)*	*T ᾱ (1/^{o}K)*	*E (GPa)*	*I (m^4)*	*K (kN/mm)*	*D*
17	20	0.60	0.30	4.0	2	1E-6	35	0.01	40	1
18	30	0.90	0.45	4.0	2	1E-6	35	0.99	60	1
19	40	1.15	0.57	5.0	2	1E-6	35	5.77	80	1
20	50	1.45	0.72	6.0	2	1E-6	35	39.60	100	1
21	60	1.75	0.87	7.0	2	1E-6	35	8.33	120	1
22	70	2.00	1	8.0	2	1E-6	35	39.50	140	1
23	80	2.30	1.15	10.0	2	1E-6	35	79.20	160	1
24	90	2.60	1.30	12.0	2	1E-6	35	123.70	180	1
25	20	0.60	0.57	4.0	2	1E-6	35	0.07	40	1
26	30	0.90	0.85	4.0	2	1E-6	35	0.99	60	1
27	40	1.15	1.09	5.0	2	1E-6	35	5.77	80	1
28	50	1.45	1.37	6.0	2	1E-6	35	39.60	100	1
29	60	1.75	1.66	7.0	2	1E-6	35	24.50	120	1
30	70	2.00	1.90	8.0	2	1E-6	35	39.50	140	1
31	80	2.30	2.18	10.0	2	1E-6	35	79.20	160	1
32	90	2.60	2.47	12.0	2	1E-6	35	123.70	180	1
33	23	2.90	1.45	4.0	2	1E-6	35	0.66	46	1
34	25	3.20	1.60	4.0	2	1E-6	35	0.91	50	1
35	28	3.50	1.75	4.0	2	1E-6	35	1.16	56	1
36	35	4.40	2.20	4.5	2	1E-6	35	2.68	70	1
37	45	5.65	2.82	5.5	2	1E-6	35	10.31	90	1
38	23	2.90	2.75	4.0	2	1E-6	35	0.66	46	1
39	25	3.20	3.04	4.0	2	1E-6	35	0.91	50	1
40	28	3.50	3.32	4.0	2	1E-6	35	1.16	56	1
41	35	4.40	4.18	4.5	2	1E-6	35	2.68	70	1
42	45	5.65	5.36	5.5	2	1E-6	35	10.31	90	1
43	23	0.70	0.35	4.0	2	1E-6	35	0.66	46	1
44	25	0.75	0.37	4.0	2	1E-6	35	0.91	50	1
45	28	0.80	0.40	4.0	2	1E-6	35	1.16	56	1
46	35	1.00	0.50	4.5	2	1E-6	35	2.68	70	1

Table 5.10. *Section and Deck Properties for Evaluation Cases part-3*

Case	*Span (m)*	*H (m)*	*N.A (m)*	*A (m^2)*	*k/m (kN/mm)*	*T ᾱ (1/^{o}K)*	*E (GPa)*	*I (m^4)*	*K (kN/mm)*	*D*
47	45	1.30	0.65	5.0	2	1E-6	35	10.31	90	1
48	23	0.70	0.66	4.0	2	1E-6	35	0.66	46	1
49	25	0.75	0.71	4.0	2	1E-6	35	0.91	50	1
50	28	0.80	0.76	4.0	2	1E-6	35	1.16	56	1
51	35	1.00	0.95	4.5	2	1E-6	35	2.68	70	1
52	45	1.30	1.23	5.0	2	1E-6	35	10.31	90	1
53	20	2.50	1.25	4.0	5	1E-6	35	0.39	100	1
54	30	3.75	1.87	4.0	5	1E-6	35	2.01	150	1
55	40	5.00	2.50	5.0	5	1E-6	35	9.69	200	1
56	50	6.25	3.12	6.0	5	1E-6	35	42.07	250	1
57	60	7.50	3.75	7.0	5	1E-6	35	27.44	300	1
58	70	8.75	4.37	8.0	5	1E-6	35	39.60	350	1
59	80	10.00	5.00	10.0	5	1E-6	35	79.20	400	1
60	90	11.25	5.62	12.0	5	1E-6	35	123.70	450	1
61	20	2.50	2.37	4.0	5	1E-6	35	0.20	100	1
62	30	3.75	3.56	4.0	5	1E-6	35	2.01	150	1
63	40	5.00	4.75	5.0	5	1E-6	35	9.69	200	1
64	50	6.25	5.93	6.0	5	1E-6	35	42.07	250	1
65	60	7.50	7.12	7.0	5	1E-6	35	132.30	300	1
66	70	8.75	8.31	8.0	5	1E-6	35	39.60	350	1
67	80	10.00	9.50	10.0	5	1E-6	35	79.20	400	1
68	90	11.25	10.68	12.0	5	1E-6	35	123.70	450	1
69	20	0.60	0.30	4.0	5	1E-6	35	0.11	100	1
70	30	0.90	0.45	4.0	5	1E-6	35	2.01	150	1
71	40	1.15	0.57	5.0	5	1E-6	35	9.69	200	1
72	50	1.45	0.72	6.0	5	1E-6	35	42.07	250	1
73	60	1.75	0.87	7.0	5	1E-6	35	7.84	300	1
74	70	2.00	1.00	8.0	5	1E-6	35	39.60	350	1
75	80	2.30	1.15	10.0	5	1E-6	35	79.20	400	1
76	90	2.60	1.30	12.0	5	1E-6	35	123.70	450	1

Table 5.11. *Section and Deck Properties for Evaluation Cases part-4*

Case	*Span (m)*	*H (m)*	*N.A (m)*	*A (m^2)*	*k/m (kN/mm)*	*T ᾱ (1/ºK)*	*E (GPa)*	*I (m^4)*	*K (kN/mm)*	*D*
77	20	0.60	0.57	4.0	5	1E-6	35	0.09	100	1
78	30	0.90	0.85	4.0	5	1E-6	35	2.01	150	1
79	40	1.15	1.09	5.0	5	1E-6	35	9.69	200	1
80	50	1.45	1.37	6.0	5	1E-6	35	42.07	250	1
81	60	1.75	1.66	7.0	5	1E-6	35	20.58	300	1
82	70	2.00	1.90	8.0	5	1E-6	35	39.60	350	1
83	80	2.30	2.18	10.0	5	1E-6	35	79.20	400	1
84	90	2.60	2.47	12.0	5	1E-6	35	123.70	450	1
85	23	2.90	1.45	4.0	5	1E-6	35	0.36	115	1
86	25	3.20	1.60	4.0	5	1E-6	35	0.62	125	1
87	28	3.50	1.75	4.0	5	1E-6	35	1.27	140	1
88	35	4.40	2.20	4.5	5	1E-6	35	4.34	175	1
89	45	5.65	2.82	5.5	5	1E-6	35	18.76	225	1
90	23	2.90	2.75	4.0	5	1E-6	35	0.36	115	1
91	25	3.20	3.04	4.0	5	1E-6	35	0.62	125	1
92	28	3.50	3.32	4.0	5	1E-6	35	1.27	140	1
93	35	4.40	4.18	4.5	5	1E-6	35	4.34	175	1
94	45	5.65	5.36	5.5	5	1E-6	35	18.76	225	1
95	23	0.70	0.35	4.0	5	1E-6	35	0.36	115	1
96	25	0.75	0.37	4.0	5	1E-6	35	0.62	125	1
97	28	0.80	0.40	4.0	5	1E-6	35	1.27	140	1
98	35	1.00	0.50	4.5	5	1E-6	35	4.34	175	1
99	45	1.30	0.65	5.0	5	1E-6	35	18.76	225	1
100	23	0.70	0.66	4.0	5	1E-6	35	0.36	115	1
101	25	0.75	0.71	4.0	5	1E-6	35	0.62	125	1
102	28	0.80	0.76	4.0	5	1E-6	35	1.27	140	1
103	35	1.00	0.95	4.5	5	1E-6	35	4.34	175	1
104	45	1.30	1.23	5.0	5	1E-6	35	18.76	225	1
105	20	2.50	1.25	4.0	20	1E-6	35	0.45	400	1
106	30	3.75	1.87	4.0	20	1E-6	35	2.28	600	1

Table 5.12. *Section and Deck Properties for Evaluation Cases part-5*

Case	*Span (m)*	*H (m)*	*N.A (m)*	*A (m^2)*	*k/m (kN/mm)*	*T ᾱ (1/^{o}K)*	*E (GPa)*	*I (m^4)*	*K (kN/mm)*	*D*
107	40	5.00	2.50	5.0	20	1E-6	35	9.69	800	1
108	50	6.25	3.12	6.0	20	1E-6	35	42.07	1000	1
109	60	7.50	3.75	7.0	20	1E-6	35	27.44	1200	1
110	70	8.75	4.37	8.0	20	1E-6	35	39.60	1400	1
111	80	10.00	5.00	10.0	20	1E-6	35	79.20	1600	1
112	90	11.25	5.62	12.0	20	1E-6	35	123.70	1800	1
113	20	2.50	2.37	4.0	20	1E-6	35	0.20	400	1
114	30	3.75	3.56	4.0	20	1E-6	35	2.01	600	1
115	40	5.00	4.75	5.0	20	1E-6	35	9.69	800	1
116	50	6.25	5.93	6.0	20	1E-6	35	42.07	1000	1
117	60	7.50	7.12	7.0	20	1E-6	35	132.30	1200	1
118	70	8.75	8.31	8.0	20	1E-6	35	39.60	1400	1
119	80	10.00	9.50	10.0	20	1E-6	35	79.20	1600	1
120	90	11.25	10.68	12.0	20	1E-6	35	123.70	1800	1
121	20	0.60	0.30	4.0	20	1E-6	35	0.11	400	1
122	30	0.90	0.45	4.0	20	1E-6	35	2.01	600	1
123	40	1.15	0.57	5.0	20	1E-6	35	9.69	800	1
124	50	1.45	0.72	6.0	20	1E-6	35	42.07	1000	1
125	60	1.75	0.87	7.0	20	1E-6	35	7.84	1200	1
126	70	2.00	1.00	8.0	20	1E-6	35	39.60	1400	1
127	80	2.30	1.15	10.0	20	1E-6	35	79.20	1600	1
128	90	2.60	1.30	12.0	20	1E-6	35	123.70	1800	1
129	20	0.60	0.57	4.0	20	1E-6	35	0.09	400	1
130	30	0.90	0.85	4.0	20	1E-6	35	2.01	600	1
131	40	1.15	1.09	5.0	20	1E-6	35	9.69	800	1
132	50	1.45	1.37	6.0	20	1E-6	35	42.07	1000	1
133	60	1.75	1.66	7.0	20	1E-6	35	20.58	1200	1
134	70	2.00	1.90	8.0	20	1E-6	35	39.60	1400	1
135	80	2.30	2.18	10.0	20	1E-6	35	79.20	1600	1
136	90	2.60	2.47	12.0	20	1E-6	35	123.70	1800	1

Table 5.13. *Section and Deck Properties for Evaluation Cases part-6*

Case	*Span (m)*	*H (m)*	*N.A (m)*	*A (m^2)*	*k/m (kN/mm)*	*T ᾱ (1/^{o}K)*	*E (GPa)*	*I (m^4)*	*K (kN/mm)*	*D*
137	23	2.90	1.45	4.0	20	1E-6	35	0.66	460	1
138	25	3.20	1.6	4.0	20	1E-6	35	1.09	500	1
139	28	3.50	1.75	4.0	20	1E-6	35	1.97	560	1
140	35	4.40	2.2	4.5	20	1E-6	35	5.89	700	1
141	45	5.65	2.825	5.5	20	1E-6	35	20.41	900	1
142	23	2.90	2.755	4.0	20	1E-6	35	0.66	460	1
143	25	3.20	3.04	4.0	20	1E-6	35	1.09	500	1
144	28	3.50	3.325	4.0	20	1E-6	35	1.97	560	1
145	35	4.40	4.18	4.5	20	1E-6	35	5.89	700	1
146	45	5.65	5.367	5.5	20	1E-6	35	20.41	900	1
147	23	0.70	0.35	4.0	20	1E-6	35	0.66	460	1
148	25	0.75	0.375	4.0	20	1E-6	35	1.09	500	1
149	28	0.80	0.4	4.0	20	1E-6	35	1.97	560	1
150	35	1.00	0.5	4.5	20	1E-6	35	5.89	700	1
151	45	1.30	0.65	5.0	20	1E-6	35	20.41	900	1
152	23	0.70	0.665	4.0	20	1E-6	35	0.66	460	1
153	25	0.75	0.712	4.0	20	1E-6	35	1.09	500	1
154	28	0.80	0.76	4.0	20	1E-6	35	1.97	560	1
155	35	1.00	0.95	4.5	20	1E-6	35	5.89	700	1
156	45	1.30	1.23	5.0	20	1E-6	35	20.41	900	1
157	20	2.50	1.25	4.0	2	1E-6	35	0.34	40	2
158	30	3.75	1.875	4.0	2	1E-6	35	0.99	60	2
159	40	5.00	2.5	5.0	2	1E-6	35	5.77	80	2
160	50	6.25	3.125	6.0	2	1E-6	35	39.60	100	2
161	60	7.50	3.75	7.0	2	1E-6	35	24.99	120	2
162	70	8.75	4.375	8.0	2	1E-6	35	39.50	140	2
163	80	10.00	5	10.0	2	1E-6	35	79.20	160	2
164	90	11.25	5.625	12.0	2	1E-6	35	123.70	180	2
165	20	2.50	2.375	4.0	2	1E-6	35	0.16	40	2
166	30	3.75	3.562	4.0	2	1E-6	35	0.99	60	2

Table 5.14. *Section and Deck Properties for Evaluation Cases part-7*

Case	*Span (m)*	*H (m)*	*N.A (m)*	*A (m^2)*	*k/m (kN/mm)*	*T ᾱ (1/^{o}K)*	*E (GPa)*	*I (m^4)*	*K (kN/mm)*	*D*
167	40	5.00	4.75	5.0	2	1E-6	35	5.77	80	2
168	50	6.25	5.93	6.0	2	1E-6	35	39.60	100	2
169	60	7.50	7.12	7.0	2	1E-6	35	245.00	120	2
170	70	8.75	8.31	8.0	2	1E-6	35	39.50	140	2
171	80	10.00	9.50	10.0	2	1E-6	35	79.20	160	2
172	90	11.25	10.68	12.0	2	1E-6	35	123.70	180	2
173	20	0.60	0.30	4.0	2	1E-6	35	0.01	40	2
174	30	0.90	0.45	4.0	2	1E-6	35	0.99	60	2
175	40	1.15	0.57	5.0	2	1E-6	35	5.77	80	2
176	50	1.45	0.72	6.0	2	1E-6	35	39.60	100	2
177	60	1.75	0.87	7.0	2	1E-6	35	8.33	120	2
178	70	2.00	1.00	8.0	2	1E-6	35	39.50	140	2
179	80	2.30	1.15	10.0	2	1E-6	35	79.20	160	2
180	90	2.60	1.30	12.0	2	1E-6	35	123.70	180	2
181	20	0.60	0.57	4.0	2	1E-6	35	0.07	40	2
182	30	0.90	0.85	4.0	2	1E-6	35	0.99	60	2
183	40	1.15	1.09	5.0	2	1E-6	35	5.77	80	2
184	50	1.45	1.37	6.0	2	1E-6	35	39.60	100	2
185	60	1.75	1.66	7.0	2	1E-6	35	24.50	120	2
186	70	2.00	1.90	8.0	2	1E-6	35	39.50	140	2
187	80	2.30	2.18	10.0	2	1E-6	35	79.20	160	2
188	90	2.60	2.47	12.0	2	1E-6	35	123.70	180	2
189	23	2.90	1.45	4.0	2	1E-6	35	0.66	46	2
190	25	3.20	1.60	4.0	2	1E-6	35	0.91	50	2
191	28	3.50	1.75	4.0	2	1E-6	35	1.16	56	2
192	35	4.40	2.20	4.5	2	1E-6	35	2.68	70	2
193	45	5.65	2.82	5.5	2	1E-6	35	10.31	90	2
194	23	2.90	2.75	4.0	2	1E-6	35	0.66	46	2
195	25	3.20	3.04	4.0	2	1E-6	35	0.91	50	2
196	28	3.50	3.32	4.0	2	1E-6	35	1.16	56	2

Table 5.15. *Section and Deck Properties for Evaluation Cases part-8*

Case	*Span (m)*	*H (m)*	*N.A (m)*	*A (m^2)*	*k/m (kN/mm)*	*T ᾱ (1/^{o}K)*	*E (GPa)*	*I (m^4)*	*K (kN/mm)*	*D*
197	35	4.40	4.18	4.5	2	1E-6	35	2.68	70	2
198	45	5.65	5.36	5.5	2	1E-6	35	10.31	90	2
199	23	0.70	0.35	4.0	2	1E-6	35	0.66	46	2
200	25	0.75	0.37	4.0	2	1E-6	35	0.91	50	2
201	28	0.80	0.40	4.0	2	1E-6	35	1.16	56	2
202	35	1.00	0.50	4.5	2	1E-6	35	2.68	70	2
203	45	1.30	0.65	5.0	2	1E-6	35	10.31	90	2
204	23	0.70	0.66	4.0	2	1E-6	35	0.66	46	2
205	25	0.75	0.71	4.0	2	1E-6	35	0.91	50	2
206	28	0.80	0.76	4.0	2	1E-6	35	1.16	56	2
207	35	1.00	0.95	4.5	2	1E-6	35	2.68	70	2
208	45	1.30	1.23	5.0	2	1E-6	35	10.31	90	2
209	20	2.50	1.25	4.0	5	1E-6	35	0.39	100	2
210	30	3.75	1.87	4.0	5	1E-6	35	2.01	150	2
211	40	5.00	2.50	5.0	5	1E-6	35	9.69	200	2
212	50	6.25	3.12	6.0	5	1E-6	35	42.07	250	2
213	60	7.50	3.75	7.0	5	1E-6	35	27.44	300	2
214	70	8.75	4.37	8.0	5	1E-6	35	39.60	350	2
215	80	10.00	5.00	10.0	5	1E-6	35	79.20	400	2
216	90	11.25	5.62	12.0	5	1E-6	35	123.70	450	2
217	20	2.50	2.37	4.0	5	1E-6	35	0.20	100	2
218	30	3.75	3.56	4.0	5	1E-6	35	2.02	150	2
219	40	5.00	4.75	5.0	5	1E-6	35	9.69	200	2
220	50	6.25	5.93	6.0	5	1E-6	35	42.07	250	2
221	60	7.50	7.12	7.0	5	1E-6	35	132.30	300	2
222	70	8.75	8.31	8.0	5	1E-6	35	39.60	350	2
223	80	10.00	9.50	10.0	5	1E-6	35	79.20	400	2
224	90	11.25	10.68	12.0	5	1E-6	35	123.70	450	2
225	20	0.60	0.30	4.0	5	1E-6	35	0.10	100	2
226	30	0.90	0.45	4.0	5	1E-6	35	2.02	150	2

Table 5.16. *Section and Deck Properties for Evaluation Cases part-9*

Case	*Span (m)*	*H (m)*	*N.A (m)*	*A (m^2)*	*k/m (kN/mm)*	*T ᾱ (1/^{o}K)*	*E (GPa)*	*I (m^4)*	*K (kN/mm)*	*D*
227	40	1.15	0.57	5.0	5	1E-6	35	9.69	200	2
228	50	1.45	0.72	6.0	5	1E-6	35	42.07	250	2
229	60	1.75	0.87	7.0	5	1E-6	35	7.84	300	2
230	70	2.00	1.00	8.0	5	1E-6	35	39.60	350	2
231	80	2.30	1.15	10.0	5	1E-6	35	79.20	400	2
232	90	2.60	1.30	12.0	5	1E-6	35	123.70	450	2
233	20	0.60	0.57	4.0	5	1E-6	35	0.09	100	2
234	30	0.90	0.85	4.0	5	1E-6	35	2.01	150	2
235	40	1.15	1.09	5.0	5	1E-6	35	9.69	200	2
236	50	1.45	1.37	6.0	5	1E-6	35	42.07	250	2
237	60	1.75	1.66	7.0	5	1E-6	35	20.58	300	2
238	70	2.00	1.90	8.0	5	1E-6	35	39.60	350	2
239	80	2.30	2.18	10.0	5	1E-6	35	79.20	400	2
240	90	2.60	2.47	12.0	5	1E-6	35	123.70	450	2
241	23	2.90	1.45	4.0	5	1E-6	35	0.36	115	2
242	25	3.20	1.60	4.0	5	1E-6	35	0.62	125	2
243	28	3.50	1.75	4.0	5	1E-6	35	1.27	140	2
244	35	4.40	2.20	4.5	5	1E-6	35	4.34	175	2
245	45	5.65	2.82	5.5	5	1E-6	35	18.76	225	2
246	23	2.90	2.75	4.0	5	1E-6	35	0.36	115	2
247	25	3.20	3.04	4.0	5	1E-6	35	0.62	125	2
248	28	3.50	3.32	4.0	5	1E-6	35	1.27	140	2
249	35	4.40	4.18	4.5	5	1E-6	35	4.34	175	2
250	45	5.65	5.36	5.5	5	1E-6	35	18.76	225	2
251	23	0.70	0.35	4.0	5	1E-6	35	0.36	115	2
252	25	0.75	0.37	4.0	5	1E-6	35	0.62	125	2
253	28	0.80	0.40	4.0	5	1E-6	35	1.27	140	2
254	35	1.00	0.50	4.5	5	1E-6	35	4.34	175	2
255	45	1.30	0.65	5.0	5	1E-6	35	18.76	225	2
256	23	0.70	0.665	4.0	5	1E-6	35	0.36	115	2

Table 5.17. *Section and Deck Properties for Evaluation Cases part-10*

Case	*Span (m)*	*H (m)*	*N.A (m)*	*A (m^2)*	*k/m (kN/mm)*	*T ᾱ (1/^{0}K)*	*E (GPa)*	*I (m^4)*	*K (kN/mm)*	*D*
257	25	0.75	0.71	4.0	5	1E-6	35	0.62	125	2
258	28	0.80	0.76	4.0	5	1E-6	35	1.27	140	2
259	35	1.00	0.95	4.5	5	1E-6	35	4.34	175	2
260	45	1.30	1.23	5.0	5	1E-6	35	18.76	225	2
261	20	2.50	1.25	4.0	20	1E-6	35	0.45	400	2
262	30	3.75	1.87	4.0	20	1E-6	35	2.28	600	2
263	40	5.00	2.50	5.0	20	1E-6	35	9.69	800	2
264	50	6.25	3.12	6.0	20	1E-6	35	42.07	1000	2
265	60	7.50	3.75	7.0	20	1E-6	35	27.44	1200	2
266	70	8.75	4.37	8.0	20	1E-6	35	39.60	1400	2
267	80	10.00	5.00	10.0	20	1E-6	35	79.20	1600	2
268	90	11.25	5.62	12.0	20	1E-6	35	123.70	1800	2
269	20	2.50	2.37	4.0	20	1E-6	35	0.20	400	2
270	30	3.75	3.56	4.0	20	1E-6	35	2.02	600	2
271	40	5.00	4.75	5.0	20	1E-6	35	9.69	800	2
272	50	6.25	5.93	6.0	20	1E-6	35	42.07	1000	2
273	60	7.50	7.12	7.0	20	1E-6	35	132.30	1200	2
274	70	8.75	8.31	8.0	20	1E-6	35	39.60	1400	2
275	80	10.00	9.50	10.0	20	1E-6	35	79.20	1600	2
276	90	11.25	10.68	12.0	20	1E-6	35	123.70	1800	2
277	20	0.60	0.30	4.0	20	1E-6	35	0.11	400	2
278	30	0.90	0.45	4.0	20	1E-6	35	2.01	600	2
279	40	1.15	0.57	5.0	20	1E-6	35	9.69	800	2
280	50	1.45	0.72	6.0	20	1E-6	35	42.07	1000	2
281	60	1.75	0.87	7.0	20	1E-6	35	7.84	1200	2
282	70	2.00	1.00	8.0	20	1E-6	35	39.60	1400	2
283	80	2.30	1.15	10.0	20	1E-6	35	79.20	1600	2
284	90	2.60	1.30	12.0	20	1E-6	35	123.70	1800	2
285	20	0.60	0.57	4.0	20	1E-6	35	0.09	400	2
286	30	0.90	0.85	4.0	20	1E-6	35	2.02	600	2

Table 5.18. *Section and Deck Properties for Evaluation Cases part-11*

Case	*Span (m)*	*H (m)*	*N.A (m)*	*A (m^2)*	*k/m (kN/mm)*	*T ᾱ (1/ºK)*	*E (GPa)*	*I (m^4)*	*K (kN/mm)*	*D*
287	40	1.15	1.092	5.0	20	1E-6	35	9.69	800	2
288	50	1.45	1.377	6.0	20	1E-6	35	42.07	1000	2
289	60	1.75	1.662	7.0	20	1E-6	35	20.58	1200	2
290	70	2.00	1.9	8.0	20	1E-6	35	39.60	1400	2
291	80	2.30	2.185	10.0	20	1E-6	35	79.20	1600	2
292	90	2.60	2.47	12.0	20	1E-6	35	123.70	1800	2
293	23	2.90	1.45	4.0	20	1E-6	35	0.66	460	2
294	25	3.20	1.6	4.0	20	1E-6	35	1.09	500	2
295	28	3.50	1.75	4.0	20	1E-6	35	1.97	560	2
296	35	4.40	2.2	4.5	20	1E-6	35	5.89	700	2
297	45	5.65	2.825	5.5	20	1E-6	35	20.41	900	2
298	23	2.90	2.755	4.0	20	1E-6	35	0.66	460	2
299	25	3.20	3.04	4.0	20	1E-6	35	1.09	500	2
300	28	3.50	3.325	4.0	20	1E-6	35	1.97	560	2
301	35	4.40	4.18	4.5	20	1E-6	35	5.89	700	2
302	45	5.65	5.367	5.5	20	1E-6	35	20.41	900	2
303	23	0.70	0.35	4.0	20	1E-6	35	0.66	460	2
304	25	0.75	0.375	4.0	20	1E-6	35	1.09	500	2
305	28	0.80	0.4	4.0	20	1E-6	35	1.97	560	2
306	35	1.00	0.5	4.5	20	1E-6	35	5.89	700	2
307	45	1.30	0.65	5.0	20	1E-6	35	20.41	900	2
308	23	0.70	0.665	4.0	20	1E-6	35	0.66	460	2
309	25	0.75	0.712	4.0	20	1E-6	35	1.09	500	2
310	28	0.80	0.76	4.0	20	1E-6	35	1.97	560	2
311	35	1.00	0.95	4.5	20	1E-6	35	5.89	700	2
312	45	1.30	1.23	5.0	20	1E-6	35	20.41	900	2

The cases 313 to 624 are the same as cases from 1 to 312 with thermal expansion coefficient = 1.2E-6 $ºK^{-1}$ and lower bending inertia.

Where:

- H: total deck depth
- I: deck section moment of inertia
- N.A: neutral axis ordinate from deck bottom surface
- A: deck cross-section area
- k/m: longitudinal stiffness per meter per track
- ᾱ: thermal expansion coefficient
- E: modulus of elasticity
- K: total longitudinal stiffness
- D: support location 1 for bridge start and 2 for bridge end

After evaluating the bridge deck cases, charts are drawn for bridge deck permissible domain rail stresses.

The maximum allowable expansion length is given according to top deck displacement. The following charts are for thermal expansion coefficient = 1E-6 $^{o}K^{-1}$, as shown in Figure 5.57 for k2, and in Figure 5.58 for k5, and in Figure 5.59 for k20.

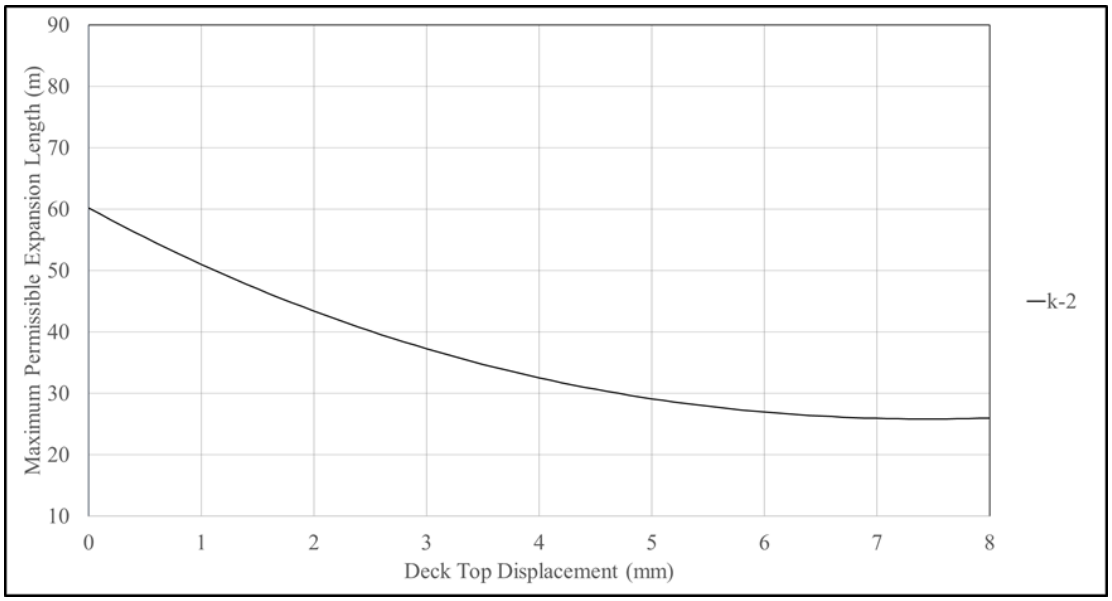

Figure 5.57. Maximum Expansion Length for Bridge Deck with Longitudinal Stiffness 2 (kN/mm/m)

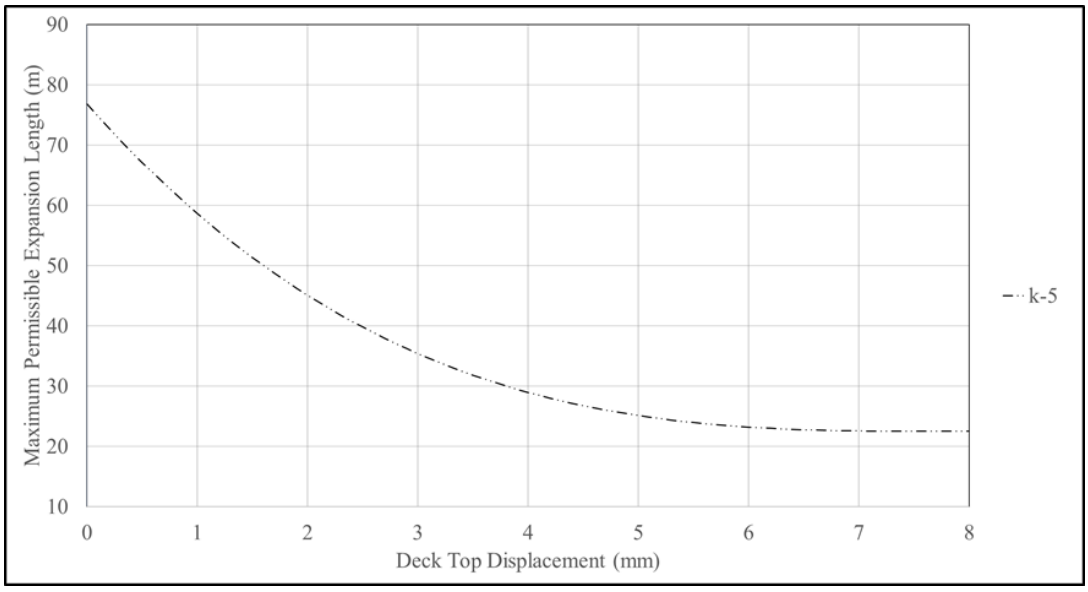

Figure 5.58. Maximum Expansion Length for Bridge Deck with Longitudinal Stiffness 5 (kN/mm/m)

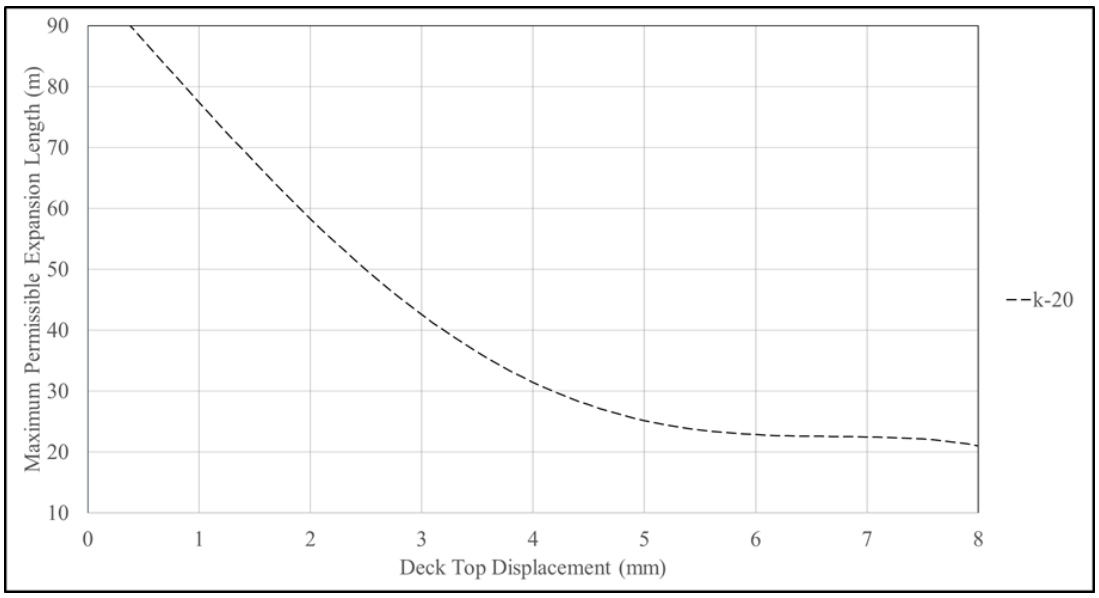

Figure 5.59. Maximum Expansion Length for Bridge Deck with Longitudinal Stiffness 20 (kN/mm/m)

The maximum allowable expansion length is given according to top deck displacement. The following charts are for thermal expansion coefficient = 1.2E-6 $^{o}K^{-1}$, as shown in Figure 5.60 for k2, and in Figure 5.61 for k5 and in Figure 5.62 for k20.

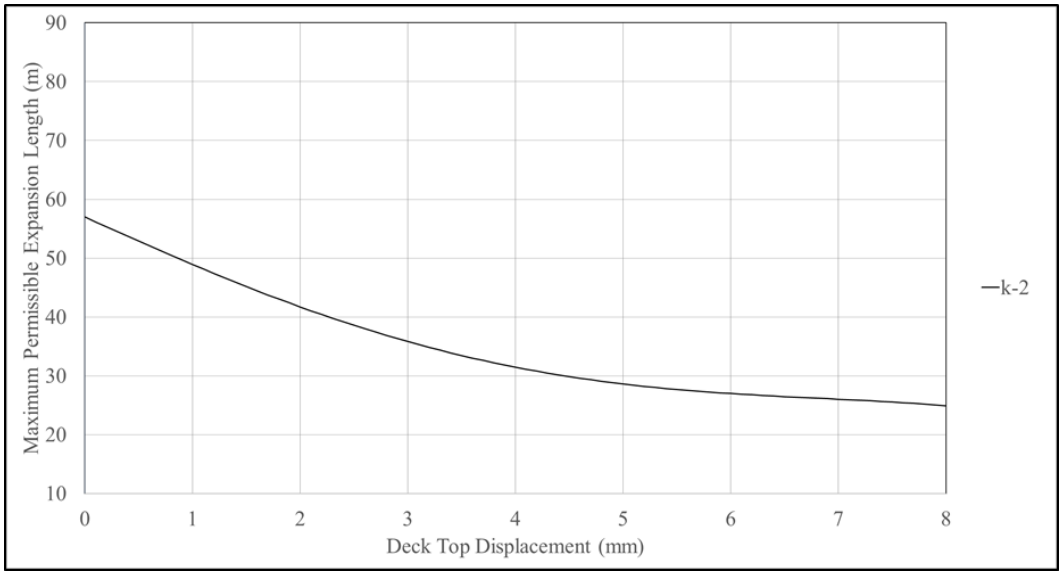

Figure 5.60. Maximum Expansion Length for Bridge Deck with Longitudinal Stiffness 2 (kN/mm/m)

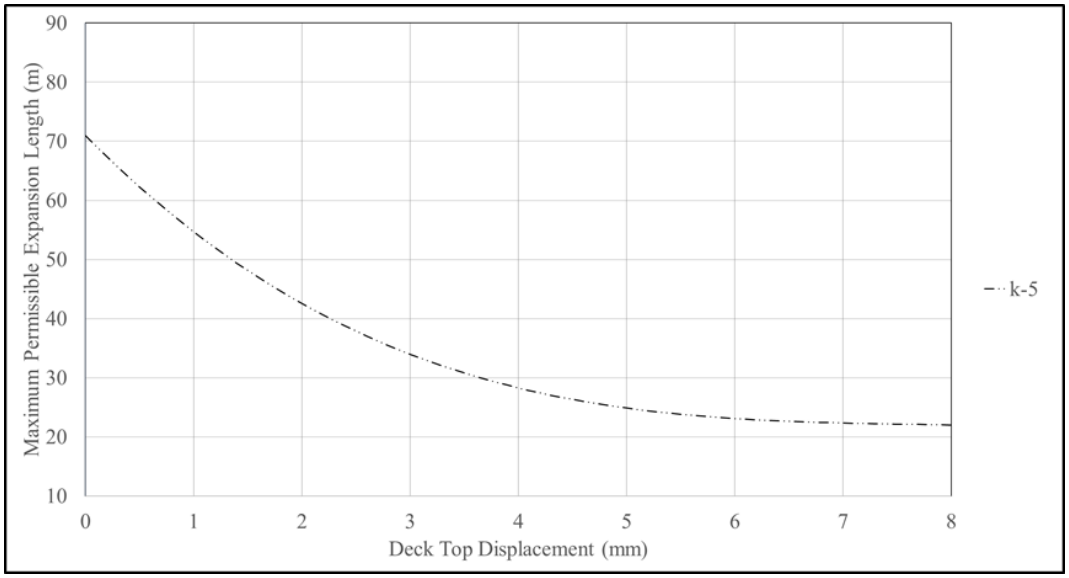

Figure 5.61. Maximum Expansion Length for Bridge Deck with Longitudinal Stiffness 5 (kN/mm/m)

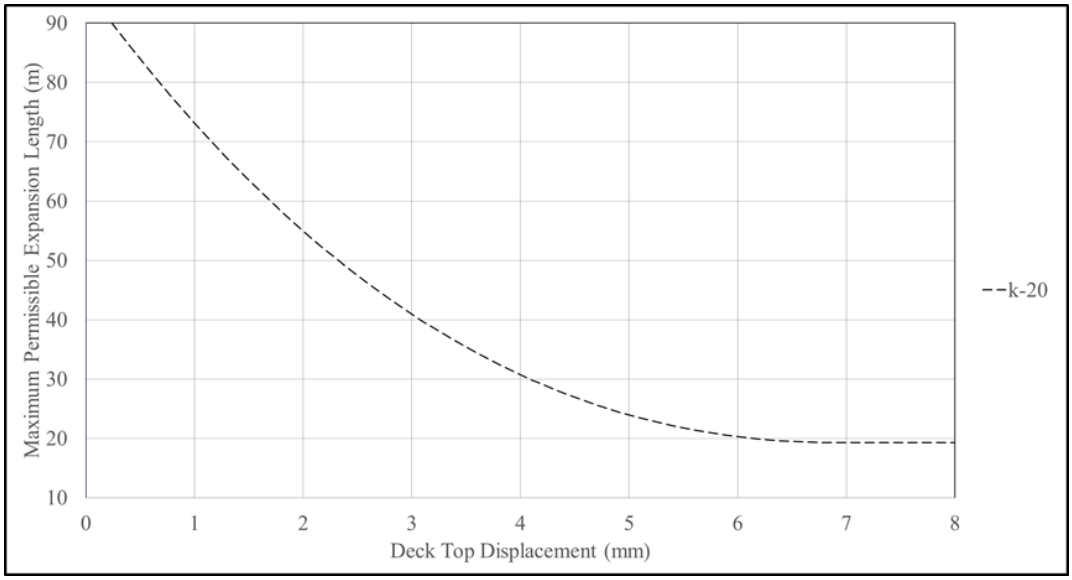

Figure 5.62. Maximum Expansion Length for Bridge Deck with Longitudinal Stiffness 20 (kN/mm/m)

The drop in maximum allowable expansion length and the increase in bending stiffness demand is shown in Figure 5.63 for k2, and in Figure 5.64 for k5, and in Figure 5.65 for k20.

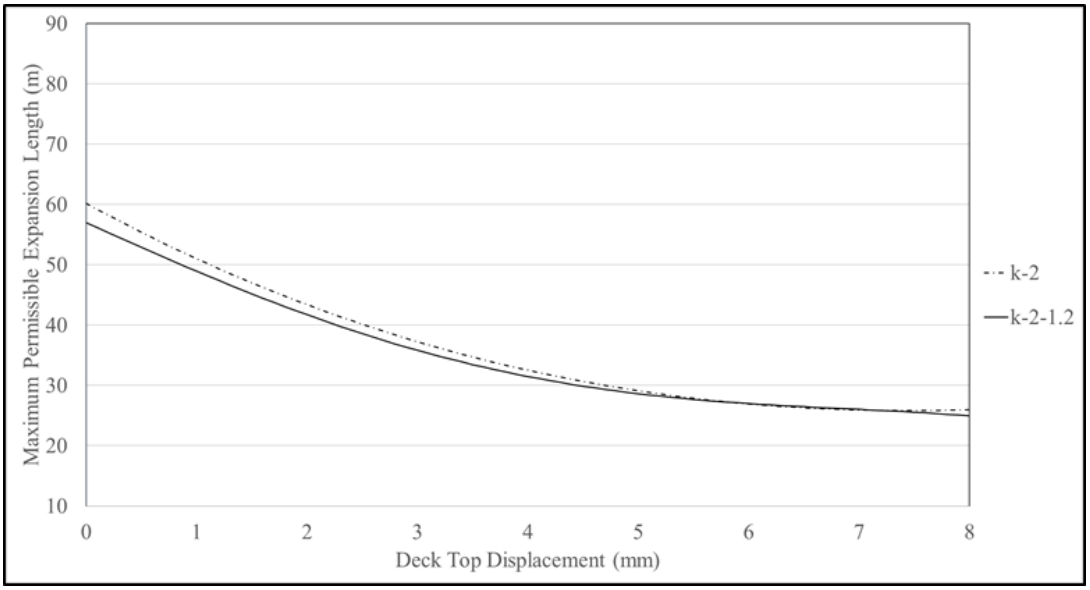

Figure 5.63. Permissible Domain for Rail Stresses for k 2 (kN/mm/m)

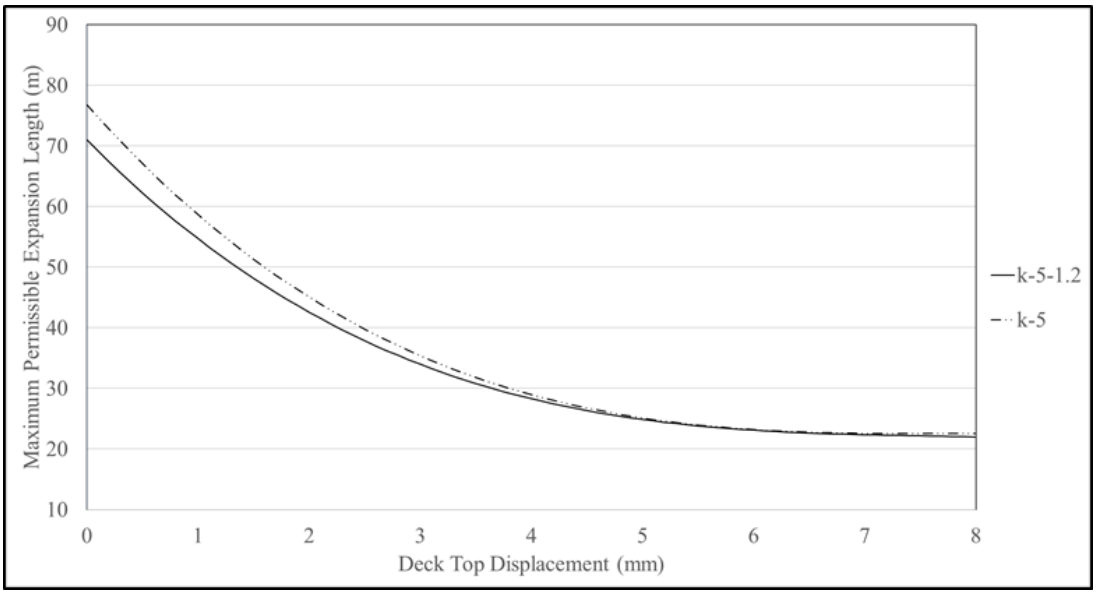

Figure 5.64. Permissible Domain for Rail Stresses for k 5 (kN/mm/m)

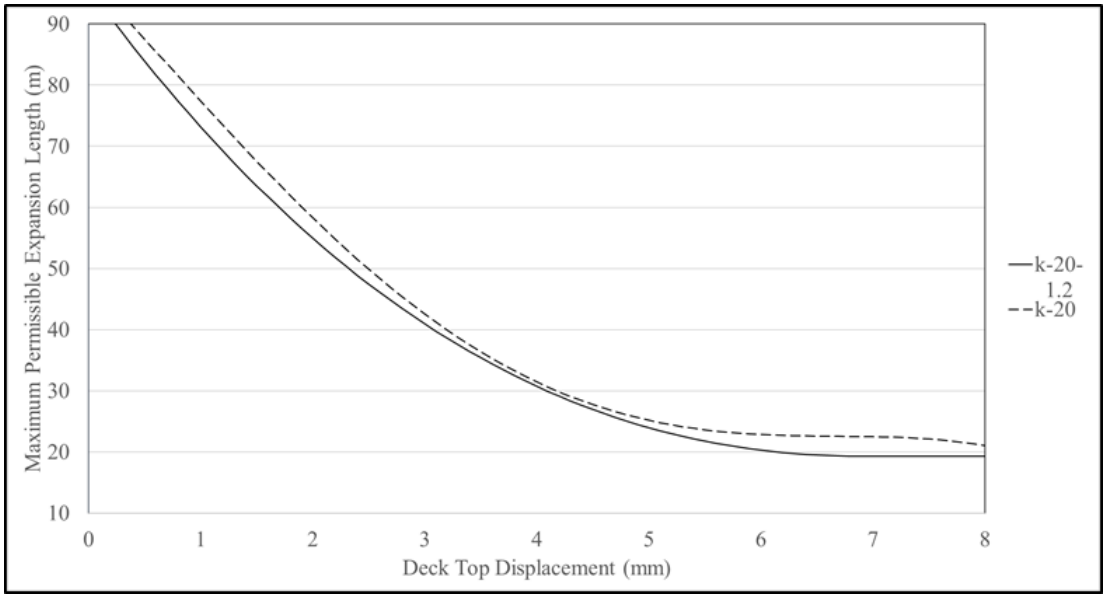

Figure 5.65. Permissible Domain for Rail Stresses for k 20 (kN/mm/m)

The maximum allowable expansion length given by Eurocode is shown in Figure 5.66, and the proposed length for different longitudinal stiffnesses with $\bar{\alpha}$ = 1E-6 $^{o}K^{-1}$ is shown in Figure 5.67.

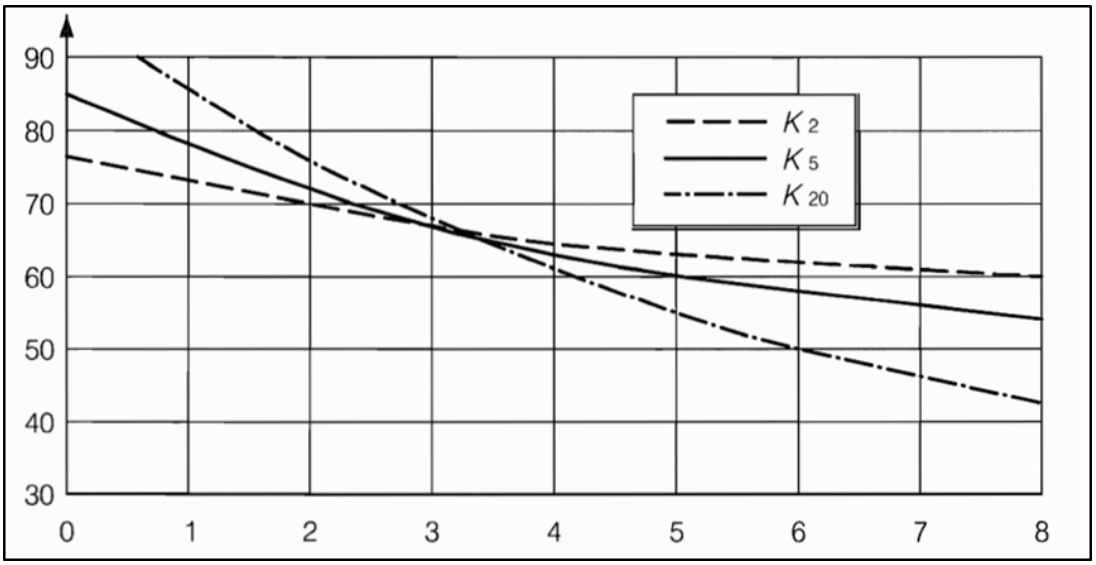

Figure 5.66. Permissible Domain for Rail Stresses Eurocode with Amplification Factor α = 1

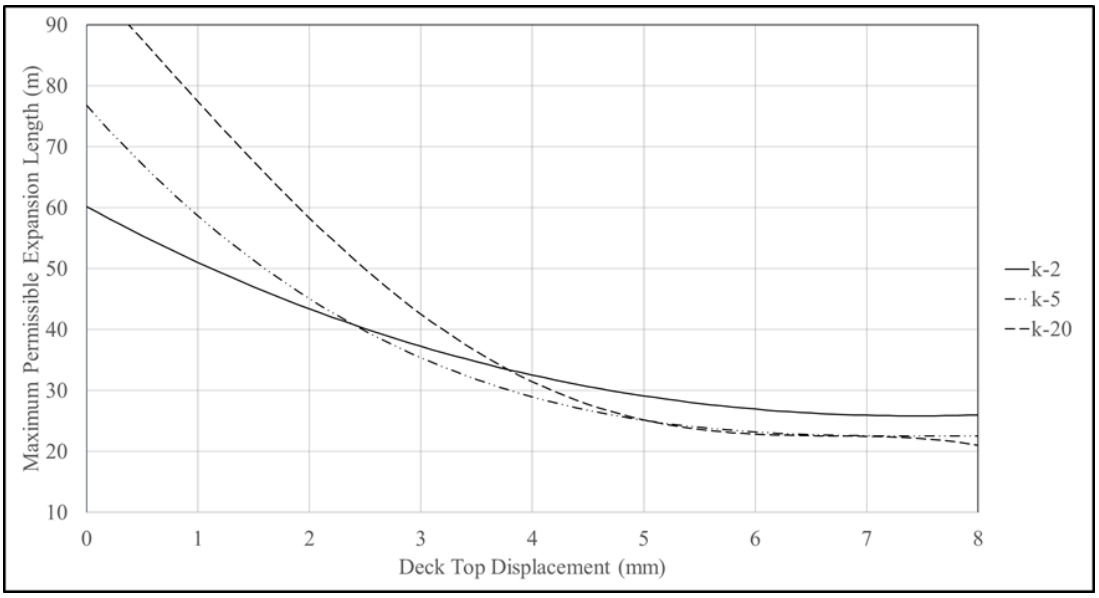

Figure 5.67. Proposed Permissible Domain for Rail Stresses α = 1.4 with Amplification Factor

The maximum allowable expansion length given by Eurocode is shown in Figure 5.68, and the proposed length for different longitudinal stiffnesses with $\bar{\alpha}$ = 1.2E-6 $^{o}K^{-1}$ is shown in Figure 5.69.

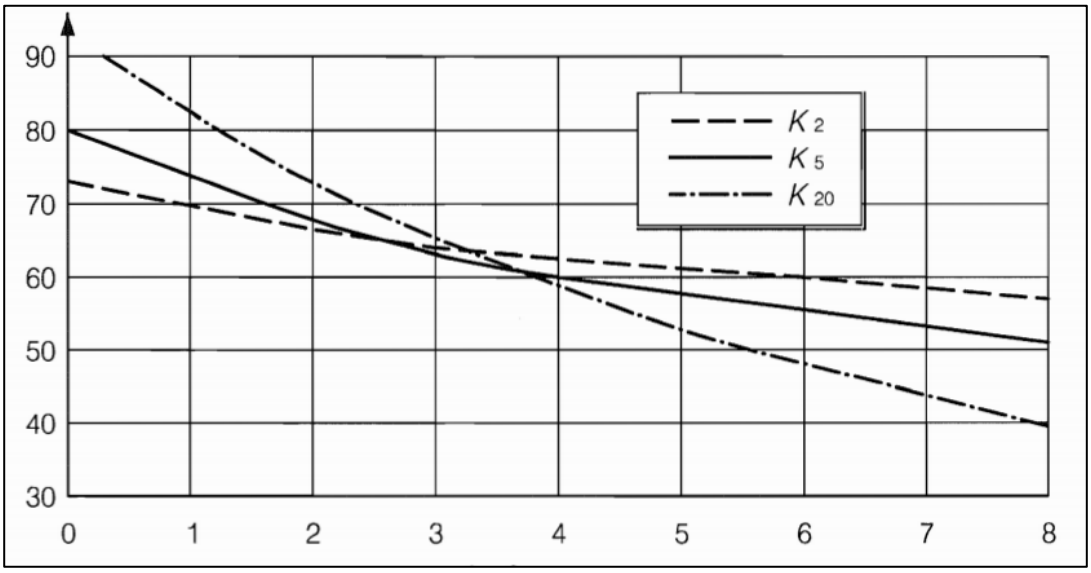

Figure 5.68. Permissible Domain for Rail Stresses Eurocode with Amplification Factor α = 1

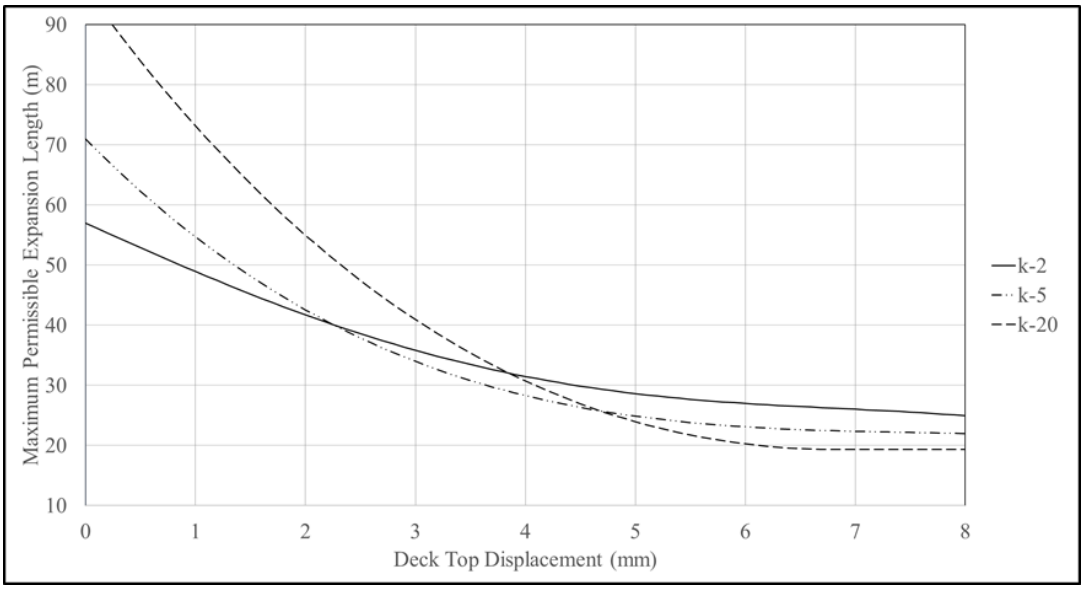

Figure 5.69. Proposed Permissible Domain for Rail Stresses with Amplification Factor α = 1.4

CHAPTER 6

SUMMARY, CONCLUSION AND RECOMMENDATIONS FOR FUTURE STUDIES

The increased speed of railways is achieved by the use of continuous welded rail as the rail is continuous. If a bridge structure is used, the bridge movement will induce deformations and additional stresses on the rail. Also, the rail will induce forces on the bridge deck resulted from traffic movement. This phenomenon is called Track-Structure interaction. The parameters affecting the track-structure interaction are defined in the literature, but how these parameters affect the total response of the structure, relative displacement, and rail additional stresses are not discussed in detail. This study is aimed to investigate the parameters affecting the track-structure interaction for high-speed railway bridges with ballasted bed track and how changing the magnitude of the parameters will affect the rail stresses. Eurocode provides a simple method for determining the maximum allowable expansion length according to the total longitudinal stiffness of the supporting system and the top deck displacement under vertical loads. This method is valid for classified vertical and horizontal loads with α alpha factor = 1. In this study, the simple method adapted by Eurocode is extended to include classified vertical and horizontal loads up to α alpha factor = 1.4.

The modeling approach used in this study is based on simple 2D models. This modeling approach is proven to save time and to provide accurate results. Comparisons between 2D and 3D modeling are found in the literature. It is found that 3D modeling is only needed when the buckling of the continuous welded rail is under investigation. However, the modeling approach and the computer software used for this study is validated according to the validation models provided by UIC. Due to the non-linear behavior of the ballast, all analyses should be non-linear. Eurocode and many design codes allow the linear sum of rail stresses resulted from a non-linear

separate analysis of variable actions. The linear sum of non-linear analysis is against the nature of non-linear systems. However, due to the complexity of the system resulted from the ballast behavior, which will change according to the ballast state of vertical load, design codes allow the linear sum of the rail stresses. Design codes define two methods of analysis: Separated simple analysis and Complete analysis, both of which are evaluated, and the difference between the two methods is shown. Loads applied to the structure are divided into three main categories vertical, horizontal, and thermal loads. The thermal loads applied to the rail are ignored since, for this study, no thermal expansion device is used. Rail stresses are shown for each loading case, and which parameters affecting the rail stresses for the specific load case are identified and different magnitudes of the variable's influence on the rail stresses are given. The results found from the study are used for constructing the data set for the proposed simple calculation method.

The analysis shows that thermal action results in additional stress on the rails according to the structural arrangement used. The rail stresses are directly affected by the expansion length of the bridge deck and the longitudinal stiffness of the supporting system. The deck cross-section area has a negligible effect. Only if the cross-section area is physically achievable. Cross-section areas close to the track cross-sectional area will change the effect of thermal action on the rail stresses, but these areas are very small and physically unachievable. Other parameters such as bridge deck height and neutral axis location have no effect on the additional rail stresses. Additional stresses in the rail increase if the expansion length is increased and/or if the longitudinal stiffness is increased. The additional stresses resulted from horizontal forces are shown to be directly affected by the bridge deck span length and the longitudinal stiffness of the supporting system if the supporting stiffness reaches high value close to the fixed behavior under horizontal forces, the rail stresses will drop and the rail stresses resulted from braking forces are not considered additional stresses because these stresses have not resulted from the bridge movement under the applied load. The rail stresses drop according to the longitudinal stiffness of the supporting

system. Moreover, for supporting systems with low longitudinal stiffness, the rail stresses increase with the increase in bridge length, but this is not the case for systems with high longitudinal stiffnesses. The stress close to the supporting point is not increased dramatically according to the span length; the effect of bridge bending stiffness, total height, and neutral axis location are neglected for bridges with low longitudinal stiffness. However, the bending stiffness starts to affect the rail stresses while the longitudinal stiffness is increasing. Bridge deck height and neutral axis location effect is related to the bending stiffness effect where higher bending effect will result in higher deck height and neutral axis effect. Bending stiffness effect is a result of the coupling force between the reaction in the bearings and the applied force on the rails. Whenever the bridge bending stiffness is high, the couple force effect is reduced. For bridges with the same longitudinal and bending stiffnesses, but with relatively high longitudinal stiffness, deck height and neutral axis location are found to be affecting the rail stresses. Deeper bridge decks will result in higher stresses, and when the neutral axis approaches the top surface, the rail stresses increase as the coupling arm is increased. For bridge decks with rigid bending stiffness, the effect of deck height and neutral axis location are neglected. Rail stresses resulted from vertical loads are directly related to the bending stiffness of the bridge deck. The relation between rail stresses and top deck displacement is non-linear affected by many factors. Longitudinal stiffness of the supporting system has a negative effect on the rail stresses resulted from vertical loads. Lower longitudinal stiffness will allow a higher back movement of the supports, this will reduce the coupling force, but for systems with higher longitudinal stresses, the coupling force is increased, so the rail stresses.

Load application on the bridge and the ballast state of vertical loads should be defined carefully. Thermal loads are only applied for un-loaded ballast resistance. Also, vertical and horizontal loads should be applied only to loaded ballast resistance. Horizontal loads shall always be accompanied by vertical loads. For the vertical load evaluation, only one embankment should be loaded, and the other embankment should be in unloaded state because the interaction is already done prior to the train leaving

the bridge. Using two loaded embankments will reduce the relative displacement and will increase the rail stresses.

The simple method proposed by Eurocode in Annex G provides an easy and time-saving approach. This approach has a drawback. It is only valid for classified loads with $\alpha = 1$. As a result of the parametric study, the data set is prepared for the evaluation and, by evaluating the bridge cases, new charts are proposed. Developing an approach in the charts is different from the Eurocode approach. Nevertheless, the results have consisted. The maximum allowable expansion length is dropped and, the bending stiffness requirement is increased as a result of the increased loads due to higher α factor. The increase in the thermal expansion coefficient resulted in a decrease in the maximum allowable expansion length, and this holds logical since increasing the value of the thermal expansion coefficient will result in higher stresses from thermal loads.

The analysis results show that expansion length over 90 m could be achieved for rail stresses criteria. Design codes haven't specified how this limit is set, but it could be found in the literature that the maximum expansion length is related to rail wearing resulted from bridge deck movement due to daily temperature variation. Design codes should incorporate the daily temperature variation as a design criterion and release the maximum allowable expansion length. This will result in a more economical and reliable design since for bridge decks with spans over 90 (m) rail thermal expansion device should be used. Introducing a rail expansion device will raise the operating cost as it requires more maintenance, and it will cause reliability problems because expansion devices are more prone to damage. The design codes didn't identify the additional stresses resulted from rail bending and shear transferred between the joints. These stresses are fixed within a value subtracted from the remaining allowable stress. If rail bending stress is calculated, this will increase the maximum allowable additional stress limit, which will lead to a more economical design. The German design code recommendations (DIN-Fb 101) allow a maximum allowable additional tensile stress up to 112 (MPa) if the rail bending is considered as a load case.

Future researches should focus on a new design criterion for continuous welded rail interaction with structures. The existing codes are very limited and do not serve the design practice. Most designers incorporate designs according to practice experience, not to know-how based experience. That’s why there is a real need for a Unified Theory of CWR made to be continuous over the bridge structures.

REFERENCES

Alabbasi, Y., & Hussein, M. (2019). Large-scale triaxial and box testing on railroad ballast: a review. SN Applied Sciences, 1(12), 1592. https://doi.org/10.1007/s42452-019-1459-3.

American Railway Engineering and Maintenance-of-Way Association (AREMA), 2008, Steel structures, in Manual for Railway Engineering, Chapter 15, Lanham, MD.

Baxter, D., & Nemovitz, D. (2012). Sensitivity analysis of rail–structure interaction force effects for direct-fixation. In Proc., Annual Conf. & Exposition AREMA, American Railway Engineering and Maintenance-of-Way Association, Lanham, MD.

Bilow, D. N., & Randich, G. M. (2000, December). Slab track for the next 100 years. In 2000 Annual Conference Proceedings of American Railway Engineering and Maintenance of Way Association.

CEN (European Committee for Standardization). (1991-2:2003E). "Actions on structures, part-2: traffic loads on the bridges." Eurocode 1, Brussels.

CEN (European Committee for Standardization). (EN 13674-1:2002E). "Railway applications - Track - Rail - Part 1, Vignole railway rails 46 kg/m and above." European Standard, Brussels.

Chen, R., Wang, P., & Wei, X.-K. (2013). Track-Bridge Longitudinal Interaction of Continuous Welded Rails on Arch Bridge. Mathematical Problems in Engineering, 2013, 1–8. doi: 10.1155/2013/494137.

Chatkeo, Y. (1985). Die Stabilität des Eisenbahngleises im Bogen mit engen Halbmessern bei hohen Axialdruckkräften. na.

Cutillas, A. (2008). Track-bridge interaction problems in bridge design. Track-Bridge Interaction on High-Speed Railways. doi: 10.1201/9780203895399.

Dai, G., Chen, G., Zheng, R., & Chen, Y. F. (2020). A New Bilinear Resistance Algorithm to Analyze the Track-Bridge Interaction on Long-Span Steel Bridge under Thermal Action. Journal of Bridge Engineering, 25(2), 04019138. doi: 10.1061/(asce)be.1943-5592.0001505.

Dai, G.-L., & Yan, B. (2012). Longitudinal forces of continuously welded track on high-speed railway cable-stayed bridge considering impact of adjacent bridges. Journal of Central South University, 19(8), 2348–2353. doi: 10.1007/s11771-012-1281-1.

Dosa, A., & Unggureanu, V. V. (2007). Discrete model for the stability of continuous welded rail. Transportation Infrastructure Engineering, 4, 25–34.

Dutoit, D. (2008). New evolutions for high speed rail line bridge design criteria and corresponding design procedures. Track-Bridge Interaction on High-Speed Railways. doi: 10.1201/9780203895399.

Esveld, C. (1996). A Better Understanding of Continuous Welded Rail Track. Rail Engineering International Edition, 4, 13–16.

Esveld, C. (2001). Modern railway track. Zaltbommel: MRT.

Esveld, Coenraad (1998). "Improved Knowledge of CWR Track" <http://www.esveld.com/Download/TUD/D202_Paris_98.PDF>.

European Rail Research Institute, Committee D202. Improved knowledge of forces in CWR track (including switches). Report DT 363/2 – Measurements of lateral resistance, longitudinal resistance and change of neutral rail temperature (NRT) for ballasted track, Volume 2. Determination of lateral and longitudinal ballast resistance of a railway track by experimental tests. Utrecht (The Netherlands): European Rail Research Institute; 1997.

Foutch, D.A., Tobias, D.H., Otter, D.E., LoPresti, J.A., and Uppal, A.S., 1997, Experimental and Analytical Investigation of the Longitudinal Loads in an Open-Deck Plate-Girder Railway Bridge, Report R-905, Association of American Railroads.

Foutch, D.A., Tobias, D., and Otter, D., 1996, Analytical Investigation of the Longitudinal Loads in an Open-Deck Through-Plate-Girder Bridge, Report R-894, Association of American Railroads.

Freystein, H. (2010). Interaktion Gleis/Brücke - Stand der Technik und Beispiele. Stahlbau, 79(3), 220–231. doi: 10.1002/stab.201001299.

Freystein, H., & Geißler, K. (2013). Interaktion Gleis/Brücke bei Stahlbrücken mit Beispielen. Stahlbau, 82(2), 78–86. doi: 10.1002/stab.201310021.

Frýba Ladislav, Kadečka Slavoš, & Man, O. (1996). Dynamics of railway bridges. Praha: Academia.

Goicolea-Ruigomez, J. (2008). Service limit states for railway bridges in new Design Codes IAPF and Eurocodes. Track-Bridge Interaction on High-Speed Railways. doi: 10.1201/9780203895399.

Guo, Y., Yu, Z., & Shi, H. (2015). Effect of rail thermal stress on the dynamic response of vehicle and track. Vehicle System Dynamic, 53, 30–50.

Holický, M., & Marková, J. THERMAL ACTIONS. Czech Technical University in Prague, Czech Republic.

International Union of Railways. (2001) 2nd edition. “Track/bridge interaction: recommendations for calculations”. UIC 774-3 R Paris.

Jones, D. R. H., & Ashby, M. F. (2019). Engineering materials. Oxford: Pergamon Press.

Kerr, A. (1976). An analysis of thermal track buckling in the lateral plane. Acta Mechanica, 30(1–2), 76–285.

Kish, A., Samavedam, G., & Jeong, D. (1982). Analysis of thermal buckling tests on U.S. railroads, FRA/ORD-82/45, Washington, D.C., USA.

Kish, A., Samavedam, G., & Jeong, D. (1985). Influence of vehicle induced loads on the lateral stability of CWR track, DOT/FRA/ ORD-85/03, Washington, D.C., USA.

Kumar, R., & Upadhyay, A. (2012). Effect of temperature gradient on track-bridge interaction. Interaction and Multiscale Mechanics, 5(1), 1–12. doi: 10.12989/imm.2012.5.1.001.

Lei, X., & Feng, Q. (2004). Analysis of stability of continuously welded rail track with finite elements. Proceedings of the Institution of Mechanical Engineers, Part F: Journal of Rail and Rapid Transit, 218(3), 225–233. doi: 10.1243/0954409042389409.

Lim, N. H., Han, S. Y., Han, T. H., & Kang, Y. J. (2008). Parametric study on stability of continuous welded rail track-ballast resistance and track irregularity. Steel Structures, 8, 171-181.

Liu, W.-S., Dai, G.-L., & He, X.-H. (2013). Sensitive factors research for track-bridge interaction of Long-span X-style steel-box arch bridge on high-speed railway. Journal of Central South University, 20(11), 3314–3323. doi: 10.1007/s11771-013-1855-6.

Liu, X., Zhao, P., & Dai, F. (2011). Advances in design theories of high-speed railway ballastless tracks. *Journal of Modern Transportation*, *19*(3), 154–162. doi: 10.1007/bf03325753.

Lonsdale, C. P., & Engineer, M. (1999). Thermite rail welding: history, process developments, current practices and outlook for the 21st century. In Proc. AREMA 1999 Annual Conf. (Vol. 1895, p. 18).

LoPresti, J.A., Otter, D.A., Tobias, D.H., and Foutch, D.A., 1998, Longitudinal Forces in an Open-Deck Steel Bridge, Technology Digest 98-007, Association of American Railroads.

LoPresti, J.A. and Otter, D.A., 1998, Longitudinal Forces in a Two-Span Open-Deck Steel Bridge at FAST, Technology Digest 98-020, Association of American Railroads.

Low, A. (2015). The Design of Railway Viaducts without Rail Joints. Structural Engineering International, 25(2), 218–223. doi: 10.2749/101686614x14043795570651.

Manovachirasan, A., Suthasupradit, S., Choi, J.-H., Kim, B.-J., & Kim, K.-D. (2018). The Evaluation of Axial Stress in Continuous Welded Rails via Three-Dimensional Bridge–Track Interaction. International Journal of Steel Structures, 18(5), 1617–1630. doi: 10.1007/s13296-018-0058-2.

Mato, F. M., & Cornejo, M. O. (2008). Track-structure interaction and seismic design of the bearings system for some viaducts of Ankara-Istanbul HSRL project. Track-Bridge Interaction on High-Speed Railways. doi: 10.1201/9780203895399.

Min, K.-H., & Yun, K.-M. (2016). An Experimental Study for Longitudinal Resistance of Ballast Track on Bridge. Journal of the Korea Academia-Industrial Cooperation Society, 17(5), 173–178. doi: 10.5762/kais.2016.17.5.173.

Mirković, N., Popović, Z., Pustovgar, A., Lazarević, L., & Zhuravlev, A. (2018). Management of stresses in the rails on railway bridges. FME Transactions, 46(4), 636–643. doi: 10.5937/fmet1804636m.

Müller, G., Jovanovıc, D., & Haas, P. (1981). Tracks-Gravel-Bridge Interaction. Computers and Structures, 13, 607–611.

Okelo, R., & Olabimtan, A. (2011). Nonlinear Rail-Structure Interaction Analysis of an Elevated Skewed Steel Guideway. Journal of Bridge Engineering, 16(3), 392–399. doi: 10.1061/(asce)be.1943-5592.0000163.

Otter, D.E., Doe, B., and Belport, S., 2005, Rail Car Lateral Forces for Bridge Design and Rating, Technology Digest 05-002, Association of American Railroads

Otter, D.E., Joy, R., and LoPresti, J.A., 1999, Longitudinal Forces in a Single-Span, BallastedDeck, Plate-Girder Bridge, Report R-935, Association of American Railroads.

Otter, D.E., LoPresti, J., Foutch, D.A., and Tobias, D.H., 1996, Longitudinal Forces in an OpenDeck Steel Plate-Girder Bridge, Technology Digest 96-024, Association of American Railroads.

Otter, D.E., LoPresti, J., Foutch, D.A., and Tobias, D.H., 1997, Longitudinal forces in an open-deck steel plate-girder bridge, AREA Proceedings, 98, 101–105.

Otter, D.E., Sweeney, R.A.P., and Dick, S.M., 2000, Development of Design Guidelines for Longitudinal Forces in Bridges, Technology Digest 00-018, Association of American Railroads.

Papp, H., & Liegner, N. (2016). Investigation of internal forces in the rail due to the interaction of CWR tracks and steel railway bridges with ballasted track superstructure. Pollack Periodica, 11(2), 65–74. doi: 10.1556/606.2016.11.2.6.

Pessel, S., & Mensinger, M. (2016). Fracture Mechanics Based Approach to the Significance of Certain Loads on the Service Life of Rails. Transportation Research Procedia, 14, 2006–2014. doi: 10.1016/j.trpro.2016.05.168.

Popović, Z., Lazarević, L., Vilotijević, M., & Mirković, N. (2017). Interaction Phenomenon Between Train, Track and Bridge. International Scientific Conference Energy Management of Municipal Transportation Facilities and Transport EMMFT 2017 Advances in Intelligent Systems and Computing, 3–11. doi: 10.1007/978-3-319-70987-1_1.

Prommersberger, G., Rojek, R. (1984). "Transmission of Longitudinal Forces on Railroad Bridges." IABSE., 12(1), 523–529.

Ramos, Ó., Schanack, F., Carreras, G. O., & Retuerto, J. D. V. (2019). Bridge length limits due to track-structure interaction in continuous girder prestressed concrete bridges. *Engineering Structures, 196,* 109310. doi: 10.1016/j.engstruct.2019.109310.

Requejo, P. G. L., & Sanguino, M. C. (2008). Numerical methods for the analysis of longitudinal interaction between track and structure. Track-Bridge Interaction on High-Speed Railways. doi: 10.1201/9780203895399.

Římal, J., & Šindler, D. (2008). Comparison of temperature loadings of bridge girders. Acta Polytechnica, 48(5).

Ruge, P., & Birk, C. (2007). Longitudinal forces in continuously welded rails on bridgedecks due to nonlinear track–bridge interaction. Computers & Structures, 85(7-8), 458–475. doi: 10.1016/j.compstruc.2006.09.008.

Ruge, P., Widarda, D., Schmälzlin, G., & Bagayoko, L. (2009). Longitudinal track–bridge interaction due to sudden change of coupling interface. Computers & Structures, 87(1-2), 47–58. doi: 10.1016/j.compstruc.2008.08.012.

Ryjáček, P., & Vokáč, M. (2014). Long-term monitoring of steel railway bridge interaction with continuous welded rail. Journal of Constructional Steel Research, 99, 176–186. doi: 10.1016/j.jcsr.2014.04.009.

Samavedam, G., Kish, A., & Jeong, D. (1983). Parametric studies on lateral stability of welded rail track, DOT/FRA/ORD-83/07, Washington, D.C., USA.

Samavedam, G., Kish, A., Purple, A., & Schoengart, J. (1993). Parametric analysis and safety concepts of CWR track buckling, DOT/ FRA/ORD-93/26, Washington, D.C., USA.

Strauss, A., Karimi, S., Kopf, F., Capraru, C., & Bergmeister, K. (2015). Monitoring-based performance assessment of rail-bridge interaction based on structural reliability. Structural Concrete, 16(3), 342–355. doi: 10.1002/suco.201500019.

Strauss, A., Karimi, S., Šomodíková, M., Lehký, D., Novák, D., Frangopol, D. M., & Bergmeister, K. (2018). Monitoring based nonlinear system modeling of bridge–continuous welded rail interaction. Engineering Structures, 155, 25–35. doi: 10.1016/j.engstruct.2017.10.053.

Strauss, A., Šomodíková, M., Lehký, D., Novák, D., & Bergmeister, K. (2018). Nonlinear Finite Element Analysis Of Continuous Welded Rail–Bridge Interaction: Monitoring-Based Calibration. Journal of Civil Engineering and Management, 24(4), 344–354. doi: 10.3846/jcem.2018.3050.

Sussmann, T. R., Hyslip, J. P., Chrismer, S. M., & Li, D. (2015). Railway Geotechnics. CRC Press.

Tobias, D.H., Foutch, D.A., Lee, K., Otter, D.E., and LoPresti, J.A., 1999, Experimental and Analytical Investigation of the Longitudinal Loads in a Multi-span Railway Bridge, Report R-927, Association of American Railroads.

Unsworth, J. F. (2010). Design of modern steel railway bridges. Boca Raton, FL: CRC Press.

Uppal, A.S., Otter, D.E., and Joy, R.B., 2001, Longitudinal Forces in Bridges due to Revenue Service, Report R-950, Association of American Railroads.

Van't Zand J, Moraal J. Ballast resistance under three dimensional loading. Delft (The Netherland): Delft University of Technology, Faculty of Civil Engineering, Laboratory of Roads and Railways. (Report 7-97-103-4).

Wenner, M., Lippert, P., Plica, S., & Marx, S. (2016). Längskraftabtragung auf Eisenbahnbrücken: Teil 2: Hintergründe des Nachweises. Bautechnik, 93(7), 470-481.

Widarda, D. R. (2009). Longitudinal Forces in Continuously Welded Rails Due to Nonlinear Track-bridge Interaction for Loading Sequences (Doctoral dissertation, Verlag nicht ermittelbar).

Yan, B., Dai, G.-L., & Zhang, H.-P. (2012). Beam-track interaction of high-speed railway bridge with ballast track. Journal of Central South University, 19(5), 1447–1453. doi: 10.1007/s11771-012-1161-8.

Yeo, I., & Lee, S. (2006) Parameter Study on the Interaction between Track and Bridge for the Behavior of CWR. Korea Railroad Research Institute, Uiwang City, Korea.